INVESTIGATION OF PHOTOFERMENTATIVE POLY-HYDROXYBUTYRATE (PHB) AND HYDROGEN PRODUCTION VIA *RHODOBACTER CAPSULATUS*

A THESIS SUBMITTED TO
THE GRADUATE SCHOOL OF NATURAL AND APPLIED SCIENCES
OF
MIDDLE EAST TECHNICAL UNIVERSITY

BY

ERTAN HOŞAFCI

IN PARTIAL FULFILLMENT OF THE REQUIREMENTS
FOR
THE DEGREE OF MASTER OF SCIENCE
IN
ENVIRONMENTAL ENGINEERING

JANUARY 2023

Approval of the thesis:

INVESTIGATION OF PHOTOFERMENTATIVE POLY-HYDROXYBUTYRATE (PHB) AND HYDROGEN PRODUCTION VIA *RHODOBACTER CAPSULATUS*

submitted by **ERTAN HOŞAFCI** in partial fulfillment of the requirements for the degree of **Master of Science** i**n Environmental Engineering, Middle East Technical University** by,

Prof. Dr. Halil Kalıpçılar
Dean, Graduate School of **Natural and Applied Sciences** _____

Prof. Dr. Bülent İçgen
Head of the Department, **Environmental Engineering** _____

Prof. Dr. Tuba Hande Bayramoğlu
Supervisor, **Environmental Engineering, METU** _____

Assoc. Prof. Dr. Harun Koku
Co-Supervisor, **Chemical Engineering, METU** _____

Examining Committee Members:

Asst. Prof. Dr. Yasemin Dilşad Yılmazel Tokel
Environmental Engineering, METU _____

Prof. Dr. Tuba Hande Bayramoğlu
Environmental Engineering, METU _____

Assoc. Prof. Dr. Harun Koku
Chemical Engineering, METU _____

Prof. Dr. İpek İmamoğlu
Environmental Engineering, METU _____

Prof. Dr. Selim Latif Sanin
Environmental Engineering, Hacettepe University _____

Date: 26.01.2023

I hereby declare that all information in this document has been obtained and presented in accordance with academic rules and ethical conduct. I also declare that, as required by these rules and conduct, I have fully cited and referenced all material and results that are not original to this work.

Name Last name: Ertan Hoşafcı

Signature:

ABSTRACT

INVESTIGATION OF PHOTOFERMENTATIVE POLY-HYDROXYBUTYRATE (PHB) AND HYDROGEN PRODUCTION VIA *RHODOBACTER CAPSULATUS*

Hoşafcı, Ertan
Master of Science, Environmental Engineering
Supervisor: Prof. Dr. Tuba Hande Bayramoğlu
Co-Supervisor: Assoc. Prof. Dr. Harun Koku

January 2023, 169 pages

The aim of this thesis study is to investigate factors affecting hydrogen (H_2) and poly-hydroxybutyrate (PHB) production via photofermentation using two strains of *Rhodobacter capsulatus* species. To this purpose, three experimental designs were set up, namely Set 1, Set 2 and Set 3.

In Set 1, various approaches in pretreatment of bacterial biomass were investigated. For *R. capsulatus* Wild Type (WT) strain, employment of different pretreatment methods did not make a significant difference, where an average of 29.6% of cell dry weight (cdw) PHB was observed. For mutant *R. capsulatus* YO3 strain, effect of drying was observed to be significant, with non-dried biomass samples yielding 40.1% of cdw average PHB compared to 28.2% of cdw for dried samples. It was concluded that YO3 should be adopted as the strain to be used in the following sets to be conducted and should not be subjected to drying. In Set 2, effect of increasing sodium (Na^+) concentration was investigated as a potential stress condition, using two different substrate types, namely acetate and sucrose. As an indirect result of Na^+ increase up to 4000 mgNa^+/L, increasing pH was observed to be a significant stress condition. Maximum PHB accumulation was observed as 57.7 ± 5.2% and 3.3

± 0.4% of cdw for acetate and sucrose, respectively. Maximum hydrogen productivities were observed as 0.58 ± 0.03 mmol/L·h and 0.73 ± 0.06 mmol/L·h, respectively for acetate and sucrose-containing reactors. In Set 3, effect of pH as a stress condition was investigated in high and low Na^+ conditions. Maximum PHB accumulation was observed to be 57.5 ± 0.2% of cdw at 8.50 pH and 33.6 ± 2.0% of cdw at 7.70 pH for low and high Na^+ conditions, respectively. Maximum hydrogen productivity was observed as 0.42 ± 0.01 mmol/L·h at pH 7.00.

Keywords: *Rhodobacter capsulatus*, PHB Production, Hydrogen Production, Sodium Accumulation, Effect of pH

ÖZ

RHODOBACTER CAPSULATUS ARACILIĞI İLE FOTOFERMENTATİF POLİHİDROKSİBÜTİRAT (PHB) VE HİDROJEN ÜRETİMİNİN İNCELENMESİ

Hoşafcı, Ertan
Yüksek Lisans, Çevre Mühendisliği
Tez Yöneticisi: Prof. Dr. Tuba Hande Bayramoğlu
Ortak Tez Yöneticisi: Doç. Dr. Harun Koku

Ocak 2023, 169 sayfa

Bu tez çalışmasının amacı, *Rhodobacter capsulatus* türlerinin iki suşu kullanılarak fotofermentasyon yoluyla hidrojen (H_2) ve polihidroksibütirat (PHB) üretimini etkileyen faktörlerin araştırılmasıdır. Bu amaçla Set 1, Set 2 ve Set 3 olmak üzere üç deneysel set kurulmuştur.

Set 1'de, bakteriyel biyokütlenin ön işleminde çeşitli yaklaşımlar araştırılmıştır. *R. capsulatus* Yabanıl Tip suşu için, farklı ön muamele yöntemlerinin kullanılması önemli bir fark yaratmamış ve hücre kuru ağırlığının (cdw) ortalama %29,6'sı PHB olarak gözlenmiştir. Mutant *R. capsulatus* YO3 suşu için, kurutulmuş numuneler için cdw'nin %28,2'ine kıyasla kurutulmamış biyokütle numunelerinde cdw'nin %40,1'i olarak gözlenen PHB'de kurutma etkisinin önemli olduğu sonucuna varılmıştır. Bundan sonra yapılacak setlerde kullanılacak suş olarak YO3'ün benimsenmesi ve kurutma işlemine tabi tutulmaması gerektiği sonucuna varılmıştır. Set 2'de, asetat ve sükroz olmak üzere iki farklı substrat türü kullanılarak potansiyel bir stres durumu olarak artan sodyum (Na^+) konsantrasyonunun etkisi araştırılmıştır. 4000 mgNa^+/L'ye kadar Na^+ artışının dolaylı bir sonucu olarak, pH'ın artmasının önemli

bir stres durumu olduğu gözlenmiştir. Maksimum PHB birikimi, asetat ve sükroz için sırasıyla cdw'nin %57,7 ± 5,2 ve %3,3 ± 0,4'ü olarak gözlenmiştir. Asetat ve sükroz içeren reaktörler için maksimum hidrojen üretkenlikleri sırasıyla 0,58 ± 0,03 ve 0,73 ± 0,06 mmol/L·sa olarak gözlenmiştir. Set 3'te, yüksek ve düşük Na^+ koşullarında bir stres koşulu olarak pH'ın etkisi araştırılmıştır. Düşük ve yüksek Na^+ koşulları için sırasıyla 8.50 pH'ta maksimum PHB birikiminin cdw'nin %57.5 ± 0.2 ve 7.70 pH'ta %33.6 ± 2.0 olduğu gözlenmiştir. Maksimum hidrojen üretkenliği, pH 7.00'de 0.42 ± 0.01 mmol/L·sa olarak gözlenmiştir.

Anahtar Kelimeler: *Rhodobacter capsulatus*, PHB Üretimi, Hidrojen Üretimi, Sodyum Birikimi, pH Etkisi

to those we love

ACKNOWLEDGMENTS

I would like to express my deepest gratitude to my supervisor Prof. Dr. Tuba Hande Ergüder Bayramoğlu for her guidance, advice, her trust in me and this study. She always knew what I was capable of and always expanded these capabilities and my perspective without me ever noticing. I also would like to express my most sincere gratitude to my co-supervisor Assoc. Prof. Harun Koku for his immensely valuable knowledge, experience, seemingly endless support for all matters regarding laboratory use and last but not least, for educating so many valuable students and conducting studies in the past for me and all biohydrogen community to refer to. I am grateful to have studied the topic of photofermentation.

I would like to thank current and former members of Environmental Biotechnology Research Group (ENVBIORG); Rayaan Harb, Tercan Çataklı, Irmak Subaşı, Dilan Laçin and Simgenur Sağdiç. Especially Rayaan, Irmak and Dilan, I am where I am now thanks to you and all your invaluable support and suggestions in laboratory equipment and analyses. I am also thankful to the members of Hydrogen Research Laboratory; Görkem Baysal, Etkin Tarlan and Lidya Midya for everything related to the lab – whether teaching me to use instruments or taking care of my bioreactors when otherwise I have been unavailable or simply just for being there for me. Undergraduate students Andri Titan Yade, Gachomba Mwangi and Candan Ateş also deserve credit for their efforts and enthusiasm in the laboratory – I sincerely hope that all of you choose to pursue your studies in this field.

I can never forget my dearest co-workers and office mates from Z-30, or biohydrogen laboratory of Environmental Engineering in other words – eventually hydrogen will take over the world, starting in our office. Aslı Onursal, Berivan Tunca and Bahar Evren, thank you for cheering my days and never neglecting to discuss everything that is going on in my life. Your advice and discussions have always been invaluable

to me. Yours sincere Mert Erkanlı, Naz Zeynep Şimşek and Cansu Polat, you are some of the most important people in my life and I am thankful to have met you.

I am especially grateful to Gülçin Balcı, my dearest friend and companion. I cannot be more thankful for her efforts for both me and this study. She has done everything that she is capable of, for both this work and for me, expecting nothing in return but a smile on my face. Thank you, for all your love and devotion to us.

My family deserves bulk of the credit, I thank my parents Erol and Tatiana for raising me to be as responsible and as conscious as possible. Without the moral values that were passed from you upon me, I would never be able to finish this study and be proud of my work. My dearest little sisters Birsen and Nazlı, thank you for being the joy of my life, with our furry little brother Nikolay Vasilyevich. Most importantly, thank you Nina Ivanovna Belyaeva, for all your love and never sparing the knowledge of me being your favorite grandkid – I only hope that I have made all of you proud. Thank you for never stopping to believe in me and supporting me all throughout my life.

TABLE OF CONTENTS

LIST OF TABLES

TABLES

LIST OF FIGURES

FIGURES

LIST OF ABBREVIATIONS

ABBREVIATIONS	
3HB	3-hyroxybutyrate
3HV	3-hyroxyvalerate
ATP	Adenosine Triphosphate
BM	Basal Medium
BP Medium	Biebl and Pfennig's Medium
CCS	Carbon Capture and Storage
cdw	Cell Dry Weight
CHL	Chloroform
CV%	Coefficient of Variation
cyt	Cytochromes
EPS	Extracellular Polymeric Substance
FID	Flame Ionization Detector
FNR	Ferredoxins
GC	Gas Chromatography
HB	Hydroxybutyrate
HPLC	High Performance Liquid Chromatography
hup	uptake hydrogenase
hup^-	uptake hydrogenase deficient
L/D	Light/Dark

LDPE	Low-density Poly-ethylene
LOD	Limit of Detection
LOQ	Limit of Quantification
MCE	Mixed Cellulose-ester
MEC	Microbial Electrolysis Cell
MPYE	Mineral-peptone Yeast Extract
NADH	Nicotinamide Adenine Dinucleotide Hydride
OD	Optical Density
P3HB	Poly(-3-hyroxybutyrate)
PHA	Poly-hydroxyalkanoate
PHB	Poly-hydroxybutyrate
PHV	Poly-hydroxyvalerate
PNSB	Purple Non-sulfur Bacteria
PTFE	Polytetrafluoroethylene
RID	Refractive Index Detector
SMR	Steam Methane Reforming
WGSR	Water-gas Shift Reaction

CHAPTER 1

INTRODUCTION

With the increase in the population and technological advances of the world, the strain on energy sources and raw materials are at its peak and is projected to only increase. This is also stated by the report prepared by International Energy Agency (IEA), in which energy demand is projected to be increased by 25% within next two decades (International Energy Agency, 2022). Considering that the most of the energy demand around the world is fulfilled by non renewable sources, it is of particular importance that the growing energy demand must be met using sustainable methods for energy production. See Figure 1.1 for the global share of energy production from various methods.

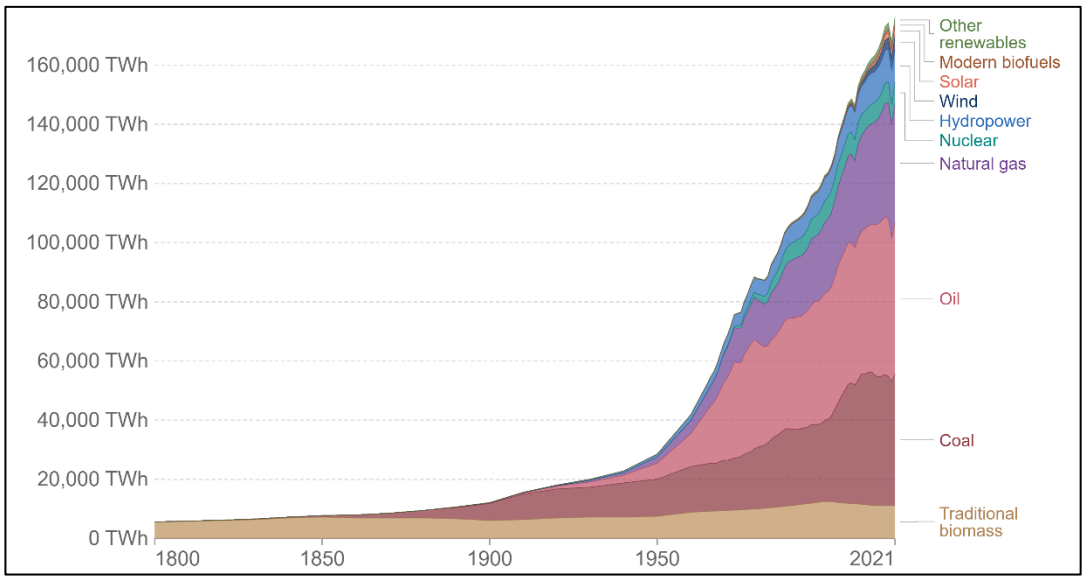

Figure 1.1. Global energy production from various sources (Statistical Review of World Energy 2022, 2022).

As can be seen from Figure 1.1, significant portion of global energy demand is met by the utilization of crude oil derived fuels. In not-too-distant future, global society

would need to abandon the already over-exploited petroleum reserves as a major energy production source and switch to renewable sources. An important aspect of crude oil should not be overlooked though, which is the hydrocarbon rich black fluid that is called petroleum is not only a fuel to burn in power generators or in vehicles, but is a mixture of different compounds that have become an integral part of modern society since its discovery centuries ago. Petroleum derived materials can be listed very broadly as liquid fuels, combustible gases, lubricants, both analytical and common quality chemicals, solvents, plastics and even road paving as asphalt (Fajobi *et al.*, 2019). Figure 1.2 summarizes the basic products derived from crude oil.

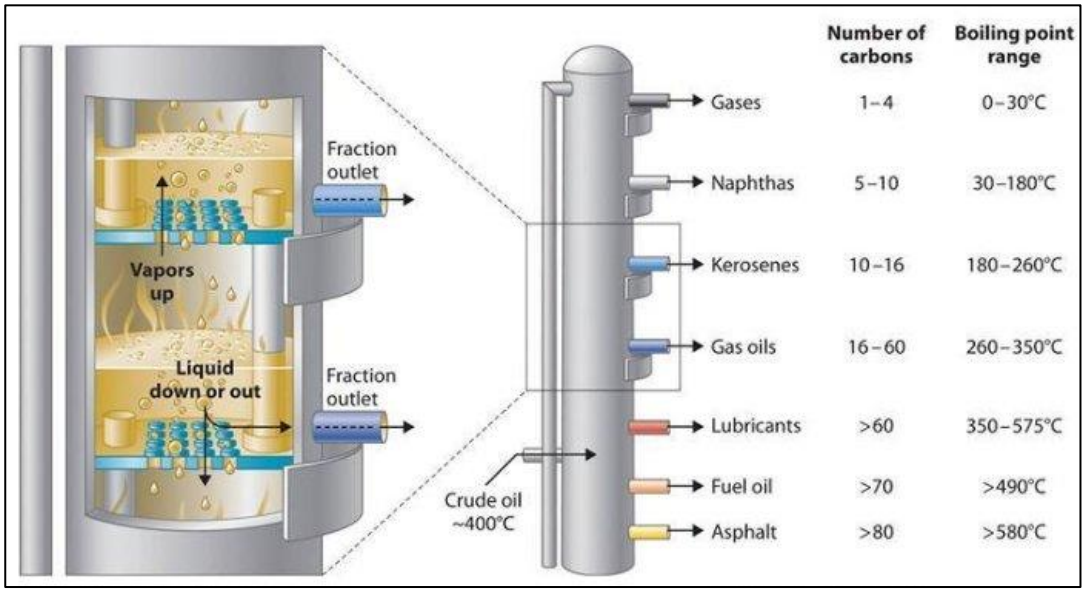

Figure 1.2. Petroleum refining products (Fajobi *et al.*, 2019).

A significant outcome of gradually abandoning crude oil as a means of major energy carrier would result in decrease in the supply of all those different petroleum derived compounds summarized above. The decrease in supply of petroleum-based products must be replaced with a sustainable alternative. Specifically, one petroleum-based product stands out in terms of potential hazards to environment and sustainability in a world without petroleum, which is plastics.

Plastics are a fundamental part of today's society with uses in countless fields and industries ranging from packaging, medical equipment, storage, electronics, daily

consumables among many others. Apart from being completely dependent upon the supply of crude oil for their production, diverse effects of plastics in both production and at the end-of-life stages have pushed the society towards a relatively new concept, namely bioplastics. Bioplastics have been in the daily lives of people for perhaps longer than one would assume, with plastics derived from biological polymers already in common use especially in the fields of medical biotechnology and food industry. There are emerging technologies such as consumable food wrappings, or established technologies utilizing bioplastics in targeted drug delivery systems (El-malek *et al.*, 2020). Most of the bioplastics are currently produced from biological material such as energy crops, and in a non-sustainable manner. In fact, biopolymers are limited in usage area and are more energy intensive to produce than conventional plastics (Schulze *et al.*, 2017). An emerging topic is to not actually produce biopolymers using energy intensive methods or dedicated energy crops, but to harvest the naturally occurring bioplastics from within microbial cells. These said bioplastics are a by-product of metabolic activity in microorganisms and are primarily used as an energy storage compound of microbial cells, just as starch in Plantae and glycogen in Animalia. These compounds bear remarkable similarities to common plastics and are synthesized naturally by most microbial species (Du & Yu, 2002).

Another rising topic for sustainable energy production is to utilize hydrogen to meet the world energy demands. Hydrogen, by its nature yields highest calorific value per unit mass when combusted, with 120.0 kJ/g net calorific value compared to 50.0 kJ/g of natural gas or 43.4 kJ/g and 42.6 kJ/g of gasoline and diesel fuel, respectively (Eng *et al.*, 2008). In addition, as can be seen from Equation 1.1 below, only output of hydrogen combustion with oxygen is water vapor, which has much less greenhouse effect than carbon dioxide or methane.

$$H_2(g) + 0.5\ O_2(g) \rightarrow H_2O\ (g),\ \Delta H = -241.8\ \text{kJ/mol}\ (-120.0\ \text{kJ/g}) \qquad (1.1)$$

To produce such an efficient fuel requires more than conventional energy production methods though. These methods can broadly be described as production of hydrogen

from fossil fuels, electrolysis and biological methods (Mahidhara *et al.*, 2019). This work focuses on the production of hydrogen via biological methods, specifically photobiological production of hydrogen.

The reason that the photobiological production of hydrogen being the focus of this thesis is due to the capabilities of the specific microorganisms used in the study, namely the group of purple non sulfur bacteria (PNSB), belonging to the phylum *Pseudomonadota* (McKinlay, 2014). PNSB are facultative anaerobes capable of photofermentation, that is, able to utilize organic carbon as the electron donor in the presence of light resulting in hydrogen production and able to utilize organic carbon in the absence of light with carbon dioxide production instead of hydrogen (Basak & Das, 2007). Some widely researched species of the group include *Rhodopseudomonas palustris*, *Rhodobacter sphaeroides* and *Rhodobacter capsulatus* (Imhoff *et al.*, 1984). These species are capable of utilizing many different varieties of substrate such as wide range of organic acids and sugars, producing hydrogen and accumulating aforementioned bioplastics at the same time without requiring complex operational parameters (Sevinç *et al.*, 2012). These bioplastics are natural compounds synthesized as a storage material of microbial cells and named as poly – hydroxyalkanoates (PHA), among which the most common PHA being poly – hydroxybutyrate (PHB) (Keshavarz & Roy, 2010). Production of hydrogen and PHB using PNSB requires only a handful of parameters investigated as of now, namely (i) mesophilic temperatures, (ii) light and (iii) high carbon/nitrogen ratio in the substrate (Tiang *et al.*, 2020). The latter is a parameter that is unique to PNSB, with high C/N ratio enhancing both hydrogen production and PHB accumulation contrary to other microbial species (Montiel-Corona & Buitrón, 2022). The exact factors affecting the PHB – hydrogen relationship are not yet fully understood though, and this is an important aspect of this thesis, to be able to relate the shift of the metabolism between H_2 and PHB production.

For the reasons said, photobiological production of hydrogen would potentially result in both energy gains in the form of hydrogen, PHB production and possibly degradation of waste materials containing high concentrations of organic carbon,

with relatively easy operation such as employment of a greenhouse to maintain mesophilic temperatures and utilizing natural sunlight to decrease the costs arising from illumination.

However, there are points still to be investigated such as substrate-H_2-PHB relationship, effects of various stress conditions on PHB accumulation and response of different strains to various stress conditions. Maximization of H_2 and/or PHB production would be advantageous for degradation of high C/N ratio wastewaters such as food, sugar and alcohol industry effluents while producing an effective energy carrier and an industrial feedstock in the form of hydrogen. The process would depend on relatively milder environmental conditions (mesophilic temperatures, neutral pH and illumination only) while also producing a valuable by-product, PHB, with the excess sludge. A sole parameter needs to be kept at sub-optimal levels to provide necessary stress conditions. To this purpose, parameters such as overall salinity and effect of various ions on the production of PHB as well as operational parameters such as pH, temperature, illumination intensity and frequency leading to highest H_2 and PHB production are worth investigating.

The scope of this thesis is to investigate the production of hydrogen and PHB using *Rhodobacter capsulatus* under different stress conditions. For this purpose, different carbon sources in the form of acetic acid and sucrose, and different operational parameters were investigated to observe the PHB and hydrogen production. Objectives of the study are;

- to operate bioreactors in order to determine the optimum biomass pretreatment method leading to the maximum PHB recovery from the microbial cells during various steps of PHB analysis method.
- to investigate the effect of sodium accumulation on PHB accumulation
    - in pH-controlled reactors
    - under two different carbon sources thus to observe the effect of substrate type on PHB and H_2 production
- to investigate the effect of pH on H_2 and PHB production.

All the objectives were based on the results of the previous sets operated for determination of optimal operational parameters and results comparison purposes. Hence, this thesis study focuses on the specific microbial strain utilized, *R. capsulatus* (Wild Type) and *R. capsulatus* (YO3) and their hydrogen and PHB production capabilities under different operational conditions with each condition leading to a different source of stress.

CHAPTER 2

LITERATURE REVIEW

This chapter aims to cover the literature survey done prior and during the experimentation stage of the study, primarily to obtain knowledge on the experimental methods, protocols and interpretation of data as well as to compare the outcomes of this study with similar studies that were conducted. The chapter also aims to identify the potential study areas that were not investigated previously and to clarify some of the unexplored areas present especially in biological systems.

2.1 Hydrogen

Lightest and most abundant element in universe, hydrogen is an element with a single proton and an electron. It is a very significant element especially in the field of life sciences, with oxidized hydrogen being the most crucial compound of life, water.

Hydrogen has an integral role in acid-base reactions, most significant element in organic chemistry after carbon and is an intermediate compound in many intracellular reactions and also most energy containing molecule in terms of heat released during combustion per unit mass basis (McCay & Shafiee, 2020). Cation of hydrogen (H^+), often termed simply as a proton, is the primary energy carrier in most biological pathways. In respiratory pathways, hydrogen donates its electrons to the electron transport chain via nicotinamide adenine dinucleotide hydride (NADH) to produce abundant energy in the form of adenosine triphosphate (ATP). Remainder H^+ cations are oxidized by molecular oxygen to form H_2O (Hambourger *et al.*, 2008). In fermentative pathways, substrate is mostly oxidized via various dehydrogenase enzymes, such as alcohol dehydrogenase (in ethanol fermentation), lactate dehydrogenase (in lactic acid fermentation) and especially iron containing

hydrogenases, releasing electrons usually via a reversible process as seen below in Equation 2.1 (Dutta *et al.*, 2018).

$$H_2 \rightleftharpoons 2\,H^+ + 2\,e^- \quad (2.1)$$

Both forward and reverse processes are catalyzed by hydrogenase; oxidation process in Equation 2.1 is achieved via uptake hydrogenase (*hup*), whereas reverse proton reduction process requires a variety of proteins such as ferredoxins (FNR) or cytochromes (*cyt*) to donate electrons (Stams & Plugge, 2009). Perhaps the most fundamental and crucial role of hydrogenase in context of this study lies in its simple reason of existence: to catalyze hydrogen production, effectively reducing the reaction's activation energy. Nonetheless, the extent of catalytic activity of hydrogenase has been proven greater than the previous best catalyst candidate, platinum (Merki & Hu, 2011). Although isolation of this enzyme is economically non-feasible as is the case with most enzymes, hydrogen production may potentially be viable with established biological systems, catalyzed by hydrogenases (H. S. Lee *et al.*, 2010). This phenomenon is usually what defines biological hydrogen production and elaborated later in this chapter.

2.1.1 Hydrogen Energy

Hydrogen may be produced from non-renewable and renewable sources alike. Broadly, hydrogen as a product is referred to as brown, grey, blue or green hydrogen with respect to the method, or the source that was utilized during the production phase, although all the terms further categorized within themselves (Tetteh & Salehi, 2023). While the most prevalent brown, grey and blue hydrogen production methods utilize fossil fuels as the primary input for hydrogen production, green hydrogen refers to utilization of renewable energy sources and currently holds the most sustainable, yet costly method for hydrogen production (Atilhan *et al.*, 2021). Carbon emissions of the said hydrogen production methods decrease in the given order, that is, highest carbon is emitted via brown hydrogen production processes and lowest,

theoretically zero carbon emissions are achieved via green hydrogen production (Yu *et al.*, 2021).

Brown hydrogen is produced from coal gasification, although in an indirect manner. Primary aim of coal gasification is to produce syngas to be used in various industrial processes, and hydrogen is both a major constituent of syngas and a byproduct of syngas production (Hong *et al.*, 2012). Grey hydrogen refers to the hydrogen produced from fossil fuels in general, typically via steam reforming method in which methane is subjected to heating in the presence of water vapor, resulting in a release of hydrogen and carbon dioxide, with carbon monoxide formed in intermediate steps. Source of methane in grey hydrogen production is typically natural gas or other fossil fuels (Ingale *et al.*, 2022). Brown and grey hydrogen terms are commonly used interchangeably by today, due to gradual emergence of green hydrogen, blurring the line between "high" carbon emissions and "slightly less than high" carbon emissions. If the brown or grey hydrogen production methods are modified to include a carbon capture and storage unit, effectively decreasing carbon emissions while still utilizing non-renewable sources as the primary fuel for hydrogen production, the product is then referred to as blue hydrogen (Howarth & Jacobson, 2021).

Green hydrogen is produced from renewable sources and theoretically has a potential for zero carbon emission. It can be further divided into biological and non-biological production of hydrogen. Prevalent green hydrogen production method currently regarded as electrolysis of water; however, the emissions of this process strongly depend on the power source that is used to produce hydrogen (Dincer, 2012). In most of the cases, energy input required to initiate the electrolysis of water is met from the electricity grid. If the grid is supplied with electricity via coal power plants, green hydrogen becomes not too different from brown hydrogen in terms of carbon emissions, although a complete life cycle assessment of the production would clarify the emissions better. Figure 2.1 below summarizes the hydrogen production methods while also including the less common yellow, pink, turquoise and other methods of hydrogen production.

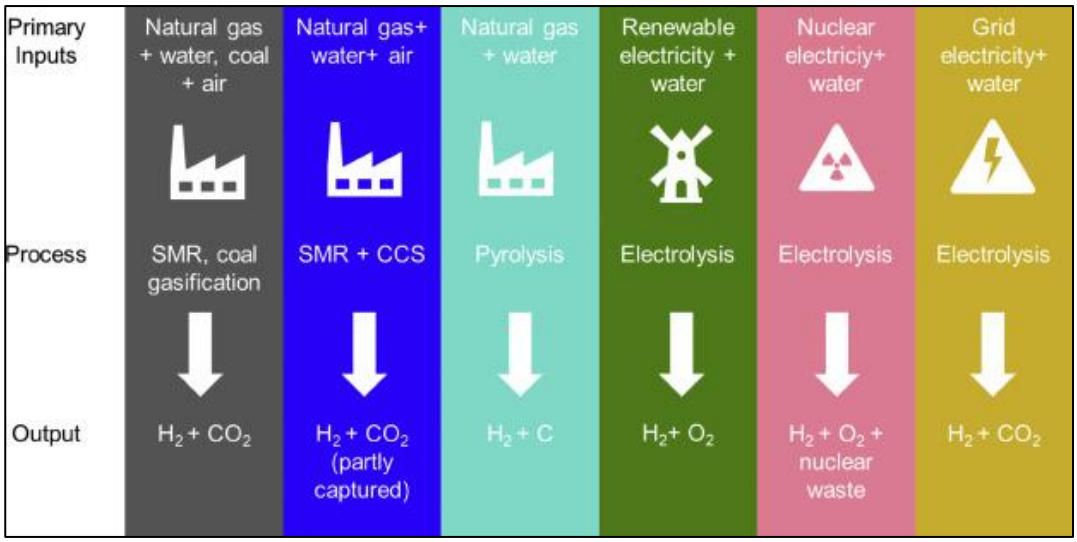

Figure 2.1. Various methods for hydrogen production (Ajanovic *et al.*, 2022).

Green hydrogen also includes the biological methods for the production of hydrogen as well, utilizing the waste-to-energy and circular economy concept, which is the main focus of this study. Biological hydrogen production methods consist of, (i) Fermentative hydrogen production, which is further divided as dark fermentation and photofermentation, (ii) Biophotolysis, direct and indirect, and (iii) Utilization of microbial electrolysis cells. See Figure 2.2 below for a summary of biological hydrogen production methods and responsible species.

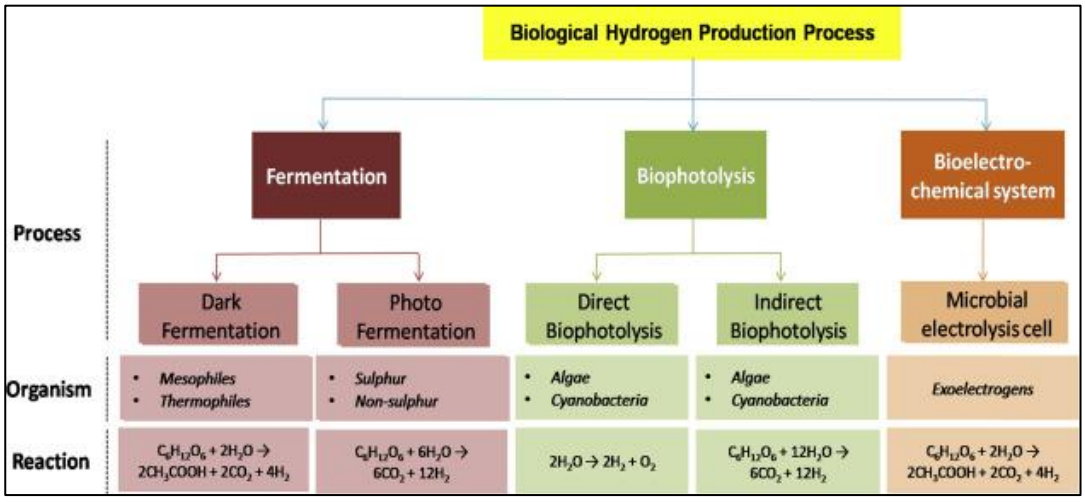

Figure 2.2. Biological hydrogen production methods (Lamb & Lien, 2020)

2.1.2 Non – Biological Hydrogen Production

As mentioned previously, non-biological hydrogen production includes hydrogen produced as a result of chemical interactions between various inputs without any biological catalyst. These methods include hydrogen production from fossil fuels or splitting of water. It is important to note that some of the non-biological hydrogen productions are considered environmentally sustainable, with little to no CO_2 emitted to atmosphere, mostly owing to carbon capture and storage (CCS) systems (Ishaq *et al.*, 2022). In context of this study, most widely practiced non-biological hydrogen production methods are briefly summarized below.

2.1.2.1 Coal Gasification

Coal gasification is the first hydrogen technology to emerge, with the initial intention being the production of syngas, which is a mixture of primarily carbon monoxide and hydrogen along with smaller parts of carbon dioxide and methane. Syngas was used as an energy carrier before the advent of natural gas which is primarily methane. In this process, coal is heated in the presence of water vapor and limited oxygen while not allowing complete combustion, producing a combustible end product with respect to Equation 2.2 below (Seyitoglu *et al.*, 2017).

$$3C + O_2 + H_2O \xrightarrow{\text{Heat}} H_2 + 3CO \tag{2.2}$$

To further produce hydrogen, product of the reaction above supplied with more water vapor, resulting in end products with respect to Equation 2.3, water-gas shift reaction (WGSR) below (Seyitoglu *et al.*, 2017).

$$CO + H_2O \rightleftharpoons H_2 + CO_2 \tag{2.3}$$

With primary outputs being hydrogen and carbon dioxide, coal gasification also results in the production of coke, tar, sulfur and ammonia, all of which can be further processed to be purified and result in various coal derived products as in crude oil refining. For relatively easy operation, presence of abundant side products and

utilizing cheap coal as feedstock, coal gasification is one of the most utilized methods for hydrogen production to this day, however even with utilization of carbon capture systems this process is not considered as a sustainable method of hydrogen production due to feedstock being coal, which is a finite resource (Kayfeci *et al.*, 2019).

2.1.2.2 Steam Reforming

Steam reforming is a similar process to coal gasification, with outputs being syngas again. Inputs of the steam reforming reaction is water vapor and hydrocarbons, most commonly methane. When methane is used as the feedstock, process is defined as steam methane reforming (SMR). In this process, methane is reacted with water with respect to Equation 2.4 below (Kayfeci *et al.*, 2019).

$$CH_4 + H_2O \rightleftharpoons 3H_2 + CO\,, \Delta H = 206\ \mathrm{kJ/mol} \qquad (2.4)$$

As in coal gasification, produced CO in SMR can also be further converted to CO_2 with WGSR (Section 2.1.2.1, Equation 2.3). Due to relatively lower carbon emissions to the atmosphere during hydrogen and feedstock production as well as the lack of by-products contrary to coal gasification, SMR is the most widely used method for hydrogen production around the world (Chen *et al.*, 2020) (Figure 2.3).

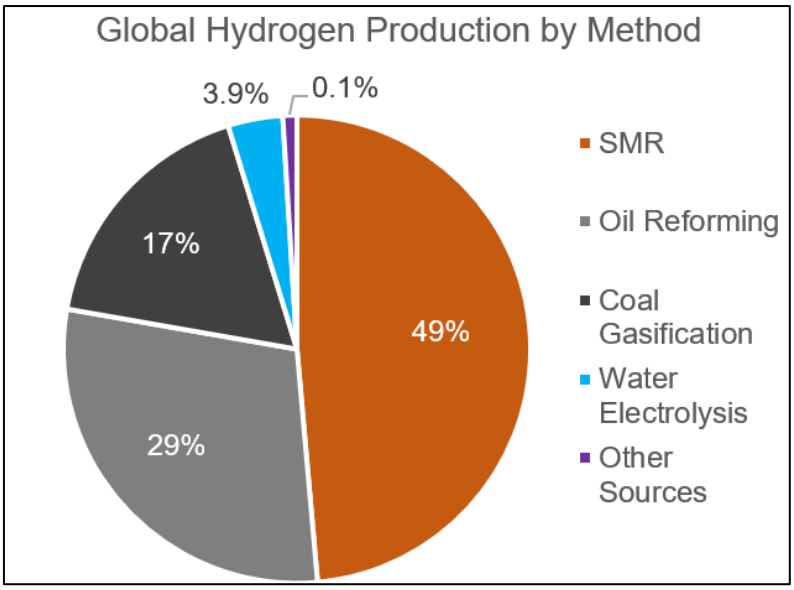

Figure 2.3. Global share of different hydrogen production methods (Dincer & Acar, 2014).

Although extensively used, SMR also has the same drawbacks as in coal gasification, that is being dependent on a non-renewable finite resource methane.

2.1.2.3 Pyrolysis

Pyrolysis is broadly defined as the decomposition of various compounds with extreme thermal energy, without allowing combustion. In other words, pyrolysis occurs in the absence of O_2 as in the case of gasification and steam reforming. Product is highly dependent on the type of feedstock, with the prevalent feedstock specifically for hydrogen production being wet biomass and methane. Pyrolysis of methane is proven to be feasible although being a relatively new technology. Primary advantage of methane pyrolysis over other non-biological hydrogen production methods is that process is relatively easy and can be operated connected to standard purity national gas grid. At high temperatures, hydrogen separates from carbon in methane easily, producing high purity hydrogen gas and solid carbon as end products. Due to producing solid carbon, CO_2 emissions to the atmosphere is

minimal and produced carbon has high commercial value due to having very high purity (Schneider *et al.*, 2020).

For its numerous advantages and utilization increasing rapidly, methane pyrolysis is also termed as turquoise hydrogen production (See Section 2.1.1).

2.1.2.4 Electrolysis

Electrolysis, or more specifically hydrogen production via water-splitting is the breakdown of H_2O molecules into molecular oxygen and hydrogen via application of an electrical current. Due to electricity and water being the primary inputs, electrolytic production of hydrogen theoretically has a potential of zero carbon emissions and therefore is also termed as green hydrogen production (Ursúa *et al.*, 2012).

The process is on the rise and conversion efficiencies are on par with SMR processes, but expected to surpass the thermal efficiency of SMR systems in the near future. Nonetheless, one critical input of electrolytic hydrogen production is the source of the electrical current applied, which varies drastically with respect to the geopolitical area where it is produced. In other words, cutting edge electrolytical hydrogen production should not be considered sustainable when the provided electrical current is produced overwhelmingly via fossil fuels (Lagioia *et al.*, 2022). This phenomenon results in spending energy to produce an energy carrier, effectively including the conversion losses of water splitting to the thermal losses due the production of electrical current. Therefore, most of the electrolytic hydrogen production processes (as well as other non-biological hydrogen production methods) around the world aim to produce hydrogen as a feedstock for industry rather than an actual energy carrier.

This issue is being addressed via utilization of energy as the input produced primarily from renewable sources, with leading alternatives as wind and solar energy. However, this method also does not contribute to green energy production via hydrogen, rather only transfers the energy from sun and wind to electricity and in

turn to hydrogen. Even when renewable sources are used, energy is already converted to electricity and ready to be used. Electrolysis process spends this already produced energy to be used as a feedstock, not utilize it in power generators.

As a summary of electrolysis and also the other mentioned non-biological hydrogen production methods, overall trend can be observed to produce hydrogen to be used as inputs in various industries rather than to produce energy. This is due to the fundamental logic behind non-biological hydrogen production methods: transferring the energy present in various fuels (coal, methane, oil, sunlight, wind) to hydrogen by spending energy, effectively accumulating the losses in those processes, eliminating the net energy gain from hydrogen.

2.1.3 Biological Hydrogen Production

Hydrogen has a critical role in cellular metabolism, and has a key role various reduction-oxidation reactions taking place in cells of the organisms of interest. Broadly, hydrogen is bound to respiratory complexes NAD^+ and FAD to form NADH and $FADH_2$ to later donate hydrogens (or protons) in the electron transport chain of the cell, accounting for the bulk of energy produced via cellular respiration. Donated by the substrate, hydrogen ions form a concentration gradient in electron transport chain, where the concentration gradient later converted to ATP via enzyme ATP synthase to be stored as energy (Vignais *et al.*, 2004).

Key enzymes involved in biological production of hydrogen can be named as nitrogenase and hydrogenase. The former is responsible from the conversion of hydrogen ions and electrons to molecular hydrogen, however with high energy requirements, seen in Equation 2.5 below (Koku *et al.*, 2002). This enzyme is activated in the presence of light, however is also deactivated in excess light, causing photoinhibition (Uyar *et al.*, 2007). Another important parameter affecting the activity of nitrogenase is the concentration of nitrogen in the media. With increasing concentrations of nitrogen containing compounds (such as ammonia or nitrite/nitrate

salts) in the media, activity of nitrogenase is dominated with N_2 fixation rather than H_2 production (Sasikala *et al.*, 1990). This leads to limited N concentration requirement for biological hydrogen production.

$$2H^+ + 2e^- + 4ATP \rightarrow H_2 + 4ADP + 4P_i \quad (2.5)$$

Hydrogenase operates reversibly with respect to Equation 2.6 below. Consumption of H_2 is achieved by uptake hydrogenase, whereas production by hydrogenase usually requires other electron donators as mentioned before (Section 2.1). Therefore, many factors inhibiting the activity of hydrogenase (Koku *et al.*, 2002) as well as mutant strains that lack the enzyme altogether are being researched (Kars *et al.*, 2008; Öztürk *et al.*, 2006; Sato *et al.*, 2017).

$$H_2 \rightleftharpoons 2\,H^+ + 2\,e^- \quad (2.6)$$

2.1.3.1 Biophotolysis

Bio-photolysis is one of the green hydrogen production methods. This process can either be carried out directly or indirectly. Microorganisms that are capable of biophotolysis primarily include phylum of cyanobacteria (or more commonly known as blue-green algae). In direct bio-photolysis, cyanobacteria use solar energy to transform water into oxygen and hydrogen (Martino *et al.*, 2021). *Chlamydomonas reinhardtii* is the most commonly used species of microalga in this procedure (Agyekum *et al.*, 2022).

In direct biophotolysis, microbial strain splits water into hydrogen and oxygen by converting solar energy to chemical energy. Cyanobacteria split water into hydrogen and oxygen ions during direct biophotolysis. The generated hydrogen ions are subsequently converted into H_2 by the enzyme hydrogenase. As with every reaction involving hydrogenase, oxygen level should be kept below 0.1% since this enzyme is oxygen sensitive. Reaction of direct photolysis is given below in Equation 2.7 (Nikolaidis and Poullikkas, 2017).

$$2H_2O \xrightarrow{\text{Light}} 2H_2 + O_2 \quad (2.7)$$

In indirect biophotolysis H_2 is produced in two steps in the presence of CO_2 and H_2O. During the first step, glucose is produced photosynthetically (Equation 2.8) and followed by a second step (Equation 2.9) that involves separation of H_2 from glucose. Both steps occur in the presence of light and under anaerobic conditions (Azwar *et al.*, 2014).

$$6H_2O + 6CO_2 \xrightarrow{\text{Light}} C_6H_{12}O_6 + 6O_2 \quad (2.8)$$

$$C_6H_{12}O_6 + 6H_2O \xrightarrow{\text{Light}} 12H_2 + 6CO_2 \quad (2.9)$$

2.1.3.2 Microbial Electrolysis Cells

Basis of microbial electrolysis cells (MEC) is formed with the use of exoelectrogenic microorganisms, which produce electrons and cations (H^+ ions) upon degradation of provided substrate. Substrate-inoculum relationship is strict in MEC process, with specific strains needed for specific substrates. Various substrates, such as acetate, lactate, glucose or cellulose may be used in MEC studies (Koul *et al.*, 2022).

In MEC, external voltage is applied to the system which results in the formation of an anode and a cathode in the solution containing the media and microorganisms. Microorganisms grown on the anode, where organic matter is degraded to result in carbon dioxide, protons and electrons, with respect to general Equation 2.10 in the anode. Protons are combined with electrons with respect to Equation 2.11 in the cathode of the reactor (Lamb & Lien, 2020).

$$\text{Organic Matter} \rightarrow CO_2 + H^+ + e^- \quad (2.10)$$

$$2H^+ + 2e^- \rightarrow H_2 \quad (2.11)$$

MECs are most commonly operated in two different types of reactors, as double or single chamber reactors, depending on the configuration of anode and cathode in the reactor. If the anode and the cathode are separated by a membrane which only permeates the passage of the H^+ ions, configuration is termed as double chamber.

Using a double chamber MEC is advantageous due to the fact that the membrane clearly separates the biomass from reaching the cathode while also preventing short-circuiting between anode and cathode. The need for maintenance of the membrane and high membrane prices are the disadvantages of the double chamber reactors. Single chamber reactors eliminate the need for using a membrane, thus the effort and costs associated with it. However, produced hydrogen in the cathode might be subjected to reuse by the electrochemically active cells, decreasing the net H_2 gain (Kadier *et al.*, 2016).

H_2 yield of MECs are significantly higher than that of dark fermentation, with up to 90 % of hydrogen in acetate converted to H_2 demonstrated. Significant disadvantages of MEC systems can be stated as the complexity of the reactor, interference of various microbial species with each other, competing for substrate and the need for further treatment of the effluent to comply with discharge standards, and significant difference of theoretical values to the observed data (Rousseau *et al.*, 2020).

2.1.3.3 Dark Fermentation

Dark fermentation is the degradation of organic molecules in the absence of light, utilizing an organic carbon as the final electron acceptor instead of molecular oxygen that is used in aerobic respiration. In dark fermentation, substrates that are rich in carbohydrates are preferred, i.e., glucose is the primary input of dark fermentation (Melis and Melnicki, 2006). There are two types of dark fermentation, classified with respect to their end products, acetic acid and butyric acid. Respective reactions are given below in Equation 2.12 and Equation 2.13 for acetate and butyrate fermentation (Roychowdhury *et al.*, 1988).

$$C_6H_{12}O_6 + 2H_2O \rightarrow 2CH_3COOH + 4H_2 + 2CO_2 \quad (2.12)$$

$$C_6H_{12}O_6 \rightarrow CH_3CH_2CH_2COOH + 2H_2 + 2CO_2 \quad (2.13)$$

Dark fermentation is widely researched topic with primary advantages being the utilization of wastewater. Employment of wastewater in dark fermentation has

proved to decrease costs, energy requirements and biodegradability issues associated with wastewater. Owing to applicability of wide variety of wastewater types such as, food and dairy industry effluent, cattle and chicken manure, wastewaters rich is cellulosic components such as paper mill effluent and yard wastes availability of substrate for dark fermentation is seldom an issue (Angenent *et al.*, 2004).

Major disadvantage of dark fermentation is the low efficiency associated with the process, with stoichiometrically 4 moles of hydrogen produced per mole of glucose during acetate fermentation. This value seldom reaches above 1-2 moleH_2/moleGlucose due to energy requirements of microbial cells and other losses during the operation of the reactors. As also seen from Equation 2.12 and Equation 2.13 above, most of the glucose change form to become other organic acids. i.e., dark fermentation process is not an efficient process for biodegradation of glucose rich wastewaters. There is a need for employing modifications to the process to degrade remainder organic acids. However, this is not strictly a disadvantage as produced organic acids still have commercial value and dark fermentation is a relatively simple process compared to other methods of biological H_2 production (Kapdan and Kargi, 2006).

2.1.3.4 Photofermentation

Photofermentation is the degradation of organic carbon in the presence of light and in anaerobic environments. It is mainly achieved by green sulfur bacteria, purple sulfur bacteria and purple non-sulfur bacteria. In this process, organic molecules are combined with energy from light to produce electrons and ATP, which are then catalyzed by nitrogenase enzyme to convert H^+ ions to H_2. Photofermentative H_2 production equations are given below for various different organic acids (Sakurai *et al.*, 2013).

$$CH_3COOH + 2H_2O \xrightarrow{\text{Light}} 4H_2 + 2CO_2 \quad (2.14)$$

$$CH_3CH_2COOH + 4H_2O \xrightarrow{\text{Light}} 7H_2 + 3CO_2 \quad (2.15)$$

$$CH_3CH_2CH_2COOH + 6H_2O \xrightarrow{\text{Light}} 10H_2 + 4CO_2 \quad (2.16)$$

Process is initiated via the energy obtained from the light, due to the positive value of standard Gibb's free energy of the equation, resulting in non-spontaneous reaction.

The advantage of photofermentation is the adaptability of the strains capable of photofermentation to various conditions with a wide optimum temperature range (15 – 45^{o}C), broad substrate requirement ranging from simple sugars and organic acids to complex wastewater constituents, relatively high substrate conversion efficiencies and simple reactor operation (Eroglu & Melis, 2011).

2.2 Poly-hydroxyalkanoates

PHAs are biological polymers serving as the carbon and energy storage compound of microbial species. It is accumulated in most of the bacterial species, although typically in lower concentrations and under certain conditions. However, there are both wild and recombinant species that accumulate PHA under every condition in excess amounts, up to 80% of dry cell mass (Chee *et al.*, 2010). Due to this rapid accumulation and similarity to conventional plastics, PHA is a viable candidate for substituting everyday plastics. The major challenge of substituting plastics with PHAs is in fact the economic problems associated with PHA production. In 2005, the cost of PHA production was reported as 7 $/kgPHA. When compared to the cost of 0.07 $/kgPlastics for conventional crude oil-based plastics, PHA production currently is not feasible. Most of the cost arises from the recovery processes employed for extraction of PHAs from microbial cells (Choi and Lee, 1997; Jung *et al.* 2020).

PHAs are biopolymers synthesized by a wide range of microorganisms. The role of PHA in microbial cells is to serve as carbon and energy storage compound, similar to glycogen and cellulose in animals and plants (Lee, 1996). PHAs are classified as short chain length (scl) PHAs and medium chain length (mcl) PHAs. scl-PHAs

include the compounds of which the amount of carbon atoms in the monomer is 3 to 5, whereas mcl-PHAs include the compounds with 6 to 14 carbon atoms in the monomer. PHA monomer is the R-hydroxyalkanoic acid (Anderson and Dawes, 1990). See Figure 2.4 for the general structure of PHAs.

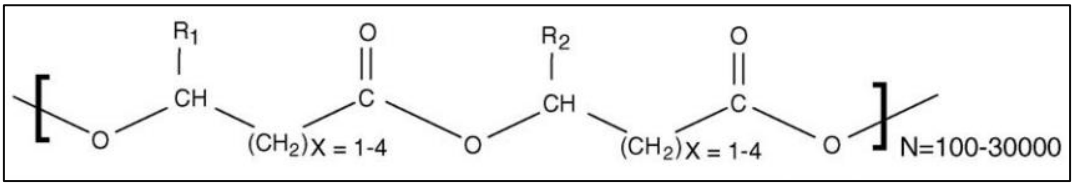

Figure 2.4. General structure of PHAs (Keshavarz and Roy, 2010).

The radical group of the monomer is affected by many factors, mainly by parent microorganism, medium, substrate and environmental conditions. Most common PHA is poly(-3-hydroxybutyrate) (P3HB), or poly-β-hydroxybutyrate (PHB) and it has been the only PHA to be produced for commercial use as of today. See Figure 2.5 for different kinds of PHAs.

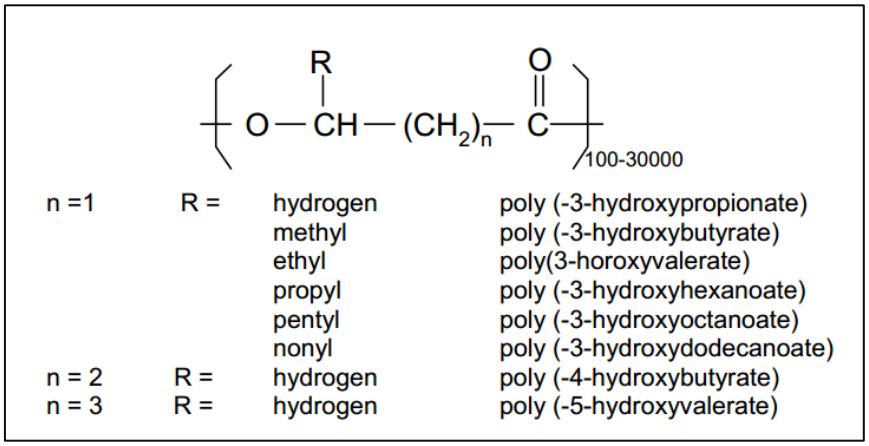

Figure 2.5. Different PHA types, varied by the monomer type and composition (Ojumu *et al.*, 2004).

2.2.1 PHB as a Viable Side Product

As mentioned previously, poly-hydroxybutyric acid (PHB) is the most common compound of the general group, poly-hydroxyalkanoates (PHA). Because of its

nature as a carbon storage compound, being accumulated in environments with abundant carbon and poor in terms of other nutrients (such as nitrogen and phosphorus) and depleted in the opposite carbon poor, N and P rich conditions, PHB is a durable yet a biodegradable material. It is a polymer that has remarkably similar properties to low-density poly ethylene (LDPE), and henceforth considered as a bioplastic (Marchessault *et al.*, 1990)

Usually, PHB is an emergency compound for the parent species, serving as an alternative substrate in the absence of an electron donor. It can be synthesized by both aerobic and anaerobic (facultative and obligate) cultures, however highest yields are observed when anaerobic processes are employed, since the main driving mechanism is to provide stress conditions for the employed culture (Steinbüchel and Füchtenbusch, 1998).

Most important aspects of PHB can be listed as biocompatibility, non-toxicity and durability with being solved easily with chlorinated compounds but extremely resistant to hydrolysis. In other words, in a sterile environment PHB can persist just as fossil-fuel derived common plastics but will degrade in the presence of microorganisms found in nature (Luengo *et al.*, 2003).

2.2.2 PHB Production

Production of PHBs can be divided into two steps. First, a microbial species capable of PHB synthesis is grown and PHB accumulation is achieved. Then, using certain methods, PHB is extracted from the biomass which is discussed in the following section (See Section 2.2.3).

PHB synthesis occurs during fermentation under stress conditions. For this reason, synthesis step is further divided into two more steps. In the first stage of the synthesis or fermentation, optimal growth conditions are supplied to the biomass and maximum possible biomass concentration is reached. In the second stage, stress conditions are applied mostly in the form of nutrient and oxygen (for facultative

aerobes) limitation. Nutrient limitation is typically achieved by reducing the amount of phosphorus or nitrogen in the media and providing excess carbon source. The maximum biomass concentration that was achieved in the first stage of the fermentation can then start to accumulate PHBs in the second stage of the fermentation (Tsuge, 2002).See Figure 2.6 for images of microorganisms accumulating PHB.

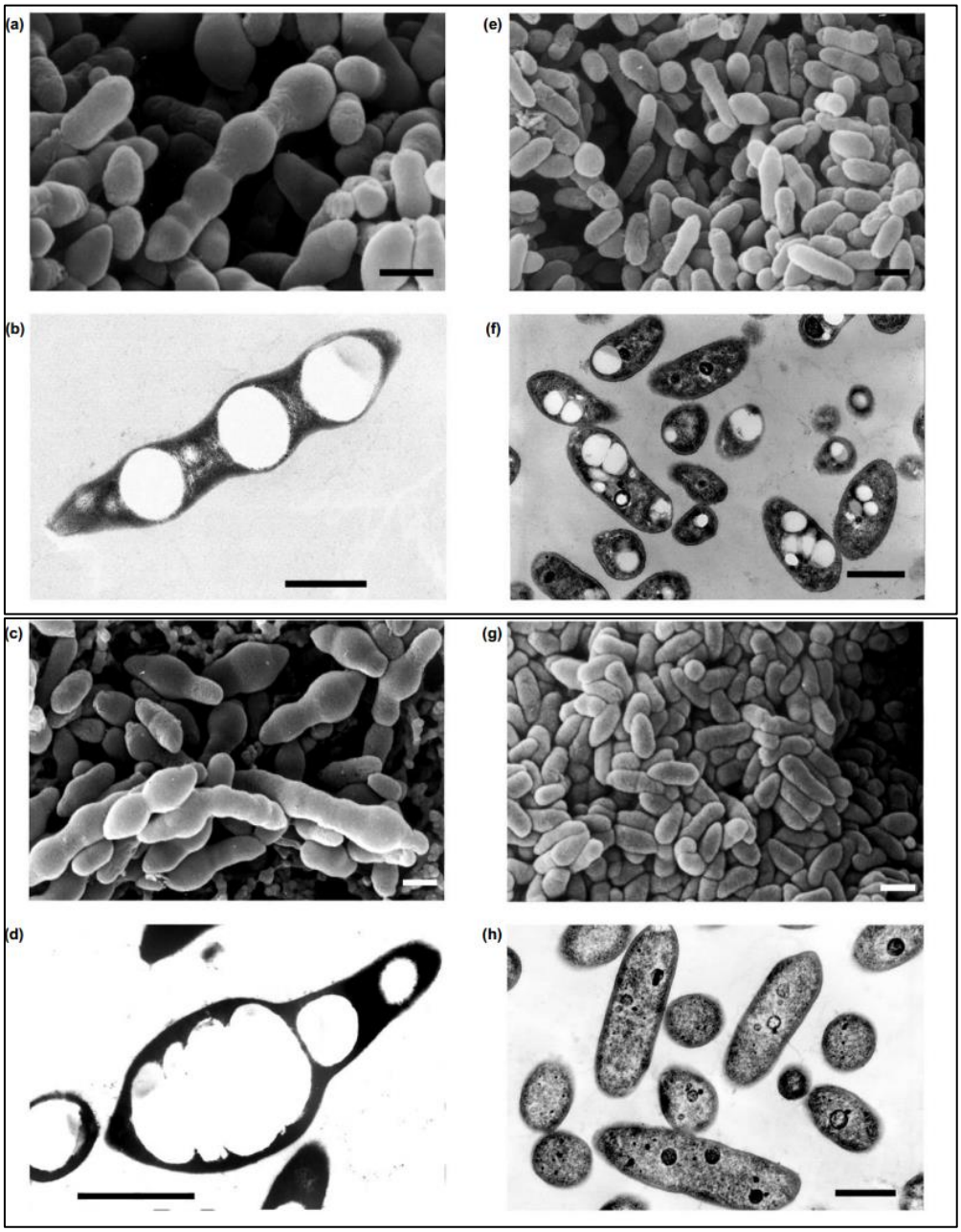

Figure 2.6. PHB granules accumulated by microorganisms (Luengo *et al.*, 2003).

2.2.2.1 PHB Producing Strains

PHB production efficiency highly depends on the parent microbial species, most importantly whether the candidate species require nutrient limitation or not. In the case of nutrient limitation, firstly biomass should be grown to maximum possible concentration and then, nutrients in the feed solution must be removed. Nitrogen, phosphorus or potassium is the most common nutrient limitation options (Merugu *et al.*, 2010).

Some microbial species may not require nutrient limitation in order to accumulate PHB. Most well-known species are (Keshavarz and Roy, 2010),

- *Azotobacter vinelandii*
- *Alcaligenes eutrophus*
- *Alcaligenes latus*

Genetically modified bacterial species generally harbor PHA synthesis genes of above species. Another significant species is the *Ralstonia eutropha*, due to having highest PHB yield. Recombinant bacteria are used (i) in order to utilize waste or by-products of certain industries instead of synthetic substrates, (ii) increase PHB production efficiency and (iii) to produce PHB without having to employ nutrient limited conditions (Higuchi-Takeuchi and Numata, 2019; Kim *et al.*, 1992; Koyama and Doi, 1995).

2.2.2.2 Substrate Types

Most common carbon source for PHB production are glucose and sucrose, due to relatively lower cost and is optimized. Glucose is fed as a concentrated solution of 700 g/L (Tsuge, 2002). Utilization of industrial or domestic wastes as the carbon source is not efficient for a wild type strain, as obtained PHB content is considerably

lower than that of purified carbon source. Recombinant microorganisms need to be considered for this kind of substrate. Lee *et al.* (1997) obtained PHB of 81% of cdw, using recombinant *E. coli* strain harboring *R. eutropha* PHA biosynthesis genes, with whey as the substrate. Lactose is a major component of whey and *E. coli* strains can utilize lactose for their growth. Substrate is supplied to the fermenter at maximum soluble lactose concentration, ≈210 g lactose/L (S. Y. Lee, 1996).

Kranz *et al.* (1997) used both wild-type and mutant *Rhodobacter capsulatus* strains for PHB production and identified that 2-12 carbon fatty acids are substrates for this species. While in general results were dependent on the specific type of strain, it was suggested that growth rates decreased with increased number of carbon atoms in the substrate. Tolerated substrate concentration also decreased with increasing number of carbon atoms (i.e., longer-chain fatty acids should be fed at lower concentrations). Highest PHA production was observed when acetone (42% cell dry weight, 100% PHB), caproate (90% cell dry weight, 100% PHB) and heptanoate (40% cell dry weight, PHB-PHV copolymer) were used as carbon source. As growth medium, RCV medium without malate and with 0.1%$NaHCO_3$ addition was used. Temperature was kept at 34^{o}C and 3000 lx illumination was supplied (Kranz *et al.*, 1997).

Merugu and Rao (2015) investigated the optimization of PHB production by *Rhodobacter capsulatus* KU002 and *Rhodopseudomonas palustris* KU003 species. It was found that *R. capsulatus* provided highest PHB yield on acetate, glucose and succinate and *R. palustris* provided highest PHB yield on glucose, succinate and acetate (Merugu and Rao, 2015).

As mentioned before, major challenge of substituting conventional plastics with PHAs is the costs associated with the PHA production. High production cost is due to the employed PHA recovery process and the fermentation media. In order to minimize the costs, cheaper medium alternatives are suggested as (Keshavarz and Roy, 2010);

- Molasses

- Corn steep liquor
- Whey
- Wheat and rice bran
- Starch
- Olive and palm oil mill effluent
- Activated sludge
- Swine waste

2.2.2.3 Limiting Substrate

Substrate limitation is applied to force the biomass to accumulate PHB. Merugu *et al.* (2010) investigated the effect of phosphate limitation on PHB synthesis on two microbial species, *Rhodobacter capsulatus* KU002 and *Rhodopseudomonas palustris* KU003. *R. palustris* accumulated slightly more PHB at lower phosphate concentrations, while PHB accumulation of *R. capsulatus* increased with increased phosphate concentration. Thus, it was concluded that phosphate limitation does not have an impact on R. capsulatus species (Merugu *et al.*, 2010).

Nitrogen limitation was observed by (Koutinas *et al.* (2007) using *Cupriavidus necator* species. It was observed that at various substrate concentrations (between 5-26 g glucose/L) PHB yield was decreased with increased free amino nitrogen.

Studies regarding the nitrogen concentration strongly suggest that limiting nitrogen is in fact the critical control parameter in PHB production, that is, after observing sufficient cell growth, nitrogen limitation should be applied to start the PHB accumulation. Some of the species that start accumulating PHB in the absence of nitrogen are *Alcaligenes eutrophus* (Koutinas *et al.*, 2007), *Methylobacterium* sp. (M. S. Kim *et al.*, 2006), *Sinorhizibum fredii* (Liangqi *et al.*, 2006) and *Rhodopseudomonas palustris* (Merugu *et al.*, 2010).

Effect of phosphate limitation on PHB production by *Ralstonia eutrophus* was also observed (Shang *et al.*, 2003).

2.2.2.4 Environmental Conditions

Other factors affecting the PHA synthesis include the fermentation temperature (30-37^{o}C, (Kim *et al.*, 1994)), reactor types (fed-batch or continuous fermentation,(B. S. Kim *et al.*, 1992; Koyama and Doi, 1995)) and lowest possible dissolved oxygen concentration (Chung *et al.*, 1997).

Reactor operation mode highly depends on the synthesizing microorganism. Kim *et al.* in his 1992 study proved that fed-batch operation mode was successful by achieving 88.8 g/L PHB concentration in 42 hours, using a Recombinant *E. coli* strain, of which the operon responsible from PHB synthesis having been cloned from *A. eutrophus* (B. S. Kim *et al.*, 1992). However, in a subsequent study in 1994, Kim *et al.* used *A. eutrophus*, which is a naturally PHB synthesizing microorganism, with the same reactor configuration to obtain 2.42 g/L of PHB within 50 hours (Kim *et al.*, 1994). Another study using fed-batch culture has been conducted by Rhee *et al.* in 1993 to produce a co-polymer of 3-hydroxybutyrate (3HB) and 3-hydroxyvalerate (3HV), using *Alcaligenes* sp. SH-69 as the microbial strain. In optimal conditions, 36 g/L of poly(3HB-co-3HV), containing 3.0 mol% 3HV was produced (Rhee *et al.*, 1993).

Continuous production of PHBs takes place in the nature, however it has been stated that continuous production is not on par with fed-batch cultures and PHB content fails to reach PHB content of fed-batch reactors (Madison and Huisman, 1999). Main reason could be that, since nutrient limitation should be applied, continuous cultures need to be periodically checked for their biomass growth rate, maximum biomass concentration and ammonium content and substrate feed should be arranged accordingly, i.e., when biomass reaches its maximum concentration, ammonium in the feed should be ceased. Studies using continuous culture was not able to reach more than 8.8 g/L of even co-polymer of 3HB and 3HV (Koyama and Doi, 1995).

PHB production rate is strongly affected by the temperature and is highly dependent on the synthesizing microorganism (Sirohi *et al.*, 2020). In general, optimal

temperature ranges are given as 25-35^{o}C (Monroy and Buitron, 2020). Keshavarz and Roy (2010) describe the optimal temperature range as 30-37^{o}C in the most general sense. Krishna and van Loosdrecht (1999) investigated PHB accumulation in activated sludge samples operated in sequencing batch reactor operation modes. Temperatures studied are in the range of 15-35^{o}C. It has been stated that all consumption rates except for PHB and NH_4^+ were increased with the temperature increase. In other words, PHB and NH_4^+ were accumulated more with the increased temperature while other inputs and intermediate products were consumed more rapidly.

The study by Johnson *et al.* (2010) investigated the effect of temperature on PHB production carried out by two stage fermentation, i.e., cell growth and PHB accumulation stages, referred to as feast and famine phases (nutrient-rich and nutrient-limited conditions). Both the short term (1 cycle) and long term (new steady state) effects of temperature are observed. For the short-term effects of the temperature on the famine phase, it has been determined that Arrhenius equation with one constant for every reaction can be used to predict the reaction rates accurately. On the feast phase, different temperature constants were identified for acetate uptake, PHB production and growth. As for the long-term effects of temperature, it has been observed that the feast phase longer in lower temperatures, due to the slower uptake of acetate. PHB yields were identified as 35wt% in 15^{o}C, 70wt% in 20^{o}C and 84wt% in 30^{o}C. It has also been stated that the temperature affects only the fermentation process and the temperature in which the experiments were conducted had no effect on the PHB yields (Johnson *et al.*, 2010).

2.2.3 PHB Recovery and Analysis

PHB is extracted from the cells using various processes and often is the most economically challenging step in large scale PHB production. As said before, PHB is produced by microorganisms commonly via fermentation under stress conditions.

After the fermentation period, biomass is separated from the slurry with one of the following methods (Lee, 1996).

- Centrifugation
- Filtration
- Flocculation-centrifugation

After the separation of biomass from the media, PHBs remain in granules within the microorganisms and need to be extracted. Various methods are developed to extract PHB granules from the cells with disadvantages and advantages for each method employed. Most common method employed in extraction of PHB using solvents in which first, the solvent modifies the membrane permeability and then, solvent solves the PHB. Separation of solvent from the mixture is then performed with solvent evaporation or precipitation in a non-solvent. The method is expensive unless solvent recycle is employed and is potentially hazardous for operators and environment (Gorenflo *et al.,* 2001). Despite being disadvantageous, the method is preferred in lab-scale studies due to its simplicity and high PHB recovery efficiency (Jacquel *et al.*, 2008). Digestion methods may be separated into chemical and enzymatic digestion, where all the material except for PHB is destroyed. Major drawback of chemically digestive extraction of PHB is that the method also severely degrades PHB, therefore complex precautions need to be taken. Enzymatic digestion does not have this issue due to the selective digestion of the material, and highest recovery efficiencies are achieved via enzymatic digestion (Kapritchkoff *et al.,* 2006). However, very expensive nature of enzymatic digestion makes this method non feasible. As of now, combination of chemical and enzymatic digestion is being researched to achieve relatively lower costs while also preventing the degradation of PHB (Sudesh and Iwata, 2008; Wang and Liu, 2013). Some other less common methods for PHB extraction involve the use of supercritical CO_2 instead of halogenated solvents, aiming to decrease the costs and hazards associated with the use of solvents at the cost of operational complexity and technical requirements (Hejazi *et al.,* 2003). Finally, cells that are over-accumulating PHB can simply burst

upon being subjected to very small amounts of stress. Centrifuged cells are treated in an ammonia solution for 10 minutes, where most of the cell debris can be separated from the solution easily. Unfortunately, the method requires the use of specialized strains which become fragile after accumulating very high amount of PHB (Page and Cornish, 1993).

Analysis of PHB is based on the method described by Braunegg (1978). Biomass pellets are taken into a chloroform solution. Acidified methanol is added to the biomass/chloroform mixture and then heated at 100^{o}C. During the heating, PHB is firstly hydrolyzed into its monomer, hydroxybutyrate (HB) and then added a methyl group (transesterification) to form hydroxybutyric acid methyl ester. Both hydrolysis and transesterification reactions may take place simultaneously. Resulting chloroform phase may be quantified using gas chromatography (GC) system (Braunegg *et al.*, 1978).

A drawback of the method is that the quantified PHB via GC will be in units of calibration, which is often in weight (mg PHB). Therefore, in order to express amount of accumulated PHB in units of % cell dry weight, weight of biomass in the sample must be predetermined. Some methods employ a drying step before mixing the biomass with chloroform (Montiel-Corona and Buitrón, 2022). However, response of microbial strains to different methods of drying is not known and must be determined before adoption of drying step. Drying could be in the form of heat-drying or freeze-drying. In the scope of this thesis study, both heat-drying and freeze-drying, as well as no-drying were investigated.

2.3 Purple Non – Sulfur Bacteria

Purple non-sulfur bacteria (PNSB) are a diverse group of photosynthetic bacteria in the phylum of proteobacteria. Closely related to purple bacteria, they are distinguished from purple bacteria by their extent of sulfur tolerance and whether oxidized sulfur is stored intracellularly or outside of the cells. The former storage

defines purple storage whereas the latter is a characteristic of purple non-sulfur bacteria. Especially in the field of microbial photosynthesis, *Rhodobacter capsulatus* and *Rhodobacter sphaeroides* belonging to the Rhodobacteraceae family and *Rhodopseudomonas palustris* belonging to Nitrobacteraceae family prevail as model species (Durand *et al.*, 2018).

PNSB are best performing candidates for photofermentative hydrogen production due to a number of reasons. PNSB are capable of utilizing a wide variety of substrates ranging from simple organic acids and sugars to wastewater with complex constituents, achieving high substrate conversion efficiencies (i.e., percent of substrate that was metabolized to form H_2) (Petushkova and Tsygankov, 2017). PNSB are facultative anaerobes, meaning that the strain can survive in the presence of oxygen, although hydrogen production is limited in this case. A number of diverse metabolic pathways exist among PNSB which include chemoautotrophy, photoautotrophy and photoheterotrophy. Pathway depends on the type of carbon source present in the medium of the microorganism, as well as presence or absence of light and oxygen. In other words, PNSB are a versatile group of bacteria that can thrive in wide variety of conditions (Imhoff *et al.*, 1984). Owing to this, relatively high number of genetic modification studies are performed to further enhance the hydrogen production capabilities of notable species such as *Rhodopseudomas palustris*, *Rhodobacter capsulatus*, *Rhodobacter sphaeroides* and *Rhodospirillum rubrum* (Lang *et al.*, 2012).

In the scope of this thesis, absence of oxygen, organic carbon and ample light is provided to the PNSB to achieve photofermentative conditions, although the growth phase of the microorganisms also includes chemoautotrophic conditions.

2.3.1 *Rhodobacter capsulatus* Wild Type (DSM1710)

R. capsulatus is a gram-negative PNSB. Depending on the environmental conditions, colonies may be formed as either rods or motile coccobacilli. The bacterium

develops chains and is spherical at pH values lower than 7 while above the pH values of 7, rod shape is observed. The length of rod morphology is also influenced by pH with the length of cells increasing with pH of the medium. They frequently form chains that are bent in character due to their rod shape. Another important aspect of the species is the filamentous growth occurring at high pH values and production of an extracellular polymeric substance as a defense mechanism. *R. capsulatus* has a distinct reddish-brown color that changes with the presence of oxygen in the media. In the presence of molecular oxygen, aerobic respiration occurs, resulting in rapid growth of microorganism, and is preferred to cultivate the microorganism. In these conditions, *R. capsulatus* has a bright red color. In the absence of O_2 and presence of light, photofermentation takes place and a brownish faded red coloration is generally observed, accompanied by high hydrogen production rates (van Niel, 1944).

R. capsulatus is known to accumulate PHB in abundant carbon and limited nitrogen conditions. Accumulation of PHB in nitrogen limited conditions is also advantageous for hydrogen production as well, since nitrogenase activity should shift towards H_2 production in limited nitrogen conditions. Therefore, limiting nitrogen both enhanced H_2 and PHB accumulation in *R. capsulatus* species, resulting in a favorable co-production condition for both of the compounds.

2.3.2 *Rhodobacter capsulatus* YO3 Mutant

As mentioned before (Section 2.1.3), key enzymes involved in biological H_2 production, or specifically photofermentative H_2 production are nitrogenase and hydrogenase. Nitrogenase is responsible enzyme for the production of N_2 from nitrogen-containing compounds (e.g., ammonia, glutamate, proteins, etc.). In the absence of nitrogen, enzyme shifts towards the production of H_2 and is antagonized by hydrogenase. In other words, biological hydrogen production is achieved primarily by nitrogenase and suppressed by hydrogenase (Sakurai *et al.,* 2013). Hydrogenase may operate reversibly as well, to produce a fraction of H_2 instead of

consuming H_2, however conditions should favor the reverse reaction (Oh *et al.*, 2011). Studies have been performed to reduce the activity of hydrogenase and increase the net H_2 gain (Golomysova *et al.*, 2010). These studies include limiting the concentration of Ni that is a part of the enzyme complex so that the enzyme could not be synthesized, continuously removing the produced hydrogen from the media before being utilized by the strain as well as genetic modifications preventing the synthesis of the enzyme itself.

R. capsulatus YO3 in this study was cultured by Öztürk *et al.* (2006) and lacks the gene responsible from the synthesis of uptake hydrogenase enzyme (hup^-). The strain was originally intended to be utilized in hydrogen production studies, however constructed carbon balances in the recent studies indicate that a previously unidentified carbon sink exists in the strains, which is speculated to be PHB.

2.4 Photofermentative PHB and Hydrogen Production

Studies regarding the PHB production via photofermentative production of PHB are limited in the literature, and are mainly achieved with PNSB. Table 2.1 below summarizes the observed PHB accumulation in some of the studies conducted using different strains, different carbon sources and concentrations.

Table 2.1. PHB accumulation observed in the literature.

Microbial Strain	***C Source and Concentration (mM)***	***Observed PHB (% of cdw)***	***Reference***
R. capsulatus DSM1710	65 mM Acetate	20.0	(Özsoy *et al.*, 2019)
R. sphaeroides KD131	40 mM Acetate	51.0	(Kim *et al.*, 2012)
R. sphaeroides KD131	60 mM Acetate	54.1	(Kim *et al.*, 2012)
R. palustris WP3-5	20 mM Acetate	10.2	(Wu *et al.*, 2012)
R. palustris WP3-5	20 mM Propionate	4.2	(Wu *et al.*, 2012)
R. sphaeroides OU001	Wastewater [1]	70.4	(Yiğit *et al.*, 1999)
R. sphaeroides WT	10 mM Acetate	38.0	(Hustede *et al.*, 1993)
R. sphaeroides WT	30 mM Acetate	70.0	(Hustede *et al.*, 1993)
R. sphaeroides WT	30 mM Glucose	31.0	(Hustede *et al.*, 1993)
R. sphaeroides WT	30 mM Fructose	27.0	(Hustede *et al.*, 1993)
R. sphaeroides WT	30 mM Succinate	4.0	(Hustede *et al.*, 1993)
R. rubrum	30 mM Acetate	53.0	(Hustede *et al.*, 1993)
R. sphaeroides	122 mM Acetate	50.8	(Brandl *et al.*, 1991)
R. sphaeroides	7.5 mM Malate	1.6	(Brandl *et al.*, 1991)
R. sphaeroides	82 mM Malate	6.4	(Brandl *et al.*, 1991)
R. sphaeroides	120 mM Crotonate	47.5	(Brandl *et al.*, 1991)

[1] Sugar industry effluent was mixed into malate containing media with 30 % (v/v) ratio.

Especially studies regarding the use of *R. capsulatus* in terms of PHB accumulation were observed to be minimal, with investigation of PHB production by *R. capsulatus* YO3 mutant almost nonexistent. Within the scope of this thesis, it was determined to investigate the capability of *R. capsulatus* in terms of PHB and hydrogen production. Some of the H_2 productivity values achieved in the literature specifically via *R. capsulatus* is also given below in Table 2.2.

Table 2.2. Observed H_2 productivities by R. capsulatus in the literature

Microbial Strain	***C Source and Concentration (mM)***	***Observed H_2 Productivity (mmol/L·h)***	***Reference***
R. capsulatus YO3	Molasses	0.69	(Oflaz and Koku, 2021)
R. capsulatus DSM1710	10 mM Acetate	0.44	(Özsoy *et al.*, 2019)
R. capsulatus DSM1710	25 mM Acetate	0.50	(Özsoy *et al.*, 2019)
R. capsulatus DSM1710	50 mM Acetate	0.44	(Özsoy *et al.*, 2019)
R. capsulatus DSM1710	65 mM Acetate	0.35	(Özsoy *et al.*, 2019)
R. capsulatus YO3	Sucrose	0.72	(Sagir *et al.*, 2017)
R. capsulatus YO3	Sucrose	2.04	(Elkahlout *et al.*, 2017)
R. capsulatus DSM1710	Acetate	0.75	(Elkahlout *et al.*, 2017)
R. capsulatus YO3	DFE[1] of thick juice	1.05	(Uyar *et al.*, 2015)
R. capsulatus DSM1710	DFE of thick juice	1.01	(Uyar *et al.*, 2015)
R. capsulatus YO3	Acetate	0.37	(Boran *et al.*, 2012)
R. capsulatus YO3	DFE of thick juice	1.36	(Özkan *et al.*, 2012)
R. capsulatus YO3	Acetate	0.51	(Androga *et al.*, 2011)
R. capsulatus YO3	DFE of molasses	0.67	(Avcioglu *et al.*, 2011)
R. capsulatus DSM1710	DFE of molasses	0.55	(Avcioglu *et al.*, 2011)
R. capsulatus DSM1710	Acetate	0.31	(Boran *et al.*, 2010)
R. capsulatus DSM155	Acetate & Lactate	0.74	(Gebicki *et al.*, 2010)
R. capsulatus YO3	Acetate & Lactate	0.32	(Özgür *et al.*, 2010)
R. capsulatus DSM1710	Acetate & Lactate	0.14	(Özgür *et al.*, 2010)

[1] DFE: Dark fermentation effluent.

CHAPTER 3

MATERIALS AND METHODS

This chapter aims to cover the information regarding the utilized microbial strains, analytical methods, experimental procedures and setup information for each conducted set, namely Set 1, Set 2 and Set 3.

3.1 Microbial Strains

Wild-type strain of *Rhodobacter capsulatus* (*R. capsulatus* WT (DSM1710)) was obtained from DSMZ German Collection of Microorganisms and Cell Cultures GmbH.

Mutant strain of *Rhodobacter capsulatus* (*R. capsulatus* YO3) was cultured by Dr. Yavuz Öztürk, Ph.D., by deleting the gene responsible from the synthesis of the enzyme uptake hydrogenase (hup^-), which is the enzyme responsible from the recycle of H_2 outside of the cell to be used as an alternative electron donor (Öztürk *et al.*, 2006).

All the cultures used in the experiments were freeze dried and stored in 30% (v/v) glycerol in -80^oC before being activated. Fully grown cultures that had not been used in experiments were used to maintain the stock cultures by inoculating fully grown cultures to 50 mL growth medium with 10% inoculation ratio. This was done on a regular basis to keep microbial cultures fresh and active. Maintained cultures were occasionally inoculated to MPYE plates with the intention of detecting any unusual colonies or contamination. Unused and older cultures were autoclaved at 120^oC for 20 minutes before being disposed of.

3.2 Media

Media used in the experiments include solid medium, growth medium, H_2 and PHB production medium as well as feed, depending on the purpose. All media were prepared using concentrated stock solutions to minimize contamination of chemical stocks and errors. Types of the media and their respective carbon and nitrogen sources are given in Table 3.1 below. Compositions of media is given in detail in their respective sections.

Table 3.1. Media used in the experimental setups and their respective carbon and nitrogen sources.

Medium	***Carbon***		***Nitrogen***	
	Source	***Concentration***	***Source***	***Concentration***
Activation medium	Yeast extract	3.0 g/L	Yeast extract Bacto-peptone	3.0 g/L 3.0 g/L
Growth medium	Acetate	20.0 mM	Glutamate	10.0 mM
1st Adaptation medium	Acetate Sucrose	20.0 mM 5.00 mM	Glutamate	10.0 mM
2nd Adaptation medium	Sucrose	5.00 mM	Glutamate	10.0 mM
H_2 and PHB production medium with acetate	Acetate	65.0 mM	Glutamate	2.00 mM
H_2 and PHB production medium with sucrose	Sucrose	10.8 mM	Glutamate	2.00 mM
Feed with acetate	Acetate	601 mM	Glutamate	18.5 mM
Feed with sucrose	Sucrose	100 mM	Glutamate	18.5 mM

3.2.1 Activation Medium

Mineral-peptone yeast extract (MPYE) medium was used as the solid medium to activate and grow the freeze-dried cultures initially. Composition of the MPYE medium is given in Appendix A Table A. 1. pH was adjusted to 7.50 using 0.5 M NaOH solution. After the addition of agar (1.5% w/v), medium was left unstirred and autoclaved for 20 minutes at 121^{o}C (NÜVE OT 90L) to achieve sterilization and dissolution of agar. Special care was taken to use much larger borosilicate bottle than the volume of prepared MPYE, as agar foaming may occur and spillage during autoclaving may interfere with the sterilization and contents of the medium. Autoclaved MPYE medium was brought to around 40^{o}C to maintain its liquidity and poured into agar plates in laminar flow cabin (Bilser BLF2000), near open Bunsen burner flame. Plates were then left to be solidified. Solidified MPYE medium can be stored either in refrigerator at 4^{o}C or room temperature.

3.2.2 Growth and Adaptation Media

As the growth medium, Biebl and Pfennig's (BP) medium is used (Biebl and Pfennig, 1981). BP medium contains phosphate buffer, calcium and magnesium salts as well as vitamin, trace element and ferric citrate solutions. Acetic acid and sodium glutamate are added as the primary carbon and nitrogen sources, in concentrations of 20 mM and 10 mM, respectively (Boran *et al.*, 2010). pH is set to 6.30 – 6.40 using 5 M NaOH solution. Medium is sterilized by autoclaving for 20 minutes at 121^{o}C (NÜVE OT 90L). Trace element, vitamin and ferric citrate solutions are prepared using sterile deionized water and filtered through 0.22 µm sterile syringe filters (ISOLAB MV-0.22/25) to achieve sterilization. Due to degradation in autoclave, trace element, vitamin and ferric citrate solutions are added after autoclaving and in laminar flow cabin (Bilser BLF2000). Composition of the growth medium is given in Appendix A Table A. 2. Trace element, vitamin and ferric citrate

solution compositions are given in Appendix A Table A. 7, Table A. 8 and Table A. 9, respectively.

Adaptation media was used to adapt the microorganisms grown in acetate as the primary carbon source to utilize sugars as their primary carbon source instead. Adaptation was done in two steps to prevent the shock loading of sugars to the culture. First adaptation medium has the exact same composition as the growth media, while also containing 5.0 mM sucrose as an alternative electron donor. Second adaptation medium replaces acetate with sucrose and is aimed to select microbial colonies that preferred to use sucrose in the first adaptation medium. Compositions of first and second adaptation media can be seen in Appendix A Table A. 3 and Table A. 4, respectively.

3.2.3 PHB and H_2 Production Media

Primary aim of PHB and H_2 production media is to achieve relevant nutrient concentrations (in terms of C, N and P) necessary for PHB and H_2. PHB and H_2 production medium also contains BP medium along with trace element, vitamin and ferric citrate solutions. To provide stress conditions necessary for the accumulation of PHB, excess carbon and limited nitrogen was supplied in the form of 65 mM of acetate and 2 mM of glutamate, respectively (Özsoy Demiriz *et al.*, 2019).

Additionally, PHB and H_2 production medium with sucrose instead of acetate was also utilized (Oflaz and Koku, 2021) to investigate the effect of substrate type, i.e., acetate and sucrose. For this purpose, carbon concentration of this medium was kept equal to carbon concentration of PHB and H_2 production medium with acetate, accounting for 10.8 mM of sucrose. Nitrogen and other essential salts concentrations were kept the same for both acetate and sucrose-containing PHB and H_2 production media. Compositions of PHB and H_2 production media is given in Appendix A Table A. 5 and Table A. 6. pH of the media was adjusted with 5 M NaOH to desired levels, which are discussed in the experimental setup of the respective sections.

3.3 Environmental Conditions

The environment in which the reactors operate consists of parameters such as temperature, headspace and light intensity, which are all maintained constant throughout operation of all sets.

All sets were operated in temperature-controlled incubators (NÜVE ES 110) and temperature was maintained at 30^{o}C throughout reactor operation.

Headspaces of the reactors were flushed with argon (Habaş Industrial and Medical Gases, 99.995% v/v) to maintain anaerobic conditions. Headspace pressure was kept constant at 1 atm during reactor operation by either fitting 50 mL sterile injectors onto reactor stoppers or keeping water displacement apparatus connected to the reactor at all times.

For all sets operated, light intensity was maintained at 2500-2600 lux and measured by a lux meter (ExTech HD450).

3.4 Analytical Methods

This section covers the experiments conducted for each set and divided as analyses conducted on the working volume of the reactors, headspace analyses and PHB analyses. Not all the analyses were conducted on a daily basis, however in the case of daily experimentation, analyses were conducted approximately the same time of day while taking note of the exact time of analysis.

Analyses applied on the working volume of the reactors include pH, cell growth, salinity, sodium, organic acids and sugar content of the sample. Sampled volume is replaced with same volume of sterile BP medium (i.e., without any C or N source) in order to maintain the headspace pressure constant at 1 atm.

Analyses applied on headspace of the reactors were qualitative and quantitative analyses of the produced biogas. Amount and composition of biogas was determined with methods described in respective sections.

PHB analyses cover the measurement of the accumulated PHB from extraction until quantification.

3.4.1 pH

pH of the sample was measured using pH meter (Mettler Toledo MP220) by taking 1 mL of the sample. pH meter was calibrated using pH = 4.01, pH = 7.00 and pH = 10.01 buffer solutions (Orion 910104, Orion 910107, Orion 910110, respectively) on a regular basis and verified before each use.

3.4.2 Cell Growth

Growth of microbial cells was measured by absorbance spectrometer (Shimadzu UV-1800), by reading optical density of 1 mL of sample at 660 nm wavelength. Spectrophotometer was calibrated separately for OD (absorbance) vs. cell dry weight (g/L) of *R. capsulatus* WT (DSM1710) and *R. capsulatus* YO3. Calibration curves and equations can be seen in Appendix C Figure C. 1 and Figure C. 2, respectively for WT and YO3 strains (Öztürk, 2005; Uyar, 2008).

For both of the strains applicability of the calibration curve was verified by taking biomass samples during various stages of growth and measuring the OD and cdw values. The calibration was verified occasionally by measuring an OD-cdw value pair for a sample and confirming that it was on the curve. For sucrose-adapted YO3 strains, a new calibration curve was constructed using the methods described in Section 3.4.6. Calibration curve can be seen in Appendix C Figure C. 3.

3.4.3 Organic Acids and Sugars

Organic acids concentration was determined using a high-performance liquid chromatography (HPLC) system (Shimadzu LC 20AT), equipped with an ion exclusion column (Altech IOA-1000, Dimensions: 7.8 mm * 300 mm) and ultraviolet (UV) detector (Shimadzu SPD-20A). 20 µL of sample was injected to HPLC via autosampler (Shimadzu SIL-20AC HT). Oven temperature was maintained at 66^{o}C throughout the run. 0.00085 M H_2SO_4 solution was used as the mobile phase with 0.5 mL/min flowrate. Wavelength of UV detector was set as 210 nm. Run time is 80 minutes. Sugar content was determined simultaneously with organic acids, using refractive index detector (RID) (Shimadzu RID-20A).

To prepare the samples for analysis using HPLC, 1.5 mL of sample was taken and placed in Eppendorf tubes. Eppendorf tubes containing the liquid sample were then centrifuged at 13,000 rpm for 10 minutes (Eppendorf MiniSpin Plus Centrifuge) to separate suspended microbial cells from the medium. Supernatant was filtered through 0.22 µm mixed cellulose-ester (MCE) syringe filters (ISOLAB MV-0.22/25). Filtered supernatant was diluted with deionized water to be in the calibration range, that is 1 – 10 mM for all organic acids and 1-5 mM for sucrose.

HPLC was calibrated using standard solutions prepared from 10 mM volatile free acids (formerly, Volatile Fatty Acids) calibration mixture (Supelco CRM46975 Volatile Free Acids Mix, 10mM), containing (i) heptanoic acid, (ii) formic acid, (iii) acetic acid, (iv) propionic acid, (v) isobutyric acid, (vi) butyric acid, (vii) isovaleric acid, (viii) valeric acid, (ix) isocaproic acid and (x) hexanoic acid, in the order of elution, as well as a separate stock solution for lactic acid (Fluka, 69775). Calibration curves and equations can be seen in Appendix D Figure D. 1 through Figure D. 11. Calibration curve for sugars, specifically sucrose, was constructed by injecting standard solutions prepared using microbiology grade sucrose (Merck Millipore, 107651) to HPLC. Calibration curve and equation of sucrose can be seen in Appendix D Figure D. 12. All injections were done in triplicate to calculate

coefficient of variation (CV%) from the Equation 3.2 seen in Section 3.5. For all compounds except for heptanoic acid and isovaleric acid, $R^2 \geq 0.99$ was obtained.

Sample chromatograms for both organic acids analyses and sucrose can also be seen in Appendix D Figure D. 13 and Figure D. 14, respectively.

3.4.4 Sodium

Na^+ content of the samples was determined using flame photometer (JENWAY PFP7), by measuring the atomic flame emissions of the sample at 589 nm wavelength. Detection limit is 0.2 ppm (0.2 mg/L in aqueous solutions) and upper limit is 199.9 ppm (≈199.9 mg/L). Required sample size is around 10 mL.

Samples to be analyzed for Na^+ content were subjected to same preparatory steps as in the HPLC analysis (See Section 3.4.3). Samples were taken into 1.5 mL Eppendorf tubes and centrifuged at 13000 rpm for 10 minutes (Eppendorf MiniSpin Plus Centrifuge). Supernatant was filtered through 0.22 µm MCE syringe filters (ISOLAB MV-0.22/25) and diluted using deionized water to be approximately in the range of calibration.

Flame photometer was calibrated using standard solutions prepared using ACS Reagent grade NaCl (Sigma-Aldrich S9888). Calibration range of the instrument is 0 – 100 mg Na^+/L. Calibration was done each time before using the flame photometer; thus, calibration equations varied daily. A sample calibration curve and equation can be seen in Appendix E Figure E. 1.

3.4.5 Conductivity

Conductivity of the samples was measured using conductivity meter (Hach Sension 378) by taking 20 mL of the sample and multiplying the reading with the dilution factor. Same sample could be used for Na^+ and conductivity measurements as both analyses need approximately the same dilution ratio for this study.

3.4.6 Cell Dry Weight

Cell dry weight (cdw) analyses were applied to construct OD vs. cdw (g/L) calibration curve for analysis in UV spectrophotometer with respect to method described by Öztürk (2005).

Microorganisms were inoculated into growth medium described in Section 3.2.2, and 30 mL of samples were taken from the growing reactors in regular time intervals. OD (Absorbance at 660 nm) value was read using absorbance spectrophotometer (Shimadzu UV-1800). Sample was aliquoted into 10 mL centrifuge tubes, which were then centrifuged at 4000 rpm for 15 minutes (Sigma 4k15 Centrifuge). Supernatant was removed with a sterile pipette and microbial pellets were resuspended by adding 1 mL of deionized water. Resuspended cultures were transferred to 1.5 mL microcentrifuge tubes to be centrifuged at 13,000 for 2 minutes (Eppendorf MiniSpin Plus Centrifuge). Supernatant was removed via a sterile pipette again and cells were resuspended in 200 µL of deionized water. Resuspended cultures in 200 µL water were then transferred to pre-weighted aluminum dishes and dried (NÜVE ES 110) at 50^{o}C for 6 hours. Then, dry weight of the sample was calculated with respect to Equation 3.1 below.

$$\text{Cell Dry Weight } \left(\frac{\text{gcdw}}{\text{L}}\right) = (\text{A} - \text{B})/(\text{Sampling Volume}) \quad (3.1)$$

Where;

A is the weight of the dish containing dried biomass (g), B is the weight of empty dish (g) and sampling volume is 0.01 L (10 mL).

Calculated cdw (gcdw/L) values are then plotted versus OD (Absorbance at 660 nm) readings which the samples were taken for drying. For each OD reading, at least three cdw analyses were done to calculate the CV % using Equation 3.2 in Section 3.5.

3.4.7 Gas Production and Composition

Headspace gas analysis includes the amount produced daily, as well as the content of the biogas. Exact hour and minute of the headspace analysis was recorded to later express the results as molar gas production rate on an hourly basis (mmol/L·h or mol/m^3·h).

Produced gas was collected either in 50-100 mL sterile injectors (Figure 3.1a) or water displacement apparatus (Figure 3.1b) depending on the volume of the reactors operated. Time of the reading and volume produced were noted daily. Every 2-3 days, gas collection apparatus was disconnected in a sterile environment and gas was discharged.

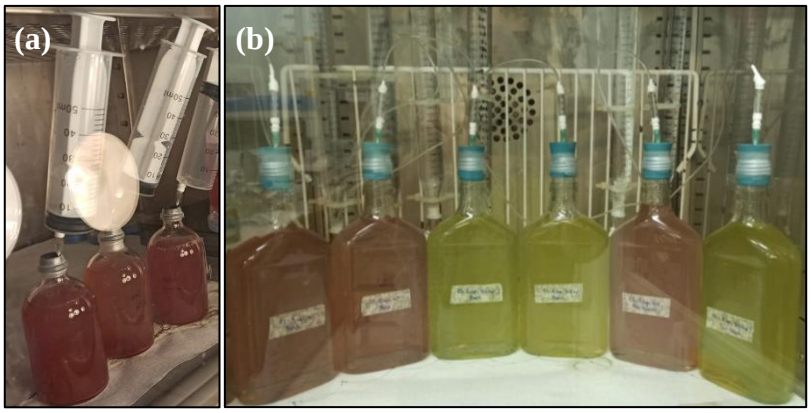

Figure 3.1. Gas collection setup, (a) sterile injectors and (b) water displacement apparatus

In order to analyze the biogas compositions, headspace gas from the reactors was sampled daily by gas tight syringe (Hamilton 1750 SL 500 µL (22/51/2) L). Content of the headspace gas was measured by injecting 100 µL of headspace gas into gas chromatography (GC) system (Agilent Technologies 6890N Network GC), equipped with Supelco Carboxen 1010 column and thermal conductivity detector (TCD), through purged pack (PP) inlet. Argon (Hat Industrial and Medical Gases, 99.999% v/v, 5.0 grade) was used as the carrier gas. Flow rate of the carrier gas was constant at 26 mL/min. Inlet, column oven and detector temperatures were constant at 160^{o}C, 140^{o}C and 170^{o}C, respectively. Run time was 9 minutes.

GC was calibrated using chromatography grade calibration gas mix (Linde HiQ 60 Calibration Gas Mixture, Hydrogen Balance), which contained 50% H_2, 10% N_2, 10% CH_4 and 30% CO_2. Calibration curves and equations can be seen in Appendix F Figure F. 1 through Figure F. 4. All injections were done in triplicate to calculate CV (%) from the Equation 3.2 in Data Analysis section. R^2 values were ≥ 0.99 for all compounds with CV $\leq$ 1%.

3.4.8 Poly – hydroxybutyric Acid (PHB) Recovery and Analysis

PHB was measured by following the procedure described by Braunegg *et al.* (1978), modified and adapted to suit the needs of this study (Özsoy, 2012). The method involves chloroform extraction of PHB from microbial cells, followed by simultaneous methanolysis and transesterification process to be able to be quantifiable by GC. All procedures involving the use of chloroform and methanol are performed under fume hood (Truva Series 120D).

3.4.8.1 Obtaining of Biomass Pellets

Biomass was separated from the medium by centrifugation (Thermo Scientific SL16R) of samples at 13,000 rpm for 20 minutes. At least 15 mL of sufficiently grown biomass (with biomass concentration around 1.0 gcdw/L) from reactors has proved to yield enough PHB to be above the quantification limit of the GC, although more sample volume is always better to minimize errors. After centrifugation, supernatant was discarded and water content of the biomass was removed by freeze drying under vacuum (lyophilization) at -80^{o}C for 24 hours (CHRIST Alpha 1-4) (Özsoy, 2012). It should be noted that in this thesis study, two more approaches for drying step, namely heat-drying and no-drying were also applied in Set 1 (See Section 3.6.2) to find the optimum approach where the PHB loss would be minimum. Therefore, PHB analysis performed for Set 2 and Set 3 follows the result of Set 1 in terms of drying step.

3.4.8.2 Extraction and Methanolysis

Following the removal of water from biomass, pellets were weighed in polystyrene weighing dishes (KERN & Sohn GmbH ABJ 220-4M), added into 2 mL chloroform in screw-capped tubes and thoroughly mixed. If biomass had not been dried, dry weight of the pellet was calculated indirectly from the OD value at the time of sampling (See Equation 3.5 in Section 3.6.2.2). 2 mL of acidified methanol solution (15% H_2SO_4 v/v) was added to the aforementioned biomass-chloroform mixture, heated and maintained at 100^oC for 4 hours using block heater (WTW CR3200) to initiate the methanolysis of the PHB. Caps of tubes were further sealed with polytetrafluoroethylene (PTFE) sealing tape to prevent the evaporation of the sample during the heating. The pictures of the samples during different steps of PHB analysis are given in Figure 3.2.

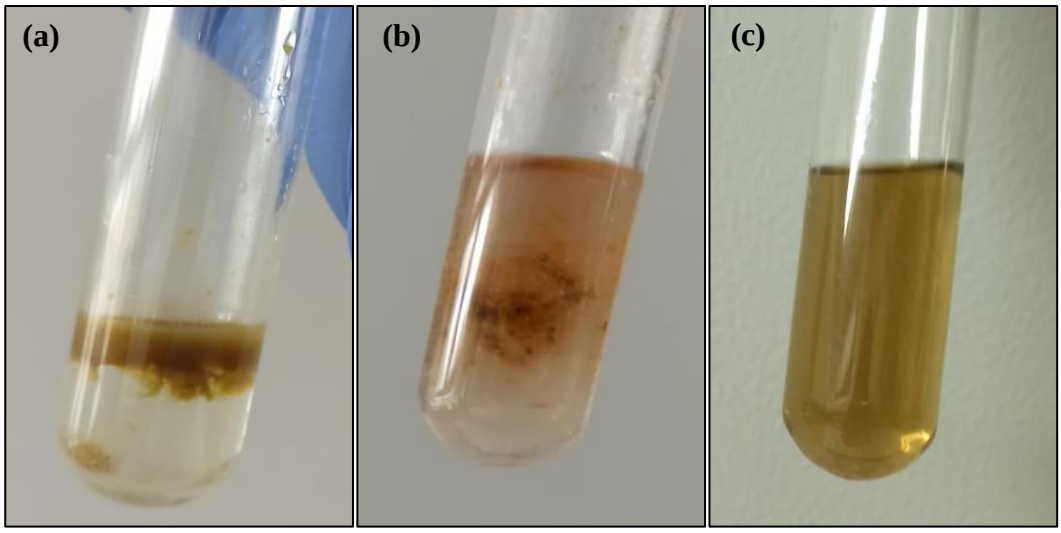

Figure 3.2. (a) Samples from reactors after 2 mL chloroform addition, (b) Samples after addition of 2 mL chloroform and 2 mL acidified methanol and (c) Samples after heating at 100^oC for 4 hours.

During methanolysis, PHB is degraded into its monomer hydroxybutyric acid. Methyl group is then added to the monomer via the simultaneous transesterification process occurring alongside methanolysis, resulting in the hydroxybutyric acid methyl ester, which in turn is quantifiable by GC.

3.4.8.3 Phase Separation and Filtration

Following methanolysis, samples were cooled down to room temperature. 1 mL of distilled water was added to the tubes and shaken for 10 minutes to achieve separation of two distinct phases, seen in Figure 3.3. Upper (aqueous) phase contains H_2SO_4 mixed with leftover methanol and distilled water, as well as soluble polar compounds that may be extracted from the microbial cells alongside PHB (Cui *et al.*, 2007). Lower phase contains hydroxybutyric acid methyl ester dissolved in chloroform. In between phases, non-soluble cell debris accumulate. Upper phase was discarded and lower phase was filtered through 0.22 µm PTFE syringe filters (ISOLAB PTFE-0.22/25) for GC analysis.

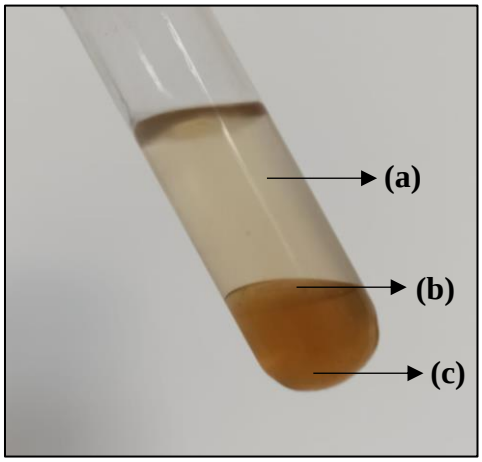

Figure 3.3. Separated phases of methanolysed samples after addition of distilled water. (a) Aqueous phase, (b) Interphase cell debris and (c) Chloroform phase

3.4.8.4 Quantification

In order to quantify the PHB accumulated in the samples (chloroform phase), GC system (Agilent Technologies 6890N Network GC), equipped with Agilent J&W, HP-FFAP capillary column (Dimensions: 30 m * 0.320 mm * 0.25 µm) and flame ionization detector (FID) through split/splitless (S/SS) inlet were used. After phase separation, the filtered sample (lower phase; chloroform phase) of 1 µL was injected using a microsyringe (Hamilton 701N 10µL) to GC system. Argon (Hat Industrial

and Medical Gases, 99.999% v/v, 5.0 grade) was used as the carrier gas with constant column pressure at 6.67 psi. Inlet temperature was 230°C with 20:1 split ratio and detector temperature was 250°C. Oven temperature was set as 70°C initially with 1-minute hold. Final oven temperature was 160°C (1-minute hold) with 8°C/min ramp. Runtime was 13.25 minutes.

In order to quantify the injected PHB, GC was calibrated using standard solutions prepared from pure PHB (Fluka 81329). Pure PHB was dissolved in chloroform to obtain a stock solution. PHB standard solutions were prepared by diluting the stock solution with chloroform to achieve appropriate concentrations. Afterwards, standard solutions of PHB were subjected to same steps as in PHB analysis of biomass, that is, methanolysis, phase separation and filtration in the order of application. Calibration curve and equation can be seen in Appendix G Figure G. 1, along with a sample chromatogram in Figure G. 2. All injections were done in triplicate.

3.5 Data Analysis

All the reactors in the study were set up as either duplicate or triplicate reactors. In case of duplicate reactor setup, mean data of the results were taken and high and low producing reactors were expressed as error bars to show the upper and lower data range in the figures. In case of triplicate reactor operation, mean results were given and error bars were expressed as the standard deviation of triplicate reactors.

Calibrations done in the study contain at least 3 data points and 3 readings per data point. Calibrations were verified by calculating the R^2 values of the best line and keeping coefficient of variation of the triplicate readings below 5%, calculated using Equation 3.2 below.

$$CV\ (\%) = \frac{\sigma}{\mu} \times 100 \qquad (3.2)$$

Where, σ and μ are standard deviation and mean peak area of three consecutive measurements of a sample.

Limit of detection (LOD) and limit of quantification (LOQ) of the instrument was calculated using Equation 3.3 and Equation 3.4 respectively, given below ("Validation of Analytical Procedures: Text and Methodology Q2(R1)," 2005).

$$\mathrm{LOD} = 3.3 * \frac{\sigma_{\mathrm{smallest}}}{\mathrm{m}} \tag{3.3}$$

$$\mathrm{LOQ} = 10 * \frac{\sigma_{\mathrm{smallest}}}{\mathrm{m}} \tag{3.4}$$

Where, $\sigma_{\mathrm{smallest}}$ is the standard deviation of triplicate analyses of the calibration standard with smallest analyte concentration and m is the slope of the calibration curve.

3.6 Experimental Setup and Procedure

This section covers the experimental design and operation of three sets conducted and purpose of each experiment. Preparatory steps to activate and grow the microbial cultures are also covered. All steps involving the inoculation of pure cultures to the sterilized media were performed in laminar flow cabin (Bilser BLF2000), near open Bunsen burner flame and using aseptic technique.

3.6.1 Initial Activation and Growth of Cultures

3.6.1.1 Activation of the Cultures

For initial activation, microorganisms that had been previously stored in -80^{o}C were inoculated to MPYE agar plates in laminar flow cabin, after thawing the culture in room temperature. Using aseptic technique, microbial culture was inoculated to MPYE plates with loop. Streak plate method was used in inoculation to observe separate bacterial colonies as well as to verify the absence of contamination. Inoculated plates were incubated at 30^{o}C in dark for about 5 – 6 days to grow sufficiently.

3.6.1.2 Growth

After the initial activation in MPYE agar plates, a loopful of culture was transferred to 2 mL growth medium in Eppendorf tubes. Newly inoculated cultures in 2 mL growth medium were incubated in dark at 30^{o}C for 4 – 5 days.

Cultures grown in 2 mL growth medium were then transferred to 15 mL growth medium. Whole content of the Eppendorf tube containing the grown culture was placed in 15 mL falcon tubes and volume was completed to 15 mL with growth medium, accounting for approximately 13.3% (v/v) inoculation ratio. 2500 – 2600 lux illumination was provided and cultures were incubated at 30^{o}C for 4 – 5 days.

After growth in 15 mL tubes, microorganisms were transferred to 50 mL growth medium with 10% (v/v) inoculation ratio. After incubating for 3 – 4 days, (corresponding to around 0.45 – 0.50 gcdw/L) at 30^{o}C and under 2500 – 2600 lux illumination, fully grown cultures were used for seeding the reactors in the experiments.

3.6.2 Set 1: Determination of Biomass Pretreatment Method for PHB Analysis

PHB quantification methodology involves many steps that the accumulated PHB could be lost during recovery or analysis. In Set 1, potential losses during centifugation, losses in drying processes and losses during methanolysis were investigated for both *R. capsulatus* WT and *R. capsulatus* YO3 strains. The set was operated for 5 days due to the fact that in previous studies 5 days of operation had been enough to accumulate PHB in sufficient amounts for reliable quantification based on the methods described in this study (See Section 3.4.8). At the end of the operation, all reactors were sampled for PHB analysis. Each biomass sample withdrawn was subjected to three drying methods;

1) No-drying
2) Heat-drying at 55^{o}C for 24 hours
3) Freeze-drying at -80^{o}C for 24 hours

The results were compared and the method leading to the lowest PHB loss was selected as the optimum drying method to be used in further PHB analyses.

3.6.2.1 Reactor Setup of Set 1

110 mL clear glass serum bottles were used in the experiment (Figure 3.4). Using batch mode of operation, triplicate reactors for both strains, namely *R. capsulatus* (WT) and *R. capsulatus* (YO3), were set up along with a control reactor; thus, a total of 7 reactors. Configuration of the reactors is given in Table 3.2. PHB and H_2 production medium with acetate was used as the medium. Effective volume was 100 mL and inoculation ratio of the reactors were 10% (v/v), accounting for 90 mL medium and 10 mL inoculum. Sterile deionized water was added to the control reactor instead of inoculum to observe any possible contamination and abiotic production of hydrogen or degradation of substrate. All the other parameters such as temperature, light intensity, sampling frequency were kept constant for all reactors operated. Produced gas was collected by fitting 50 mL sterile injectors onto stoppers of the reactors. Fitting sterile injectors was found to be more reliable for the collection of gas in previous studies (Tarlan 2022).

Table 3.2. Reactor setup for Set 1

Reactor	***Inoculum***	***Medium***	***T(^{o}C)***	***Light Intensity (lux)***
R0	-	PHB and H_2 production medium	30	2500 – 2600
R1	*R. capsulatus* WT			
R2	*R. capsulatus* WT			
R3	*R. capsulatus* WT			
R4	*R. capsulatus* YO3			
R5	*R. capsulatus* YO3			

R6	*R. capsulatus* YO3

Figure 3.4. Set 1 after the setup. From left to right: control reactor, triplicate WT strain reactors, triplicate YO3 strain reactors.

3.6.2.2 Operation of Set 1

Gas production and headspace gas content were measured on a daily basis. pH, growth and organic acids analyses of the set were conducted at the beginning and end of the set operation (t = 0 and t = 5 days). PHB was measured at the end of the set operation. See Table 3.3 for the summary of analyses applied.

Table 3.3. Summary of analyses conducted for each reactor in Set 1.

Time (d)	***Analyses***					
	Gas Production	***Gas Content***	***pH***	***Growth***	***Organic Acids***	***PHB***
0	✓	✓	✓	✓	✓	
1	✓	✓				
2	✓	✓				
3	✓	✓				
4	✓	✓				
5	✓	✓	✓	✓	✓	✓

After the cessation of the operation, each reactors biomass was withdrawn for PHB analyses. As mentioned above, PHB analyses were conducted using three different approaches for drying, namely;

1) No-drying.
2) Oven-drying at 55ºC for 24 hours (Şimşek Laborteknik ETS120)
3) Freeze-drying at -80ºC under vacuum (lyophilization) for 24 hours (Christ-Alpha 1-4D)

Furthermore, each method for drying and no-drying were further analyzed with (and without) adding 2 mg of PHB standard to investigate the losses during centrifugation and methanolysis steps. All the analyses were done by preparing six 15 mL aliquots from each reactor. Table 3.4 below shows the breakdown of PHB analyses. In the case of no-drying approach, weight of biomass was indirectly calculated by using the cdw vs. OD calibration (Appendix C, Figure C. 1 and Figure C. 2), and the equation given in Eq. 3.5. Thus, OD value at Day 5 was used.

Table 3.4. PHB analyses performed for each reactor with six different approaches in drying step.

Aliquot #	***No drying***		***55ºC Drying***		***-80ºC Freeze Drying***	
	Without Standard	***With Standard***	***Without Standard***	***Without Standard***	***Without Standard***	***With Standard***
1	✓					
2		✓				
3			✓			
4				✓		
5					✓	
6						✓

In the case of drying approaches, weight of biomass was obtained directly by weighing in analytical balance.

$$\mathrm{W\ (mg)} = (\mathrm{OD} * \mathrm{a} + \mathrm{b}) \frac{\mathrm{mg}}{\mathrm{mL}} * 15\mathrm{mL} \quad (3.5)$$

Where, W is the cell dry weight (mg) of the 15 mL aliquot, OD is the absorbance value read at 660 nm at t =5 days and a and b are the slope and intercept of the calibration curve, respectively.

Following the drying and obtaining of the biomass pellets step, same procedure for the analysis of PHB described in Section 3.4.8 was applied on each sample. Results for all drying approaches were compared and the approach resulting in highest PHB observation was selected as the preferred method for following studies. By conducting this study for both WT and YO3 strains, it was aimed to observe if the strain would affect the preferred PHB analysis method. Furthermore, it was aimed to observe the higher PHB accumulating strain so that the said strain would be utilized in the following set operations as well.

3.6.3 Set 2: Effect of Na^+ Concentration

The aim of the Set 2 was to investigate the effect of increasing Na^+ concentration on the *R. capsulatus* YO3 using two different carbon sources, namely acetate and sucrose. In a previous study (Oflaz, 2019), solar tubular photobioreactors were operated with molasses as the carbon source in continuous mode of operation, maintaining a pH value of 7.00 using automated NaOH dosing system. It was observed that with increasing sodium concentrations, microbial strain lost its distinctive greenish color and turned white, with hydrogen production gradually decreasing while maintaining high rate of substrate utilization. The decrease in H_2 production with high rate of substrate utilization might be due to PHB production. Therefore, in Set 2 of this thesis study, it was aimed to investigate a step further and observe if accumulating Na^+ concentration decreases H_2 production and leads to PHB accumulation or not. Accordingly, photobioreactors were operated in fed-batch mode, pH was kept constant, mimicking the Oflaz (2019)'s study as close as possible.

3.6.3.1 Reactor Setup for Set 2

360 mL clear glass flat bottles were used as photobioreactors. Reactors were operated in fed-batch mode with controlled pH via each feeding. Feeding was done once the concentration of the carbon source in the reactors decreased to half of its initial value. A total of 8 reactors were set-up utilizing two different carbon sources, namely acetate and sucrose, with 4 reactors per carbon source. Acetate was preferred to compare the results with the previous studies, whereas sucrose was preferred to mimic the high sucrose content of the substrate (molasses) used previously (Oflaz, 2019).

One reactor per carbon source was set up as control, containing no inoculum and exact same conditions as the test reactors (Table 3.5 and Figure 3.5). Sterile deionized water was added into control reactors instead of the inoculum. One reactor per carbon source was set up as pH control reactor, also containing *R. capsulatus* YO3 as the inoculum. Headspace of this reactor was opened to atmosphere with every feeding, adjusting pH (with NaOH) and then purged with argon. Exact amount of NaOH was added to the other reactors without opening their headspace to the atmosphere. pH control reactors for both carbon sources were discontinued after a while, once the response of the reactors to the NaOH was understood and amount to be added could be approximated without the need for pH control reactors. The remaining two reactors per carbon source were set up as test reactors, while the results of the set expressed as the mean results of two test reactors with high and low producing reactors expressed as the upper and lower range, respectively.

PHB and H_2 production medium with acetate, and PHB and H_2 production medium with sucrose were used as the media. Effective volume was 350 mL and inoculation ratio of the reactors were 10% (v/v), accounting for 315 mL medium and 35 mL inoculum. C concentration in the reactors were aimed to be 130 mM, which accounts for 65 mM acetate or 10.8 mM of sucrose. Nitrogen concentrations in both media, was arranged as 2 mM, accounting for 2 mM of glutamate. Produced gas was collected by fitting 100 mL sterile injectors onto stoppers of the reactors (Figure 3.5).

Table 3.5. Reactor setup for Set 2

Reactor	***Purpose***	***Inoculum***	***Carbon Source***	***Medium***
C0	[1]	-	Acetate	PHB and H_2 Production Medium
T0	[2]	*R. capsulatus* YO3		
T1	[3]	*R. capsulatus* YO3		
T2	[3]	*R. capsulatus* YO3		
C0	[1]	-	Sucrose	
T0	[2]	*R. capsulatus* YO3		
T1	[3]	*R. capsulatus* YO3		
T2	[3]	*R. capsulatus* YO3		

[1] Control reactor: To account for abiotic activity in the reactor and clear observation of possible contamination.
[2] pH control reactor: To prevent subjecting the test reactors to high risk of contamination by only opening the headspace of this reactor and adjusting pH, these were discontinued.
[3] Test reactor: To obtain data in regards to the aim of the set.

Figure 3.5. Set 2 after the setup. From left to right: Acetate-containing C0, T0, T1, T2 and sucrose-containing T0, T1, T2 and C0. Reactors were arranged in a crescent pattern to distribute light equally.

3.6.3.2 Operation of Set 2

Daily analyses done on each reactor can be listed as,

i. Biogas production
ii. Biogas composition
iii. Biomass growth
iv. pH
v. Substrate utilization
vi. Sodium concentration
vii. Conductivity
viii. PHB

During the first 4 days of reactor operation, PHB samples were not taken due to biomass amount needed being relatively high (See Section 3.4.8.1). Rather, reactors were only sampled for first 7 analyses listed above, all of which can be done with 5 mL sample from reactors' content. Once biomass had reached certain concentration (after Day 4), PHB samples were started to be taken, accounting for 20 mL of sampling daily. Sample was replaced with basal medium (BM), containing only essential salts and buffer solution with no C or N source. Although 20 mL sample was taken from all reactors, only the samples from test reactors were subjected to PHB analysis. 15 mL sample from control and pH control reactors were discarded.

Once the concentration of the carbon source in the reactors decreased to around half of its initial value, 20 mL of sample taken was replaced with PHB and H_2 production medium with concentrated C and N, instead of BM, effectively raising concentration of the carbon source back to its initial value. The term "feed" refers to this aforementioned concentrated medium. Calculation of feed carbon source concentration can be seen in Appendix B. Feeding the reactors also introduced Na^+ ions to the system due to the NaOH addition to the feed to raise the pH to neutral levels. Nitrogen concentration in the feed was arranged to keep the same initial C/N

ratio, that is 65 mM Acetate/2 mM Glutamate. Concentrations of the other essential salts and buffer solution were kept same as PHB and H_2 production media.

3.6.4 Set 3: Effect of pH

Based on the observations that had been made during the operation of Set 2, another set was planned to investigate the effect of pH on the accumulation of PHB. In Set 2, pH of the reactors with acetate as the carbon source had elevated from 7.50 up to 8.00 in between Days 32 - 44. Highest PHB accumulation of the reactors also occurred in between these days. Moreover, there was also substantial production of valeric acid as a byproduct of metabolic activity. It has been definitive in between days 32 – 44 that operation of the system shifted to favor the production of PHB. Thus, it was aimed in Set 3 to investigate whether it had been due to increase in pH or the increasing pH had been another result of the system shifting to PHB accumulation. To this purpose, reactors maintained at three different pH levels, that was 7.00, 7.70 and 8.50, were operated in Set 3.

3.6.4.1 Reactor Setup of Set 3

As in Set 2, 360 mL clear glass flat bottles were used to set up the reactors. Reactors were operated in fed-batch mode with daily pH control/adjustment. Similar to previous set, feeding was done once the concentration of the carbon source in the reactors decreased to half of its initial value. Two reactors per pH value were set up with three different pH levels, 7.00, 7.70 and 8.50, accounting for a total of 6 reactors. Reactor configuration for Set 3 is given in Table 3.6 and Figure 3.6. Results of the set were expressed as the mean results of two test reactors per pH value with high and low producing reactors expressed as the upper and lower range, respectively.

PHB and H_2 production medium with acetate was used as the media. Initial carbon and nitrogen concentrations were arranged to be 130 mM and 2 mM in the form of

65 mM acetate and 2 mM glutamate, respectively. Acetate was preferred as the primary carbon source since sucrose-containing reactors had been observed to accumulate minimal amounts of PHB in the previous set. pH of the media was adjusted with 5 M NaOH solution to the desired levels. After the adjustment of pH, Na^+ concentrations of the media were determined and equalized by addition of analytical grade NaCl to pH 7.00 and pH 7.70 media, effectively making the media same as each other in terms of Na^+ concentration (and electrical conductivity values) while keeping pH as the single variable parameter. In other words, since pH 7.00 and 7.70 media contained less Na^+ ions than pH 8.50 medium, missing Na^+ ions were added to pH 7.00 and 7.70 media in the form of NaCl. No NaCl was added to pH 8.50 medium. Reactors were set up with effective volume of 350 mL and 10% (v/v) inoculation ratio. Produced gas was collected by fitting 100 mL sterile injectors onto stoppers of the reactors.

Table 3.6. Reactor setup for Set 3.

Reactor	***pH***	***Inoculum***	***Medium***	***Carbon Source***	***T(°C)***	***Light Intensity***
R7.00-1 R7.00-2	7.00	*R. capsulatus* YO3	PHB and H_2 Production Medium	Acetate	30°C	2500 – 2600 lux
R7.70-1 R7.70-2	7.70					
R8.50-1 R8.50-2	8.50					

Figure 3.6. Set 3 after the setup. From left to right: R7.00-1, R7.00-2, R7.70-1, R7.70-2, R8.50-1 and R8.50-2. Reactors were arranged in a crescent pattern to distribute light equally.

3.6.4.2 Operation of Set 3

Operation of the set was the same as Set 2, with daily analyses done on the reactors being, biogas production, biogas composition, growth, pH, substrate utilization, sodium concentration, conductivity and PHB. On par with Set 2, PHB samples were not taken during the first 4 days of reactor operation. Samples from the reactors were replaced with sterile basal medium (BM), containing only essential salts, NaCl to keep the sodium concentration constant and buffer solution without any C or N source. Towards the depletion of acetate in the reactors, 20 mL of sample taken was replaced with PHB and H_2 production medium, containing much more concentrated amounts of acetate and glutamate instead of BM. Addition of concentrated medium elevated the substrate concentration in the reactors back to its initial value, while also increasing Na^+ concentration inevitably. This addition of concentrated medium was done only once during the operation of this set.

CHAPTER 4

RESULTS AND DISCUSSIONS

This chapter presents the results and discussions of three experimental sets conducted, namely, Set 1, Set 2 and Set 3. Set 1 aims to improve the pretreatment method used in PHB analysis, and to determine a sutaible PHB analysis procedure that is to be used in the subsequent sets, whereas Set 2 aims to investigate the effect of accumulation of Na^+ ions as a potential stress condition to the system, whether increase in Na^+ concentration would enhance the PHB yield or not, using two different carbon sources. Observations and modifications to the PHB analysis process were made in Set 1 and adapted to be used in subsequent sets. Set 3 aims to investigate the results observed during the prolonged operation of Set 2 in a shorter duration of operation and consequently, variable parameter in Set 3 was determined as the pH of the system. As described in Chapter 3, all experiments were carried out indoors, using either incubators or water baths to keep the temperature constant. Light was provided at all times and was constant for all the sets operated.

As a summary, modifications to PHB analysis method were determined in Set 1, effect of sodium concentration was investigated in Set 2 and effect of pH was researched in Set 3 of this study.

4.1 Results of Set 1: Determination of Biomass Pretreatment Method for PHB Analysis

PHB quantification methodology involves many steps that the accumulated PHB could be lost during recovery or analysis. In Set 1, potential losses during centrifugation, losses in drying processes and losses during methanolysis were investigated. Six aliquots (15 mL each) that were prepared from each reactor are listed below.

1) No drying, no PHB standard addition, biomass obtained by direct resuspension of wet pellet with chloroform before removing from centrifuge tubes.
2) No drying, 2 mg PHB standard addition, biomass obtained by direct resuspension of wet pellet with chloroform before removing from centrifuge tubes.
3) Drying at 55^{o}C, no PHB standard addition, biomass obtained by resuspension of dried pellet with chloroform after removal from centrifuge tubes.
4) Drying at 55^{o}C, no PHB standard addition, biomass obtained by direct resuspension of dried pellet with chloroform before removing from centrifuge tubes.
5) Freeze drying at -80^{o}C, no PHB standard addition, biomass obtained by resuspension of dried pellet with chloroform after removal from centrifuge tubes.
6) Freeze drying at -80^{o}C, 2 mg PHB standard addition, biomass obtained by resuspension of dried pellet with chloroform after removal from centrifuge tubes.

Listed aliquots were prepared per reactor and results are expressed in figures as the averages of triplicate reactors. Comparisons of aliquots are listed below in Table 4.1.

Table 4.1. Possible PHB losses that were investigated through Set 1.

Compared Aliquots	***Investigated Parameter***
1-3-5	PHB losses during various drying processes
1-2	PHB losses during methanolysis of wet biomass
3-4	PHB losses during centrifugation
5-6	PHB losses during methanolysis of dried biomass
2-6	Impact of presence of H_2O during methanolysis

To ensure that the photobioreactors were working as expected and thus, PHB production was guaranteed, daily gas measurements and initial and final analyses for the working volume of the reactor contents were also made. Figure 4.1 and Figure

4.2 show the cumulative hydrogen productions and hydrogen productivity values, respectively, for both strains. Maximum hydrogen productivity of 0.41 ± 0.09 mmol/L·h and 0.53 ± 0.03 mmol/L·h was obtained for *R. capsulatus* WT and YO3, respectively, which is in line with the values observed in the literature (Section 2.1.3.4).

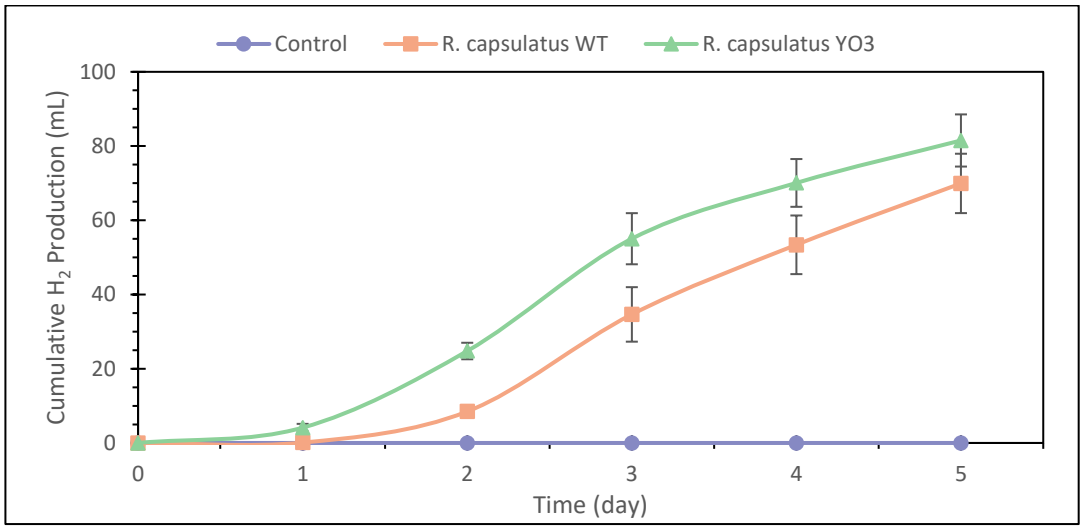

Figure 4.1. Cumulative H_2 production graph of Set -1. Reactors were operated for 5 days. Error bars indicate standard deviation among triplicate reactors.

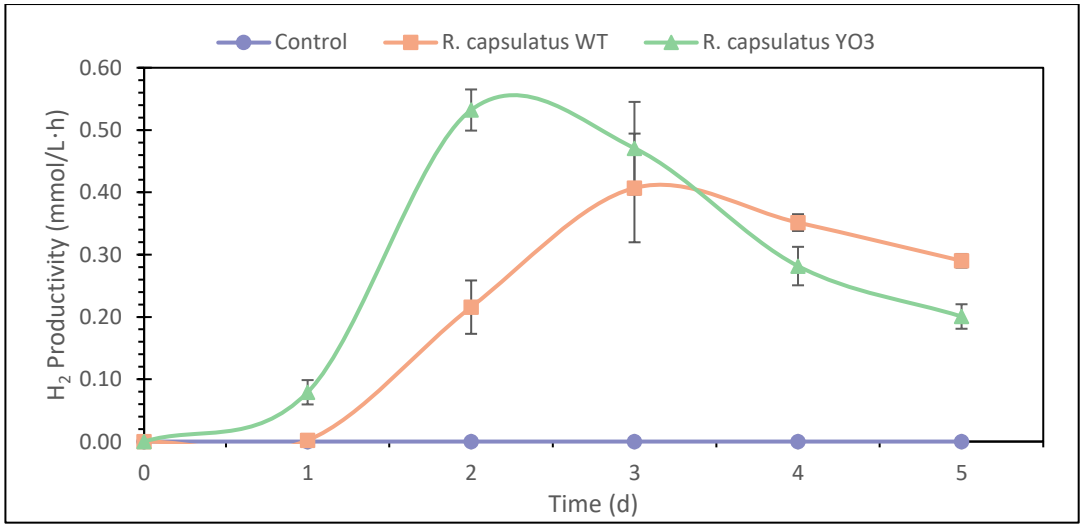

Figure 4.2. Hydrogen productivities (mmol/L·h) of Set -1. Maximum productivity of 0.41 ± 0.09 mmol/L·h and 0.53 ± 0.03 mmol/L·h was obtained for *R. capsulatus* WT and YO3 at t = 3 and t = 2 days, respectively. Error bars indicate standard deviation among triplicate reactors.

For both strains, headspace gas content was observed to be around 90% H_2 at the end of the operation (Figure 4.3), mostly owing to utilization of acetate as the primary carbon source.

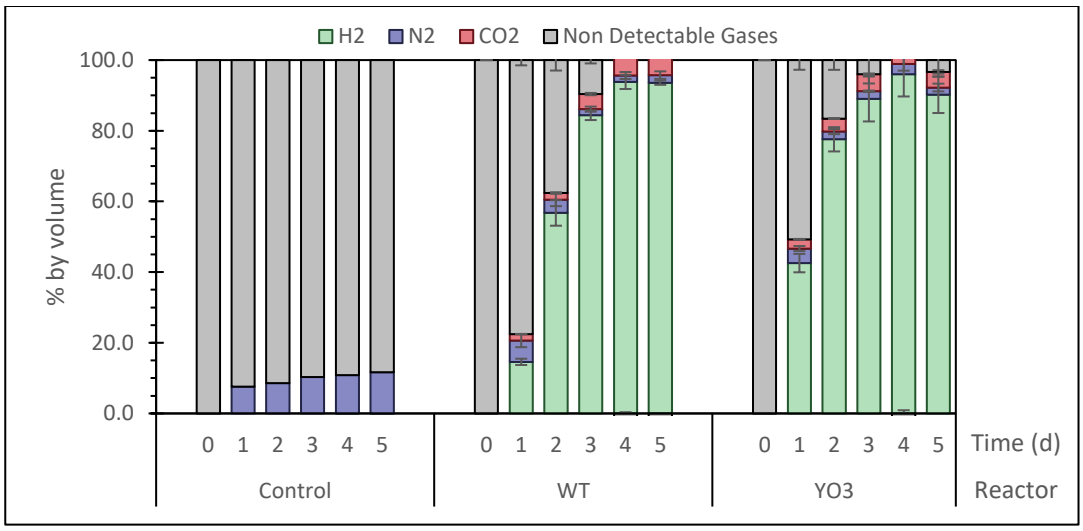

Figure 4.3. Headspace gas composition for control, WT and YO3 reactors in Set 1. Error bars indicate standard deviation among triplicate reactors.

CO_2 production of the reactors were negligible as can be seen from the $\%CO_2$ in the headspace in Figure 4.3. Cumulative CO_2 production of the reactors throughout 5 days of operation was around 4 mL, as seen in the Figure 4.4 below. Error bars indicate the standard deviation among triplicate reactors.

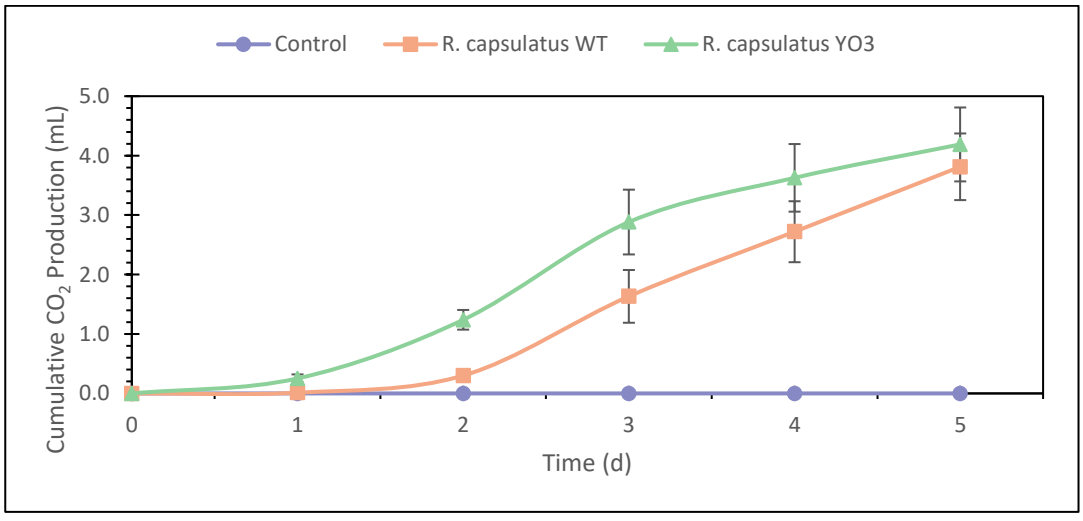

Figure 4.4. Cumulative CO_2 production graph of Set -1.

Organic acids analyses were not carried out in a daily basis. However, it can still be interpreted from Figure 4.5 that the YO3 strain consumed more acetic acid than the WT strain over the course of 5 days of operation. This resulted in higher pH value in the YO3 reactors at the end of the set operation, in spite of reaching slightly less biomass concentration at the end of the operation. Growth of the strains can be seen in Figure 4.6. pH of the reactors adjusted to be around 6.40 at the beginning of the set operation and was observed to increase to 7.30 and 7.51 for WT and YO3 strains, as seen in Figure 4.7, respectively, due to the utilization of acetic acid. With the utilization of acetic acid, increase in pH and also increase in the concentration of formic acid, a metabolic by-product of fermentation of acetic acid, was observed while reactors maintained a consistent growth to reach their theoretical maximum biomass concentration which is around 1.0 gcdw/L. As expected, there was no growth of biomass in control reactor, as well as no significant change in the pH or organic acids consumption.

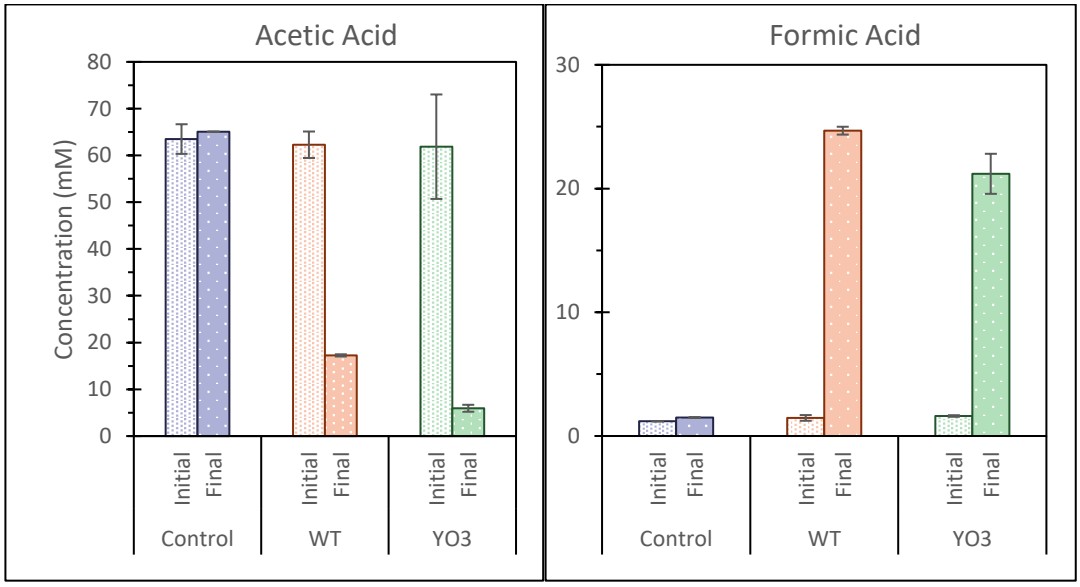

Figure 4.5. Acetic acid concentration and formic acid production of Set 1.

Error bars in Figure 4.5 above represent the standard deviations of three consecutive analyses of control reactor, and standard deviations among triplicate reactors for WT and YO3 reactors. For both strains, initial acetic acid concentration was set as 65.0 mM and verified as 62.3 ± 2.82 mM and 61.9 ± 11.2 mM for WT and YO3,

respectively. Difference in acetic acid concentrations at the end of operation has been observed to be significant, with YO3 strain consuming 10.9 mM of more substrate than the WT counterpart, accounting for 16.9±7 % more substrate utilization over the course of 5 days.

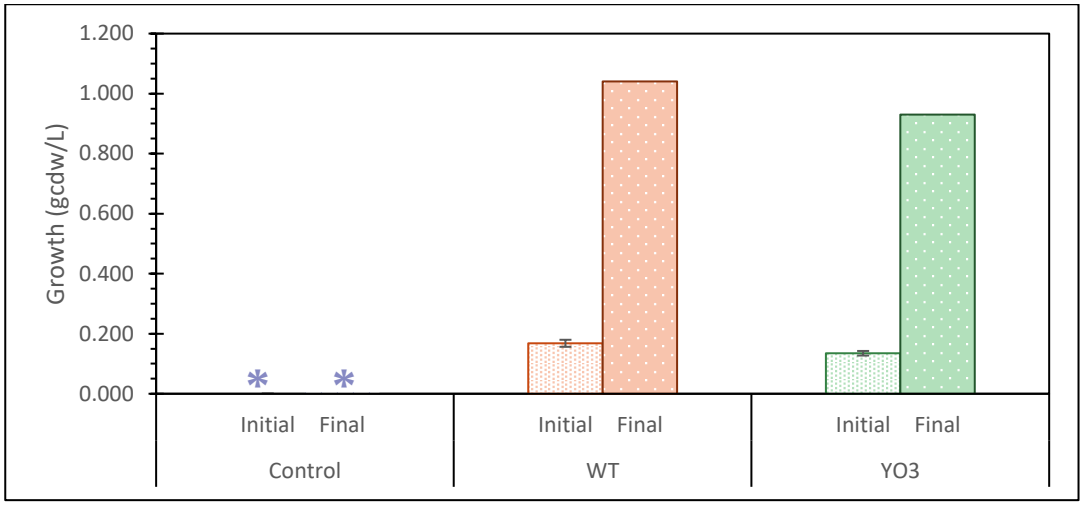

Figure 4.6. Initial and final cell dry weight values observed in Set 1. The asterisk (*) indicates zero values within measurement sensitivity.Relatively higher utilization of the substrate by YO3 strain translates to higher cumulative hydrogen production and increase in pH, however does not result in more biomass or by-product formation. Therefore, another carbon sink should be present which indeed is PHB, as suggested by Figure 4.8 below.

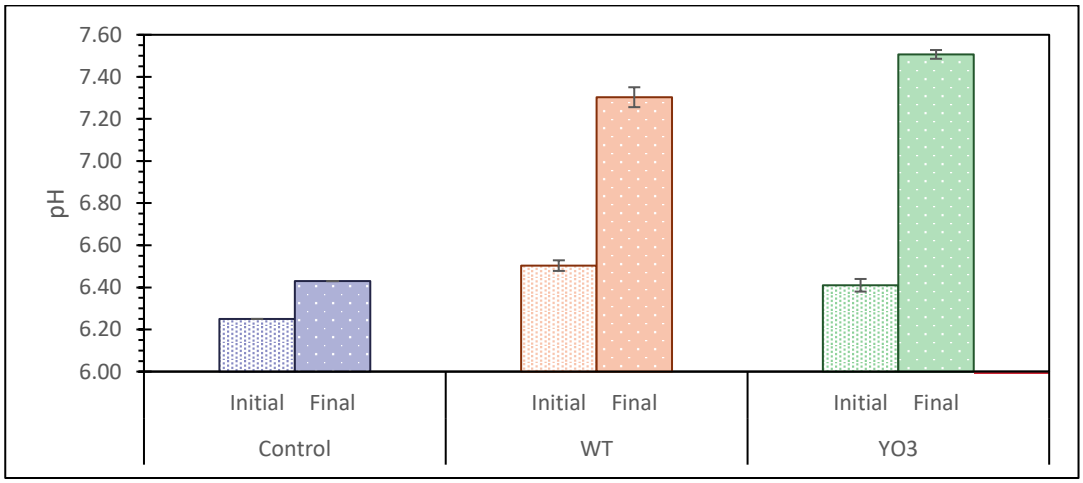

Figure 4.7. Initial and final pH values observed in Set 1.

As the main objective of the set is to identify and minimize the losses during PHB analysis, results of this set focus on PHB accumulation with every possible step in PHB analyses investigated in their respective sections. However, to complete the results regarding the substrate-hydrogen-growth-PHB relationship, PHB accumulation results of the reactors with the determined method and optimizations (no – drying approach, discussed in Section 4.1.4) are given in Figure 4.8 below.

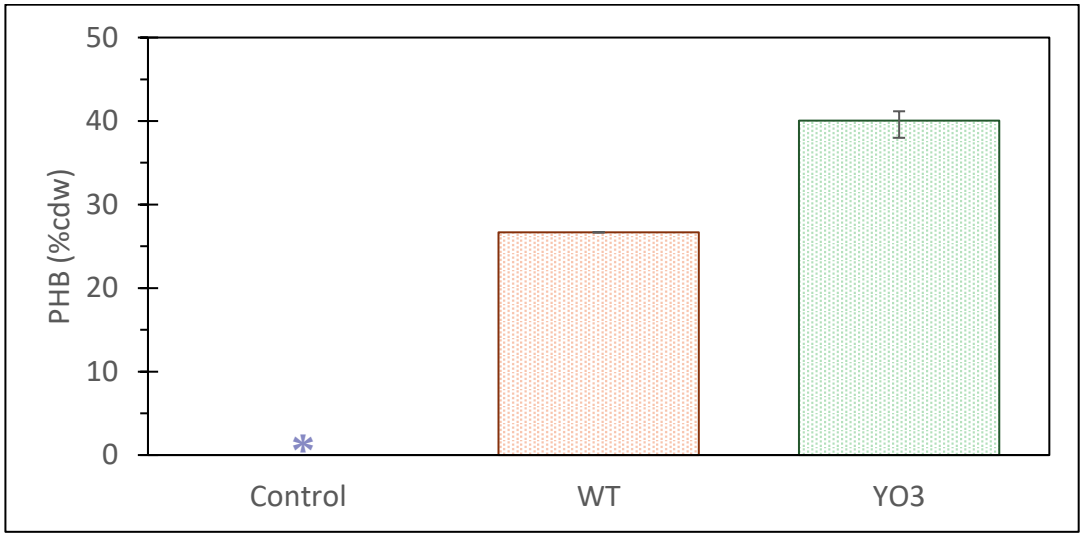

Figure 4.8. PHB accumulation as percent of cell dry weight for control reactor, WT and YO3 strains in Set 1. The asterisk (*) indicates zero values within measurement sensitivity.

Error bars indicate the highest and lowest PHB accumulation as percent cdw. As expected, YO3 strain had higher PHB accumulation than the WT strain. Results prove the opposite of general point of view, that the hydrogen production and PHB accumulation are inversely related to each other. YO3 strain proved to yield both higher amounts of hydrogen as well as PHB than the WT strain. This can be attributed to the overall higher metabolism of the YO3 strain. As mentioned previously, YO3 strain degraded more substrate, and at a higher rate compared to the WT strain. Possible reason for that might be the inability of YO3 strain to utilize hydrogen as the alternative energy donor, owing to the lack of uptake hydrogenase enzyme, resulting in complete dependence of YO3 on electron donation by acetic acid.

With regards to the strain selection, results of this set clearly indicated that the YO3 strain was superior to the WT strain for co-production of hydrogen and PHB, thus it was decided to operate next sets using *R. capsulatus* YO3 as the inoculum (Section 4.1.4). It is also observed that during the first 4 days of reactor operation, PHB samples should not be taken so that the biomass may continue unhindered growth. To analyze PHB while the biomass is still in its early growth phase, more sampling volume is needed to be able to reliably quantify the accumulated PHB as cell concentration is relatively low in this phase.

With the clear indication of reactors operating as intended, reactors were shut down and the working volume aliquoted with respect to Table 4.1 Processes that each aliquot was subjected to is given in Figure 4.9.

Aliquots 3 and 4 included same drying method and different methods for obtaining dried pellets. Said aliquots were then analyzed to compare potential PHB losses during centrifugation of reactor samples, discussed in Section 4.1.1.

Aliquots 1, 3 and 5 were subjected to different methods of drying processes with same method for obtaining pellets, except for analysis of wet biomass. These aliquots were compared to account for the losses that might be arising due to different methods of drying and discussed in Section 4.1.2.

Aliquots 1, 2, 5 and 6 included different methods of drying along with 2 mg PHB standard added to 2 and 6. Those samples were intended to be analyzed whether 2 mg of PHB would be observed after the quantification process, discussed in Section 4.1.3.

Aliquots 2 and 6 contained wet and dry biomass, respectively, and 2 mg of PHB standard to observe whether presence of H2O in the aliquot 2 would interfere with the methanolysis efficiency, also discussed in Section 4.1.3.

In the Figure 4.9, direct addition of chloroform (CHL) refers to addition of chloroform into dried and non-dried biomass without weighing and explained in detail in Section 4.1.1.

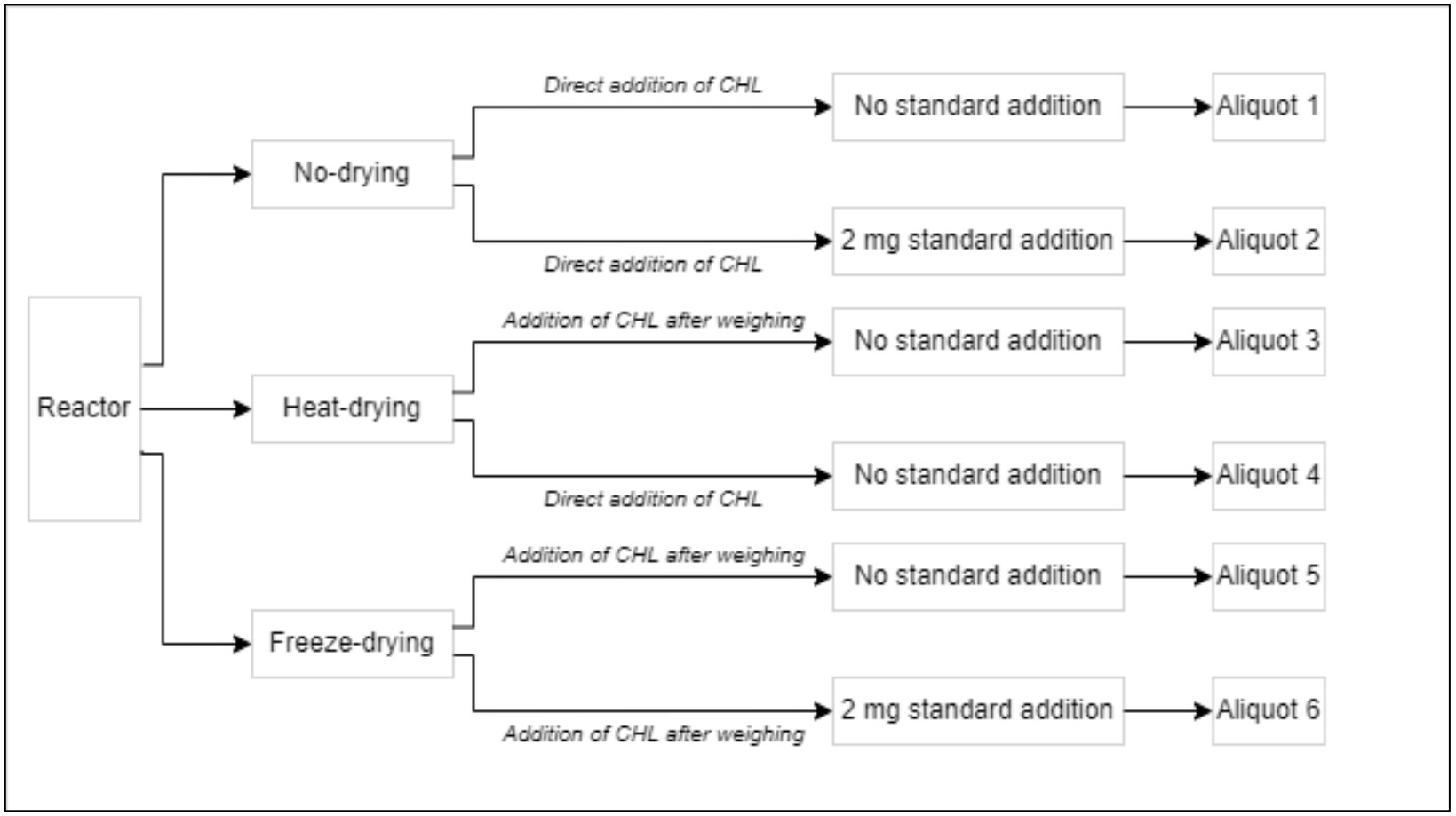

Figure 4.9. Summary of methods applied to each reactor in order to obtain the aliquots listed in Table 4.1. (CHL = chloroform).

4.1.1 PHB Losses During Centrifugation

The first step of the PHB analysis is the removal of biomass from the reactor content via centrifugation (See Section 3.4.8.1). Separation of PHB from the cells by centrifugation is a widely researched topic in the literature as well, where cells are destroyed via centrifugation on purpose to recover accumulated PHB (van Wegen *et al.*, 1998). In preliminary experiments performed (data not shown), it was observed that when the centrifuged biomass pellets had been dried using various methods (i.e., oven drying at 55^{o}C and freeze drying at -80^{o}C for 24 hours), two distinct formations occurred. First formation (i) was the expected biomass and usually was in a sturdy solid form after the drying. The second formation (ii) was an oily, cloudy compound that could be an extracellular polymeric substance (EPS) secreted by microorganisms. This compound could not be weighed accurately in analytical balance as its density was significantly lower than the density of biomass, as well as sticking to the sides of the centrifuge tubes during drying. It was suspected that the centrifugation could have been destroying cells that became fragile due to high accumulation of PHB, and consequently could have been left in that biofilm/EPS-like formation without being subjected to PHB analysis. Therefore, in this study, pellets dried at 55^{o}C for 24 hours that would be subjected to PHB analysis were obtained by one of two methods listed below:

- Method 1: Adding 2 mL chloroform directly into centrifuge tubes containing dried pellets, solving the pellets in chloroform and transferring the mixture to methanolysis vials (Direct addition of chloroform).
- Method 2: Removing as much material as possible from centrifuge tubes, weighing the obtained material in analytical balance, transferring the material to methanolysis vials and then adding 2 mL chloroform onto the recovered material (Addition of chloroform after weighing).

Any difference in the observed PHB would be due to inability to accurately obtain and weigh the aforementioned second oily, cloudy formation (ii) occurring after drying the centrifuged pellets. In other words, of the two formations occurring after

the drying of the centrifuged pellets, the method involving addition of chloroform directly into centrifuge tubes is able to successfully obtain formations (i) and (ii), whereas weighing the dried pellet and transferring the pellet to methanolysis vials inevitably leaves some of the formation (ii) in the container. It can be interpreted that the difference between the two methods of obtaining the biomass would be due to the PHB present outside of the cells, separated during centrifugation of the biomass. To express the results, PHB accumulation as % of cell dry weight was compared in Figure 4.10 to account for the possible release of PHB from microbial cells to outside of the cells due to centrifugation.

Along with the samples obtained from control, WT and YO3 reactors, a blank sample containing only 2 mL chloroform was also analyzed for its PHB content to negate the possibility of errors due to contaminated equipment or problems with the instruments.

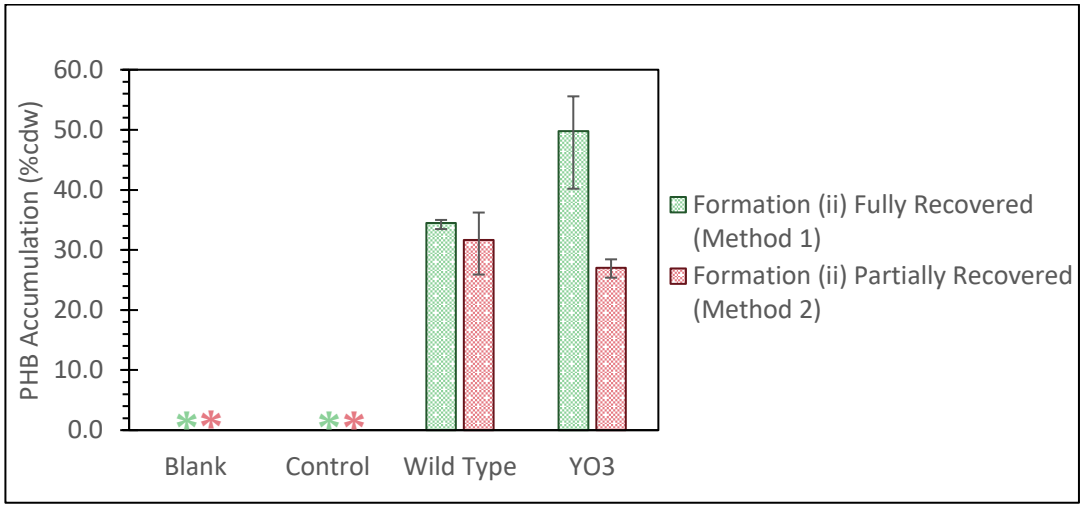

Figure 4.10. Observed PHB accumulation as % cdw for drying for 24 hours at 55^{o}C, using two methods to obtain dried microbial pellets, involving partial and full recovery of formation (ii). The asterisk (*) indicates zero values within measurement sensitivity.

Error bars represent the data of highest and lowest accumulating reactors in the figure above. The difference between two methods was not observed to be significant in WT strains with similar PHB accumulation observed for both methods, with an average of 34.5 % and 31.6 % for samples obtained with Method 1 and Method 2,

respectively. In the case of YO3 strains, very significant difference in results was observed as an average of 49.8 % and 27.0 % PHB accumulation. This significant variance in results supported the previously stated over-accumulation of PHB resulting in the bursting of cells during centrifugation and releasing PHB granules to the biofilm phase, preventing precise quantification via conventional weighing methods.

A relatively insignificant difference of 4.6 % PHB accumulation was observed between WT and YO3 strains using Method 2. This result also supports the hypothesis of a critical PHB accumulation or a weaker cellular structure of YO3 strain. YO3 cells with higher PHB accumulation might have gotten disrupted in centrifuge and only PHB from intact cells could have been quantified, thus yielding approximately same results as the WT strain. In the case of WT strain, most of the cells could have remained undisrupted during centrifuge, possibly due to cellular structure of WT being stronger than YO3 or the latter strain accumulating more PHB and becoming fragile.

4.1.2 PHB Losses During Drying

Methodology used in the PHB quantification by preliminary studies (data not shown) included freeze-drying of the biomass pellets to be able to reliably quantify the weight of the cells and consequently expressing the amount of PHB accumulation (as weight of PHB) per unit weight of microorganisms. However, it was observed that the biomass became increasingly electrostatic especially after prolonged reactor operation, resulting in difficulties in accurately weighing the dried biomass and prone to errors, regardless of the drying method used.

Previously used PHB analysis method was based on the method described by Braunegg *et al.* (1978). In Braunegg's article it is stated that the centrifuged pellets are practically ready to be methanolysed without any further processes applied. The method had been modified to include a freeze-drying step to be able to determine

weight of pellets without subjecting the pellets to heat, in order not to propagate premature degradation of PHB during drying (Özsoy Demiriz *et al.*, 2019). As stated, however, drying has its own disadvantages with the electrostatic effects being the most significant one, along with possible losses of biomass in drying and degradation of PHB.

Due to reasons listed above, PHB content of the biomass was also determined in this study without applying a drying process. Dry weight of the biomass was calculated using the optical density readings at the time of the PHB sampling. 2 mL chloroform was directly added to the centrifuged pellet in centrifuge tubes similar to the process described in Section 4.1.1. It was assumed that no biomass was lost during resuspension of the biomass in chloroform. Along with a no-drying method, effect of drying the pellets at 55°C for 24 hours was also investigated since freeze-drying equipment is not widely available and is an energy intensive process. It was aimed to observe the possibility of using heat-drying process (i.e., heat-drying at 55°C for 24 hours instead of freeze-drying at -80°C for 24 hours) if the drying step cannot be omitted at all.

Figure 4.11 depicts the average observed PHB accumulation for both strains, using three different pretreatment methods. Error bars show the highest and lowest observed PHB accumulation for the respective strain and method.

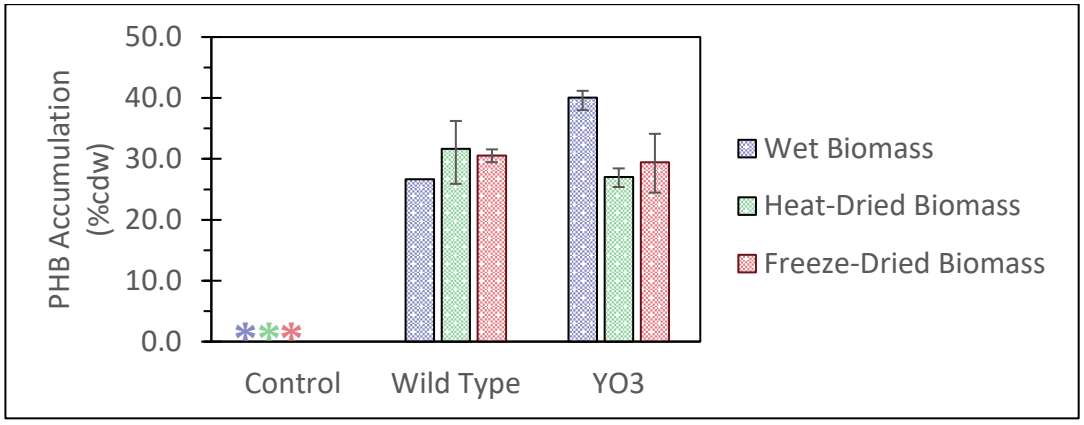

Figure 4.11. Observed PHB accumulation as % of cell dry weight using three different methods of drying. The asterisk (*) indicates zero values within measurement sensitivity.

It is seen that both WT and YO3 strains yield approximately similar % PHB accumulation for heat-drying and freeze-drying methods. Average % PHB accumulation was observed as 31.6 % and 30.6 % for WT strain for heat-drying and freeze-drying methods, respectively. For YO3 strain, average % PHB accumulation was observed as 27.0 % and 29.4 %, respectively. In the case of no-drying; however, the results differed drastically. Reactors inoculated with YO3 strain were observed to accumulate an average of 40.1 % PHB, compared to 26.7 % average PHB accumulation observed for WT strains. Observed PHB did not change drastically when using different drying methods for WT strain, but, in the case of YO3, a relative 11.9 % increase in the observed PHB was seen while using no-drying method (shown as wet biomass in Figure 4.11). This might be a result supporting the hypothesis stated in the previous section (Section 4.1.1), where effect of centrifuging was investigated. Since in the no-drying method pellet must be obtained by direct addition of chloroform without weighing the pellet as well, increase in observed % PHB might be due to inclusion of PHB polymers to the analyses which might have been separated from the cells and released to the media. The results also supported the fact that the YO3 strain might have been accumulating either much higher amounts of PHB such that over-accumulating cells burst during centrifuge, or that the YO3 strain has a weaker cellular membrane than WT counterpart, again, resulting in destruction of the cells during centrifugation. In either case, separated mushy-cloudy compound (i.e., formation ii) which was observed especially after centrifuging of YO3 samples, can only be obtained completely by directly adding chloroform into centrifuged pellets without removing the pellets from the centrifuge tubes. Complete recovery of formation ii seems to contribute to the observed PHB % significantly. In Figure 4.12b, the separated formation ii can be seen more clearly.

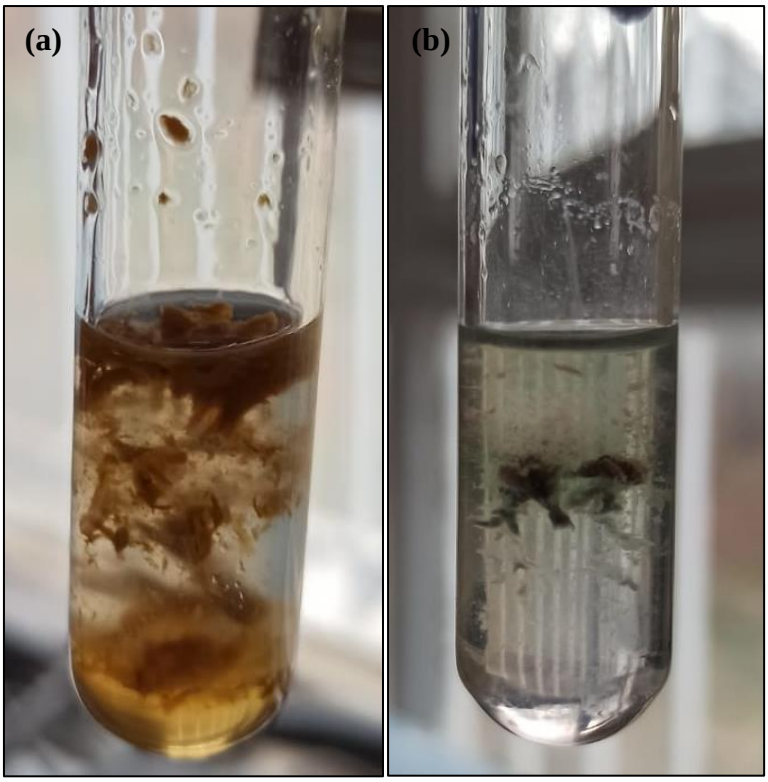

Figure 4.12. (a) *R. capsulatus* WT and (b) *R. capsulatus* YO3 samples in chloroform/acidified methanol mixture.

4.1.3 PHB Losses During Methanolysis

Methanolysis process, where bacterial pellets mixed with chloroform and acidified methanol were subjected to 100^{o}C temperature for 4 hours, was also identified as a possible source of PHB loss. This is due to the fact that if methanolysis does not complete fully, PHB molecules will not be monomerized into hydroxybutyric acid methyl ester and consequently, cannot be quantified by the GC. To investigate PHB losses during methanolysis, 2 mg of pure PHB standard was added to the biomass/chloroform/methanol mixture right before sealing of the tubes and initiation of methanolysis. In theory, samples with PHB standard addition and without addition should yield exactly 2 mg of PHB difference at the end of quantification via GC. Samples from control, WT and YO3 reactors were compared for both wet biomass and freeze-dried biomass to observe whether drying process would impact the

efficiency of methanolysis. A blank sample containing only chloroform and chloroform + 2 mg PHB standard was also analyzed to account for the errors that might have caused by the instruments. Figure 4.13 depicts the results of the observation.

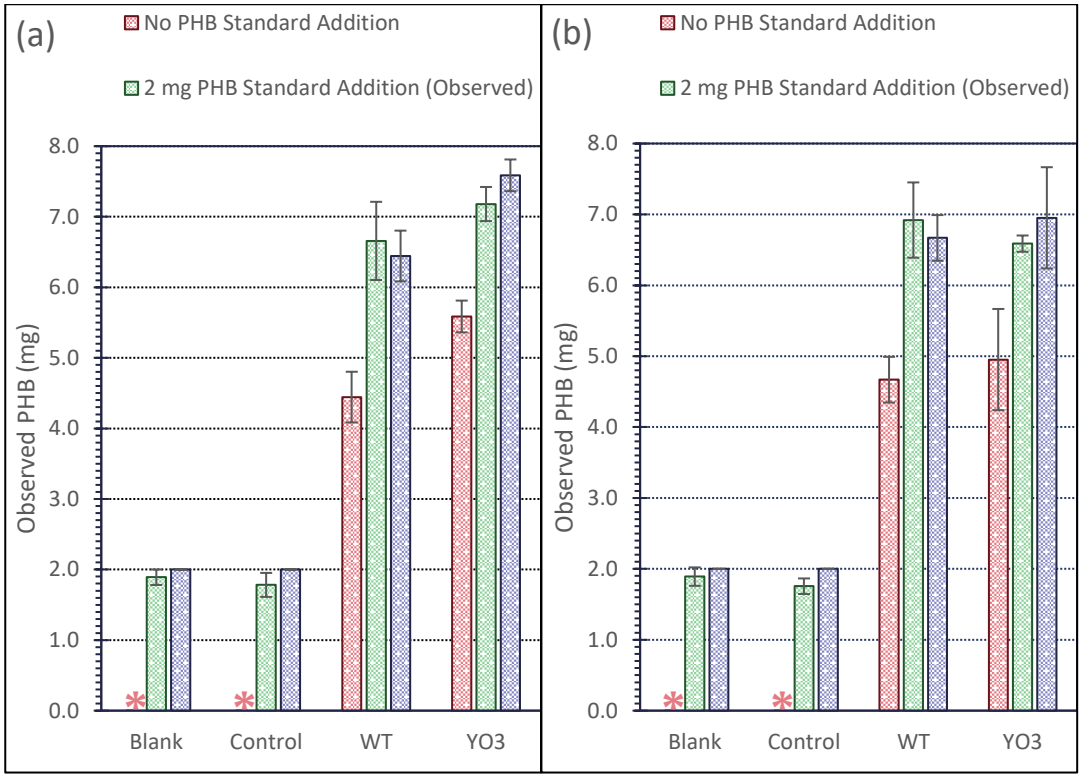

Figure 4.13. Average PHB observed (mg) among samples that did not contain PHB standard, that contained PHB standard and theoretical PHB that should have been observed for (a) Wet biomass and (b) Freeze-dried biomass. The asterisk (*) indicates zero values within measurement sensitivity.

In Figure 4.13, for WT and YO3 samples, error bars represent the standard deviations among triplicate reactors. For control and blank samples (containing no biomass), triplicate GC injection from single sample was made and error bars indicate standard deviation of three consecutive injections. Closer the observed PHB amount in the samples to theoretical PHB amount, less loss in methanolysis was observed. Status of the instruments and calibration curve was verified with the blank sample yielding 1.89 mg of PHB, which is 5.5 % less (0.11 mg) than the theoretical 2 mg PHB difference, as well as control reactor yielding approximately same amount of PHB

for no-drying and freeze-drying conditions, as 1.78 mg and 1.76 mg, respectively. Note that there was almost no solid content remaining in the centrifuge tube after centrifuging the control reactor since there was no presence of biomass, hence control sample can also be considered the same as the blank sample.

Since no-drying method included very small volumes of H_2O within the centrifuged pellets that can only be removed by drying, impact of presence of H_2O on efficiency of methanolysis could also be observed to not have a significant impact. Control, WT and YO3 samples were observed to have approximately similar amounts of average PHB difference (0.02 mg, 0.04 mg and 0.05 mg for control, WT and YO3, respectively) with respect to their counterparts without PHB standard. Therefore, it can be said that if the biomass was to be subjected to PHB analysis without drying, presence of H_2O left in the pellets did not affect the result.

In no-drying case, WT reactors yielded an average of 2.21 ± 0.30 mg PHB difference compared to 2.00 mg of theoretical difference, corresponding to 10.5 % more PHB observed. YO3 reactors had 1.59 ± 0.38 mg average difference, corresponding to 20.5 % less PHB observed than expected. Despite the difference in the observed PHB, error margins included theoretical 2 mg difference, therefore it can be stated that no losses in PHB occur during the methanolysis. This statement was also proven by the blank and control samples, which were observed to have 1.89 ± 0.11 mg and 1.78 ± 0.17 mg average PHB difference, respectively.

Despite error bars containing the expected PHB difference, it might be speculated that there might have been other reasons that made the reactors differ from each other since triplicate reactors of the same strain did not have such differences among each other. All samples contained same amount of PHB standard, yet PHB was observed more in WT reactors than the theoretical amount and less than theoretical in YO3 reactors. A possibility is that there might have been an extracellular substance likely to be linked with the hydrogenase enzyme and produced by only one of those strains which enhanced or inhibited the methanolysis rate of PHB. If the said substance is an inhibitory compound, it would have been produced by YO3 strain or if the

compound is a co-enzyme for uptake hydrogenase, it might have been accumulated in the media without being utilized by the YO3 strain. It is possible that a compound with aforementioned properties might have been interfering with the methanolysis process and binding the methyl radicals. This case would have left no methyl radicals in the solution to bind with hydroxybutyrate. Conversely, the compound might have enhancing properties on either hydrolysis of poly-hydroxybutyrate or methanolysis of hydroxybutyrate. This case implies that the compound should have been found more in the reactors with WT strain.

The latter case would also mean that the pure PHB standard had not been hydrolyzed into its monomers to begin with. This would have resulted in incomplete transesterification reaction. Consequently, GC would have been calibrated with sub-optimal purity of hydroxybutyric acid methyl ester solutions. It was decided that this case would be a subject to further verification, where commercially available hydroxybutyric methyl ester solution should be prepared to have same number of moles as a PHB standard solution would have at the end of stoichiometrically 100 % efficient methanolysis. Peak signals from the GC for both hydroxybutyric acid methyl ester standard solution and derivatized poly-hydroxybutyric acid standard solution should be compared. Any difference would indicate incomplete transesterification reaction taking place when preparing methyl ester standards from derivatization of PHB standard.

There was also the possibility of human errors, with most prevalent errors resulting from working with small masses and volumes, such as inaccurate weighing of 2 mg of PHB standard, losses during the transfer of weighted PHB into samples, non-homogenous sampling from reactors, slight volume changes from evaporation of chloroform as the solvent and chemical contamination in the reaction vessels.

4.1.4 Summary of Results of Set 1

For the operated set, peak hydrogen productivities were observed as 0.41 ± 0.09 mmol/L·h and 0.53 ± 0.03 mmol/L·h for *R. capsulatus* WT and *R. capsulatus* YO3 strains, respectively. In this context, the highest PHB accumulation was observed as 36.2 % for WT, using heat-dried biomass for PHB analysis while a maximum of 45.3 % PHB accumulation was observed for YO3 strain with wet biomass. PHB accumulation was observed to be approximately same for WT and YO3 when biomass was dried (for both heat-drying and freeze-drying). An average of 4.6 % and 1.2 % difference in accumulated PHB was observed using heat-drying and freeze-drying methods, respectively. However, analysis of wet biomass yielded 13.4 % more PHB accumulation in YO3 strains. Assuming that no further PHB was being accumulated during the analysis, this result indicates that the recovery of PHB from dried YO3 cells was less efficient compared to wet biomass.

Observing higher substrate consumption (WT: 40.03 ± 2.99 mM, YO3: 50.92 ± 11.26 mM acetic acid), higher cumulative hydrogen production (WT: 69.93 ± 8.00 mL, YO3: 81.50 ± 7.02 mL), less growth (WT: 1.04 ± 0.01 gcdw/L, YO3: 0.93 ± 0.01 gcdw/L), less by-product formation (WT: 24.68 ± 0.32 mM, YO3: 21.19 ± 1.62 mM formic acid) and more PHB accumulation (WT: 28.47 ± 2.30 %, YO3: 40.05 ± 1.61 %), and the fact that there is no study regarding the PHB accumulation, *R. capsulatus* YO3 strain was selected as the strain to be used in consequent sets. Summary of results can be seen in Figure 4.14.

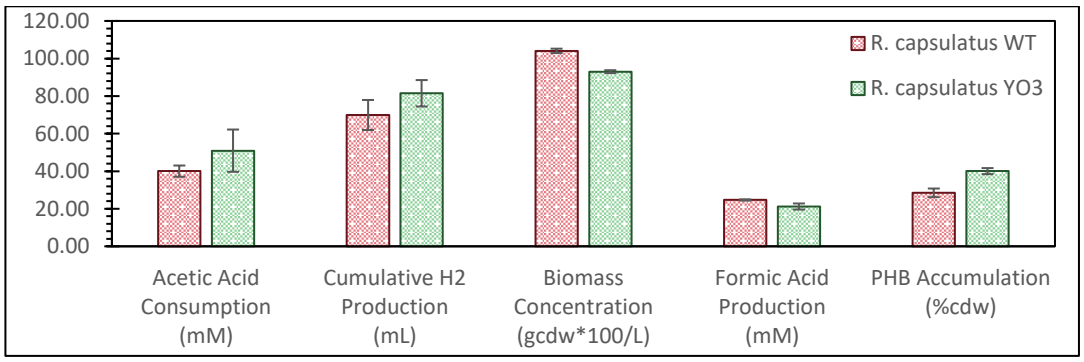

Figure 4.14. Summary of results obtained during the operation of Set 1.

Moreover, PHB analysis procedure was modified to omit the drying step due to observation of higher recovery rates and to conserve time and energy in the analysis steps. Consequent sets are conducted using methanolysis of wet biomass.

4.2 Results of Set 2: Effect of Na^+ Concentration

Second set was operated in fed-batch mode over the course of 79 days, with various dilutions to keep the reactors running. A total of 8 reactors were operated with 4 containing acetic acid as the primary carbon source and 4 containing sucrose as the primary carbon source. In other words, for each carbon source, 1 control and 3 test reactors (replicates) were set-up. Relation between substrate consumption, hydrogen production and PHB accumulation was investigated for all the reactors. Reactor operation timeline was divided into numerous phases, listed in Table 4.2 and Table 4.3, respectively, for acetate and sucrose-containing reactors in their own respective sections.

4.2.1 Acetate-Containing Reactors

Table 4.2 shows the phases and days of phases during the operation of acetate-containing reactors. During the first 4 days of Phase I, only 5 mL sampling was done daily to allow for sufficient growth of the biomass. All the parameters listed in Section 3.4 were measured except for PHB, which requires larger sampling volume. Starting in Day 5, sampling volume was increased from 5 mL to 20 mL and PHB content was measured on a daily basis, employing modifications to PHB analysis procedure that had been determined during Set 1 (See Section 4.1). At Day 44, reactor activity had almost faded away, due to increasing sodium concentrations in the reactors. Therefore, reactors were diluted with PHB and H_2 production medium on Day 44 to decrease the sodium concentrations drastically, indicating the start of Phase II of operation. After dilutions, reactor activities resumed. Before cessation of the reactor operation, effect of light/dark (L/D) cycles were also investigated (Days

61-64). Primary reason for L/D operation is that there had been a suspicion of a possible H_2 production via dark fermentation pathway in sucrose-containing reactors owing to their high H_2 and CO_2 productivities (further discussed in Section 4.2.2.2). Acetate-containing reactors were also subjected to L/D operation in line with sucrose-containing reactors. At Day 69, reactors were diluted once again (Phase III) to decrease the sodium concentration before concluding the run at Day 79. Reason for second dilution was also to be in line with sucrose-containing reactors, in which color of the strain had faded almost completely due to accumulating Na^+ ions. It was aimed with the dilution to investigate whether the loss of biomass color in sucrose-containing reactors was a reversible process and consequently, acetate-containing reactors were diluted alongside the sucrose-containing reactors.

Table 4.2. Phases of operation in Set 2 for acetate-containing reactors.

Phase	***Days***	***Description of the Phase***
I	0-44	Increasing Na^+ conditions
II	45-69 (61-64)	Operation after 1st dilution period (Investigation of light/dark cycle effect)
III	70-79	Operation after 2nd dilution period

4.2.1.1 Operational Indicators

pH of the reactors throughout the operation can be seen below in Figure 4.15. Reactors had started operation with initial pH set to 6.80 – 7.00. pH was initially intended to be controlled; however, it was seen that the pH value was stable around 7.20 during most of the time of operation. Hence, instead of constantly decreasing pH with HCl solution and therefore increasing the overall ionic strength of the working volume due to constant influx of Cl^- ions, it was decided to operate the reactors at the equilibrium pH of around 7.20 and observe the accumulation of Na^+ ions.

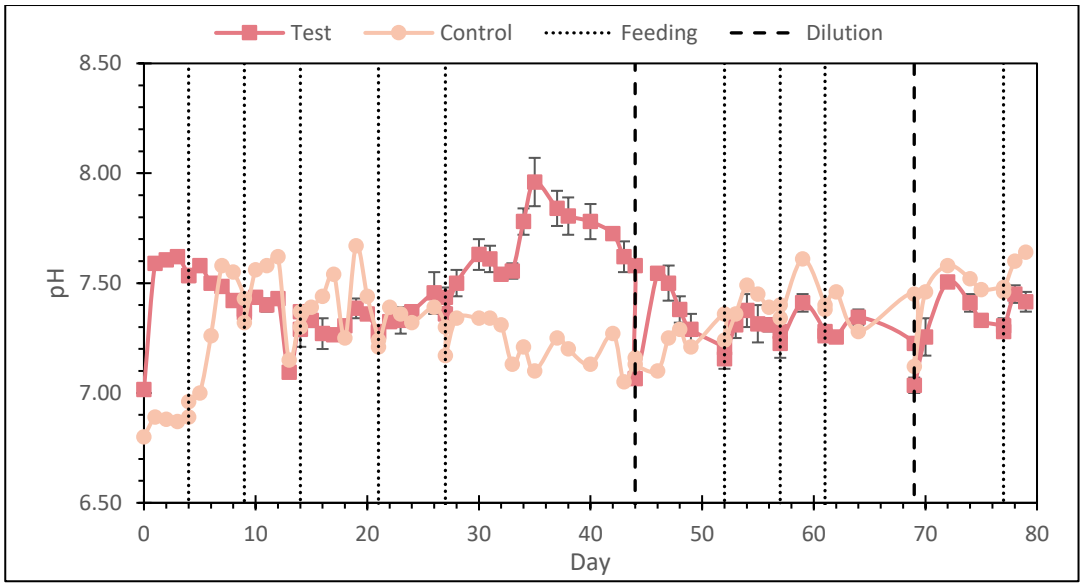

Figure 4.15. pH of acetate-containing reactors in Set 2. Error bars indicate upper and lower values of duplicate reactors.

Reactors were started with initial cdw value of 0.2 g/L; however, control reactor got contaminated with inoculum right after the first feeding (t = 4 days). Reason of contamination was most likely due to a sampling injector. Biomass concentration of the reactors can be seen in Figure 4.16. Biomass concentration peaked at Day 4 with 0.913 gcdw/L, where only 5 mL sampling had been done daily. Once sampling size was increased to 20 mL, an overall slight decrease was observed throughout the run. Despite the slow decline, it can still be said that biomass concentration was maintained generally steady between 0.8 – 0.9 gcdw/L until 5th feeding at Day 27. Significance of the inoculation ratio was also observed with the contamination of the control reactor. As seen in Figure 4.16, control reactor followed almost exactly the same trend with the test reactors, peaking at 0.822 gcdw/L, which had also occurred 4 days after contamination. In the case of control reactor, inoculum volume due to the contamination could not have been any larger than a droplet, hence control reactor could only reach until 0.822 gcdw/L compared to 0.913 gcdw/L of the test reactors.

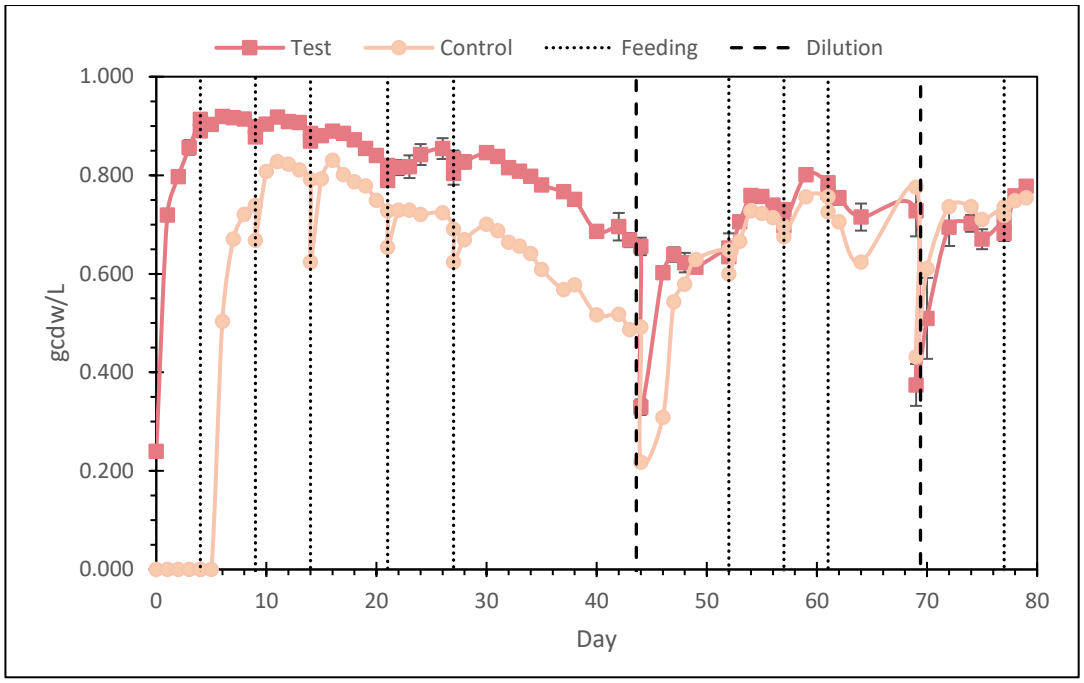

Figure 4.16. Biomass concentrations in the acetate-containing reactors in Set 2 based on OD measurements at 660 nm wavelength. Error bars indicate upper and lower values of duplicate reactors.

With the 4th feeding (Day 21) the highest Na^+ concentration of 4295 mgNa^+/L was reached (Figure 4.17a). After 5th feeding on Day 27, Na^+ concentration reached a second peak at 4059 mgNa^+/L. This concentration was observed to be the threshold value of reactor operation, due to the fact that both the cdw values (Figure 4.16) and hydrogen productivities (Figure 4.21) of the reactors had begun to gradually decrease. Yet, in spite of the decreasing cdw and H_2 productivities, acetic acid consumption rates were similar as the previous days (Days 0 – 21) (Figure 4.18). It might be speculated that consumed acetic acid might be converted to PHB, which would be discussed in Section 4.2.1.3.

pH of the reactors had been kept uncontrolled still, resulting in an increase up to 7.96 ± 0.11 by Day 35 due to degradation of acetic acid but relatively lower production of CO_2 and H_2 to equilibrate the pH. The decrease in Na^+ concentrations between Days 27 – 44 is due to the sampling frequency, where 20 mL sample taken was replaced with BM that contains much less amount of Na^+ ions.

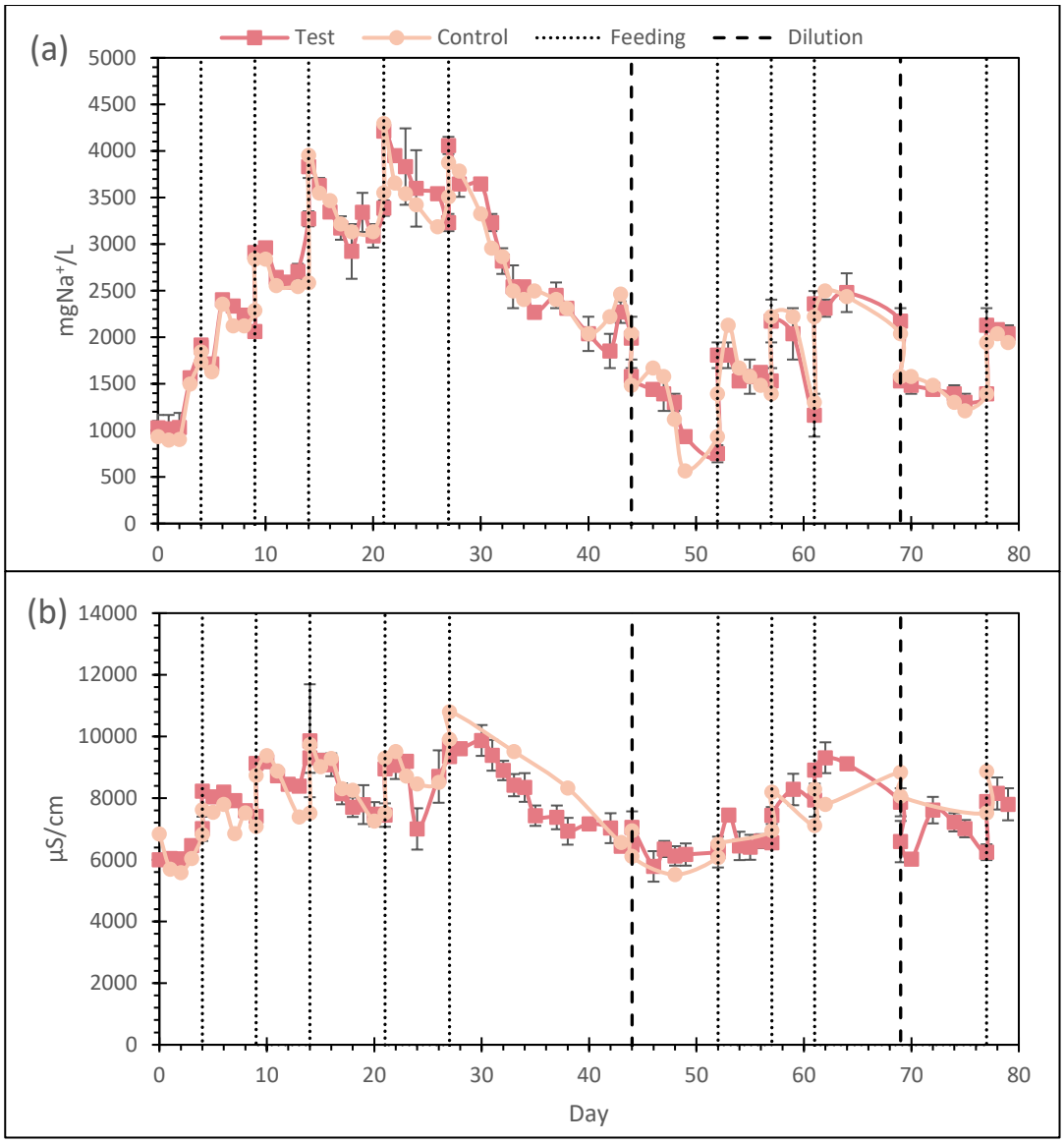

Figure 4.17. (a) Sodium concentrations and (b) conductivities of the acetate-containing reactors throughout the Set 2 operation. Error bars indicate upper and lower ranges of duplicate reactors.

After reaching the mentioned potential threshold Na^+ concentration of around 4000 $mgNa^+/L$ by Day 27 during operation, increase in valeric and hexanoic acid concentrations and decrease in formic and isobutyric acid concentrations were observed alongside the increase in pH in test reactors. Results of organic acids analysis is shown in Figure 4.18.

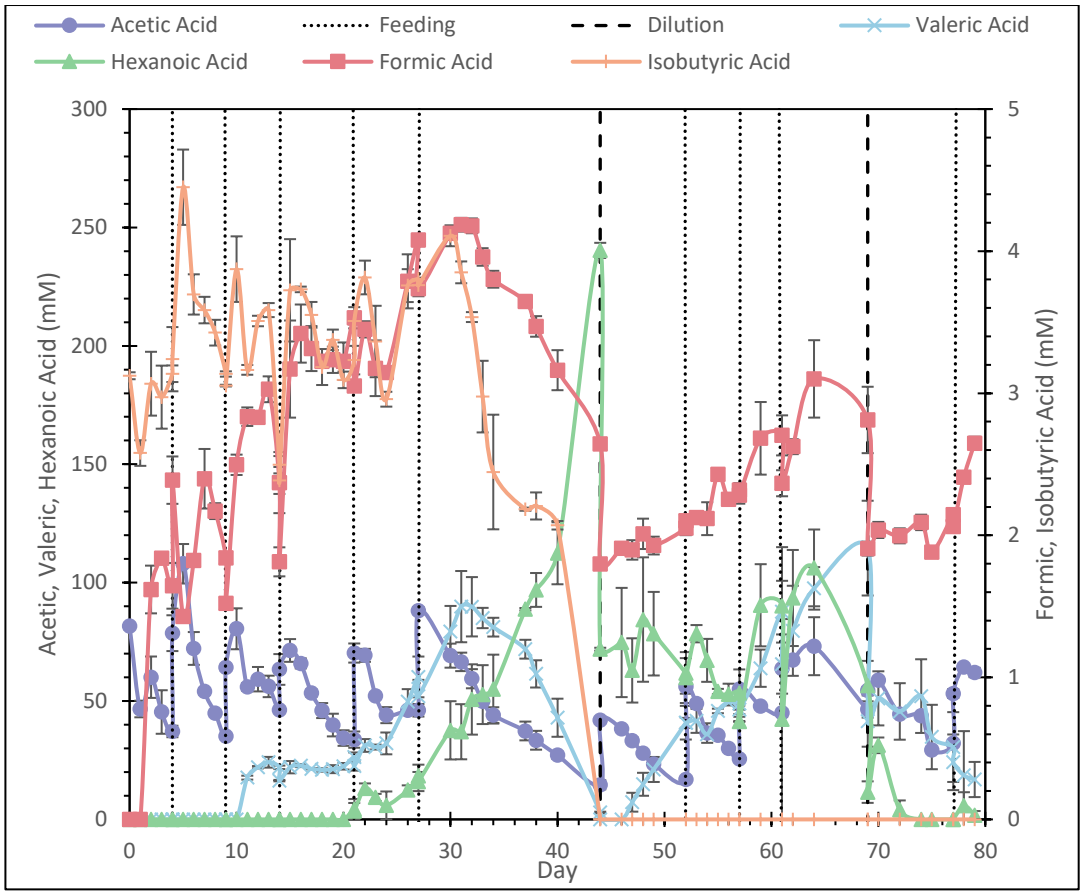

Figure 4.18. Organic acids analysis of acetate-containing reactors of Set 2 in test reactors. Error bars indicate upper and lower ranges of duplicate reactors.

Because control reactor was contaminated at the beginning of the set operation, results of control reactor are not discussed in here anymore but given in Appendix H. Most critical result in terms of organic acids analysis can be stated as the valeric acid and hexanoic acid. Until around Day 21 days, after 4th feeding to be exact, both organic acids were observed to be constant in test reactors (Figure 4.18). However, after Day 21 of operation (4th feeding), valeric and hexanoic acid started to accumulate in the reactors, with valeric acid peaking at 90 ± 15 mM at approximately similar days of maximum PHB accumulation (Day 36 – 38) was observed. It is definite that a shift in the metabolism had occurred after reaching approximately 4 g/L of Na^+ concentration by Day 21, being more apparent for PHB production after Day 27. As said previously, it is also during this time period (Days 27 – 44) that the PHB production peaked as well, as discussed in the following sections (Section

4.2.1.3). No hexanoic acid was observed until Day 21, after which also started to be accumulated, in much larger concentrations. The accumulation in both acids might be the reason of the elevated pH observed in the reactors; smaller organic acid molecules (acetic acid in the feed) might have been converted to larger molecules (i.e., valeric and hexanoic acid) by the YO3.

As mentioned before, heavier acids accumulation started after Day 21, with pH also increasing, possibly resulting in a stress condition together with high Na^+ and/or conductivity that might enhance PHB accumulation, which is discussed in the following sections (See Section 4.2.1.3). Overall, with the increasing pH and/or high Na^+ concentration/conductivity values, previously produced side products formic and isobutyric acids gradually decreased, while valeric and hexanoic acid taking the new form of prevailing side products.

4.2.1.2 Hydrogen and CO_2 Production

At the beginning of the operation, rate of gas production in the test reactors was at its highest, up to an hourly average 5.50 mL/h production, as can be seen in Figure 4.19. For most of the days of the operation, produced gas was quantified to contain ~90 % H_2 (v/v) (Figure 4.20). As said previously, control reactor did not produce any biogas until its contamination at Day 6 (Figure H. 2).

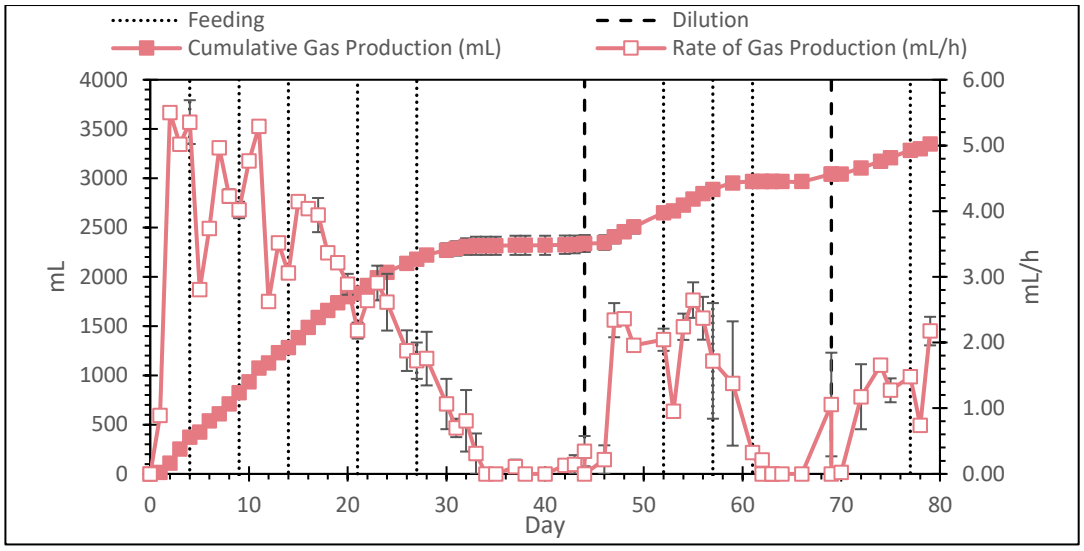

Figure 4.19. Cumulative and hourly biogas production of acetate-containing test reactors in Set 2. Error bars represent upper and lower ranges of duplicate test reactors.

At the end of operation, total produced gas was observed to be approximately ~3300 mL (Figure 4.19). Produced gas was analyzed for its H_2, N_2 and CO_2 content daily, and results are shown for test reactors in Figure 4.20 below. H_2 and CO_2 production of the reactors are shown in Figure 4.21 and Figure 4.22 respectively. Error bars in both Figure 4.21 and Figure 4.22 represent the upper and lower range of duplicate reactors.

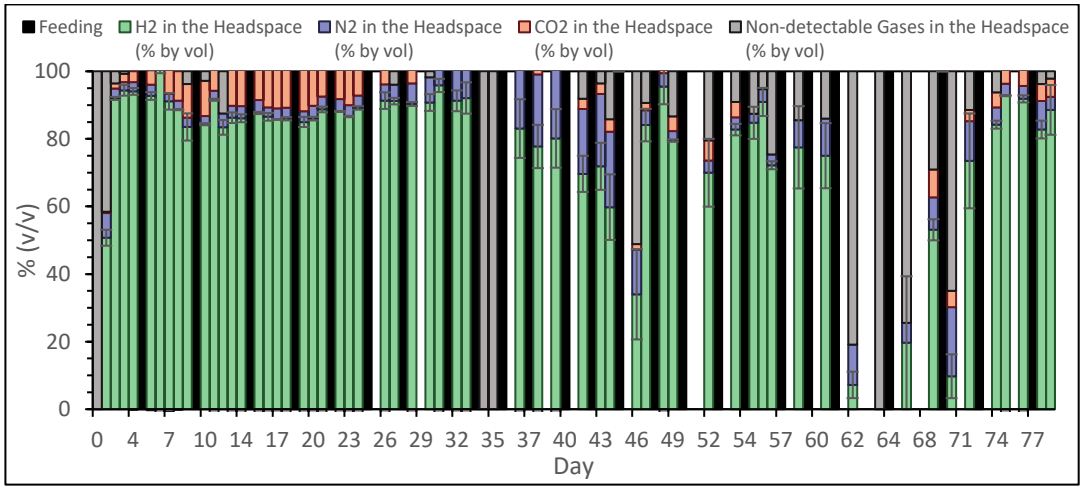

Figure 4.20. Headspace gas composition for acetate-containing test reactors throughout Set 2 operation. Error bars indicate upper and lower ranges for duplicate reactors.

Non detectable gases in Figure 4.20 represent mostly the argon gas which the reactors had been purged with at the beginning of the operation, and prevail during the first days of operation as well as the days when the reactors were diluted (Day 44 and Day 69). Other occurrences of prevalence of non-detectable gases are due to mistakes during the sampling of the reactors. There have been some sampling days where there had been accidental intrusion of O_2 to the reactors. These mistakes were corrected immediately by purging the headspace of the reactors with argon for 4 minutes.

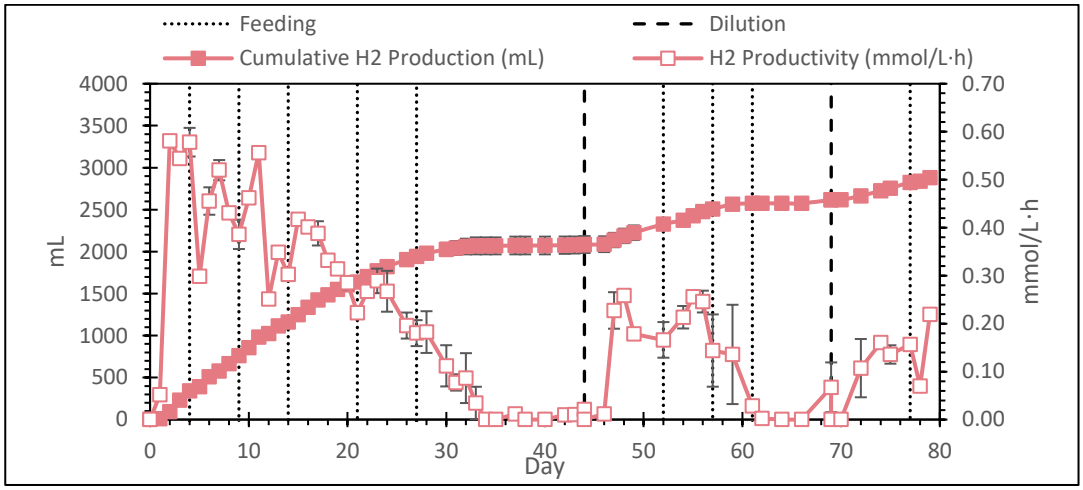

Figure 4.21. Cumulative H_2 production and H_2 productivities observed in acetate-containing test reactors of Set 2.

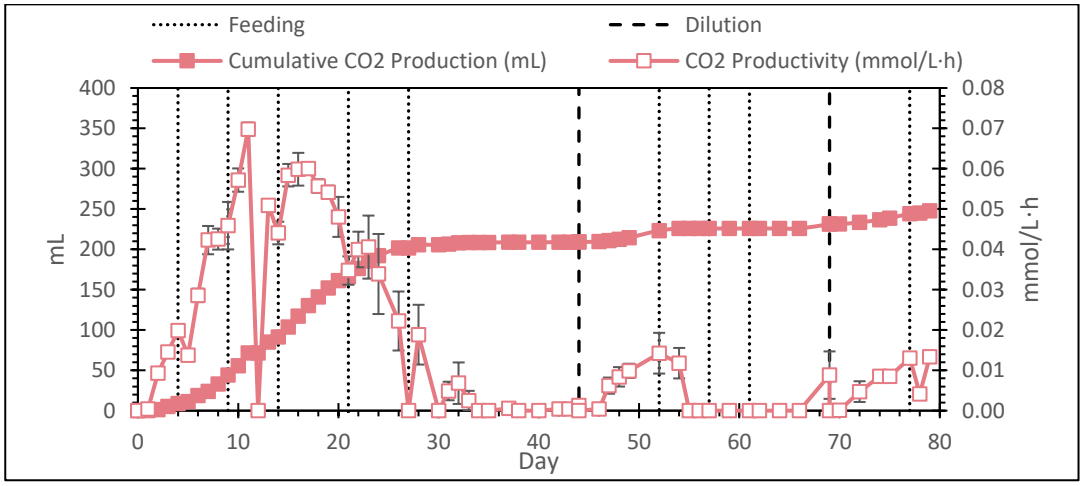

Figure 4.22. Cumulative CO_2 production and CO_2 productivities observed in acetate-containing test reactors of Set 2.

Since headspace gas composition was more or less constant in test reactors, hydrogen productivities follow the same trend with gas production rate. Maximum H_2 productivity of test reactors was observed as 0.58 ± 0.03 mmol/L·h at Day 4, just before 1st feeding. Productivity values are comparatively higher with respect to the values observed in literature (Section 2.1.3.4), although it should be noted that the inoculum is a unique strain with exact characteristics not known yet, therefore comparative studies are limited. Throughout the set operation, 2881 ± 44 mL of H_2 was produced. A sharp decrease in H_2 productivities were observed in test reactors after Day 21 (4th feeding), and had most likely been caused by the increase in the Na^+ concentration as well as pH of the reactors. Hydrogen productivity of test reactors diminished in 7 days (Days 21 – 28). Much less amount of CO_2 was produced by acetate-containing reactors, totaling for 200 mL for the test reactors (Figure 4.22).

After the observation of the absence of hydrogen production and growth in acetate-containing reactors (Figure 4.21 and Figure 4.16, respectively), reactors were diluted on Day 44 with PHB and H_2 production medium to observe if the hydrogen production and cdw would recover. Dilution effectively lowered Na^+ concentrations back to 1577 mgNa^+/L, with biomass concentration and hydrogen productivities gradually recovering, although not as high as the first days of reactor operation (Days 0-4). Maximum hydrogen productivity of test reactors after 1st dilution was observed as 0.26 ± 0.01 mmol/L·h (Figure 4.21).

To understand if there had been a dark fermentative pathway for CO_2 and H_2 production in the reactors, light dark (L/D) cycle operation was performed for 4 days between Day 61 – 64. The reason was that the observation of very high CO_2 production in sucrose-containing reactors and whether it could have been a product of dark fermentation. In parallel with sucrose-containing reactors, acetate-containing reactors were also subjected to L/D operation. No hydrogen production was observed in acetate-containing test reactors during the dark phase of L/D operation, with minimal production in light phase. This reveals that hydrogen production in acetate-containing test reactors was solely due to photofermentation.

2nd dilution for acetate-containing reactors was made on Day 69 in parallel with the sucrose-containing reactors, with the primary aim for the acetate-containing reactors being reducing the Na^+ concentrations to recover the hydrogen production. Na^+ concentration was reduced to 1531 mgNa^+/L with the dilution (Figure 4.17a) and H_2 production recovered, although with even lower productivity than that of 1st dilution. Maximum hydrogen productivity of test reactors after 2nd dilution was observed as 0.22 ± 0.01 mmol/L·h (Figure 4.21).

4.2.1.3 PHB Production

Consistent with the results obtained for organic acids accumulation and pH throughout the run, PHB accumulation was observed to peak after 5th feeding (on Day 27), as seen in Figure 4.23.

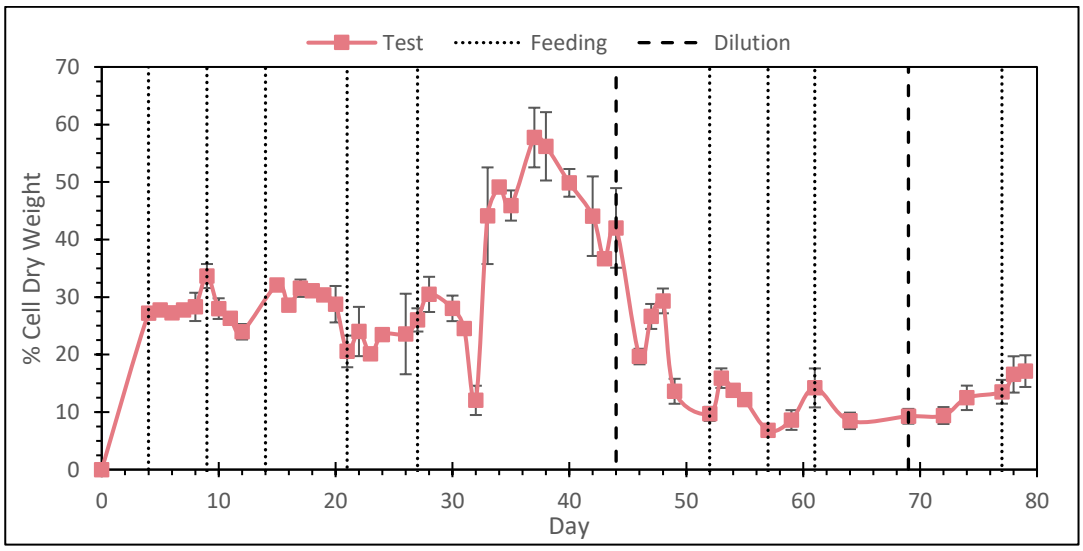

Figure 4.23. PHB Accumulation of acetate-containing reactors of Set 2. Error bars represent the upper and lower PHB values in duplicate reactors.

Until the critical Na^+ concentration of 4 g/L (Figure 4.17), PHB accumulation of the reactors remained rather stable. PHB accumulation of the reactors were thought to be linked to a number of factors, with pH and Na^+ concentrations being the most significant ones. At Day 14, valerate was observed in the reactors for the first-time

during operation, with H_2 production starting to decrease on this day. Na^+ concentration at Day 14 was observed to be around 3900 mgNa^+/L. Until the next feeding on Day 21, valerate remained stable with no consumption or production. With the feeding on Day 21, peak Na^+ concentration of 4295 mgNa^+/L was reached. This critical concentration also marked the beginning of the increase in valerate and hexanoate (Figure 4.18) and also pH (Figure 4.15). A second Na^+ peak was reached with feeding on Day 27 as 4059 mgNa^+/L. With the second Na^+ peak, rate of increase of valerate, hexanoate and pH increased. Valerate was observed to be at its highest concentration on Day 32 as 90 mM (Figure 4.18). pH of the reactors peaked at 7.96 on Day 35. Following the peak value of pH, highest PHB accumulation was observed as 57.7 % of cdw on Day 37. A delayed effect might be speculated in this case, where valerate, pH and PHB peaked at Days 32, 35 and 37, respectively. As mentioned before, hydrogen productivity had started decreasing (Figure 4.21) once Na^+ concentration was reached to 3900 mgNa^+/L, and completely ceased on Day 34.

As a summary, it was speculated that increasing Na^+ concentrations in the reactors triggered the production of valerate and decline in H_2 production. Starting as early as Day 14, increasing valerate production resulted in the elevated pH in reactors, due to the fact that the overall moles of organic acids decreasing in the reactors (i.e., large number of small acids converted by the strain to small number of larger acids, decreasing the free H^+ ions in the working volume). Increased pH as well as high concentration of Na^+ resulted in a double stress condition which completely eliminated H_2 production and shifted the metabolism completely to PHB accumulation. Maximum PHB accumulation was observed on Day 37 as 57.7 ± 5.2 % of cell dry weight. PHB accumulation of the reactors fluctuated around 25 % until 4 g/L of Na^+ concentration and increased to around 45 % until the dilution at day 44. After the dilution, the metabolism was observed to shift to H_2 production and growth, with PHB accumulation falling to around 10 %.

It is important to note that PHB accumulation was observed to be constant in between feedings, since feeding was applied once acetic acid concentration had decreased to half of its initial concentration. Therefore, assuming relatively similar rate of

degradation for both the carbon and nitrogen source in the feed, it is more important to keep C/N ratio constant rather than keeping both the parameters high. In other words, as long as the reactors do not starve for substrate, PHB accumulation can be sustained and does not degrade when acetic acid concentration becomes lower.

Results of the acetate-containing reactors in terms of PHB production indicated that there was indeed a stress caused by pH and/or Na^+ concentration/conductivity values in the reactors. To further investigate this observation, another set (Set 3) was planned to operate a number of reactors at different pH values on low and high Na^+ conditions (Discussed in Section 4.3).

4.2.2 Sucrose-Containing Reactors

Table 4.3 shows the phases of operation described for sucrose-containing reactors. As with the case of acetate-containing reactors, during first 4 days of Phase I only 5 mL sample was taken daily to allow for sufficient growth of the biomass. All the parameters listed in Section 3.4 were measured except for PHB, which requires larger sampling volume. Starting in Day 5 of Phase I, sampling volume had been increased from 5 mL to 20 mL and PHB content was measured on a daily basis. PHB analysis procedure was modified to suit the needs of the study and had been determined during Set 1 (See Section 4.1). Effect of light/dark cycles was also investigated simultaneously with the acetate-containing reactors towards the end of the Phase I (Days 61 – 64). No decline in reactor activity in terms of hydrogen production was observed during the operation. One dilution was applied on Day 69 due to very high Na^+ concentrations and conductivity values in the reactors, commencing Phase II to see if there would be any enhancement of already present hydrogen production or concentration of the biomass.

Table 4.3. Phases of operation in Set 2 for sucrose-containing reactors.

Phase	*Days*	*Description of the Phase*
I	0-69	Increasing Na^+ and conductivity conditions
	(61-64)	(Investigation of light/dark cycle effect)
II	70-79	Operation after 1st dilution period

4.2.2.1 Operational Indicators

Sucrose-containing reactors in Set 2 required much more frequent feeding and consequently pH adjustment, compared to acetate-containing reactors of the set. Similar with the acetate-containing reactors, feeding was applied once the concentration of the carbon source had decreased to approximately half of its initial value. pH of the reactors was elevated with every feed, back to 6.80 – 7.00. pH values throughout the set operation can be seen in Figure 4.24.

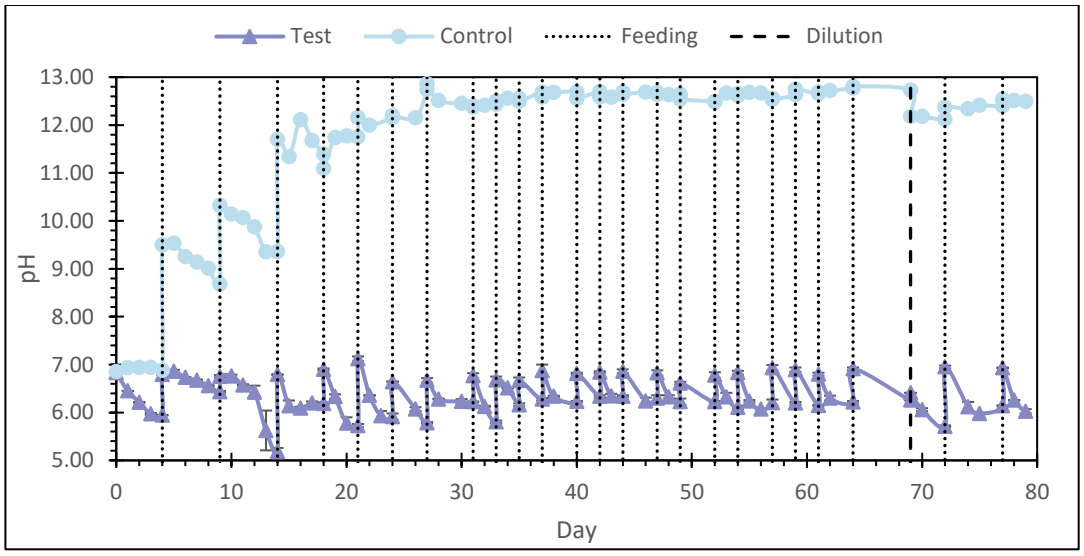

Figure 4.24. pH of sucrose-containing reactors during Set 2 operation. Error bars represent upper and lower range of duplicate reactors.

Same amount of NaOH that had been used to elevate the pH of test reactors was also added to the control reactor (which contained no inoculum), providing the information on the pH that there had been no microbial activity. This constant

addition of NaOH into the reactor with no inoculum resulted in increase in pH well above 12.00 on Day 27 and remained stable until the end of operation.

Biomass concentration in the reactors can be seen in Figure 4.25 below. It was observed that biomass was washed out from the reactors throughout the operation of the set. Despite the decrease in biomass concentration, both substrate consumption rate and hydrogen productivities of the reactors remained similar (Figure 4.28 and Figure 4.32, respectively). However, as stated in Section 3.4.2, cell concentrations in the reactors were derived from the OD values of the reactors. It was speculated that increasing Na^+ and/or salinity in the working volume of the reactors would have resulted in the loss of color of the microbial cells (Figure 4.26). Consequently, the loss of color would have been responsible from the low OD readings of the reactors. To account for this fact, direct measurement of cell dry weight using the method described in Section 3.4.6 was done and proximity of the sampling point to the calibration curve was verified.

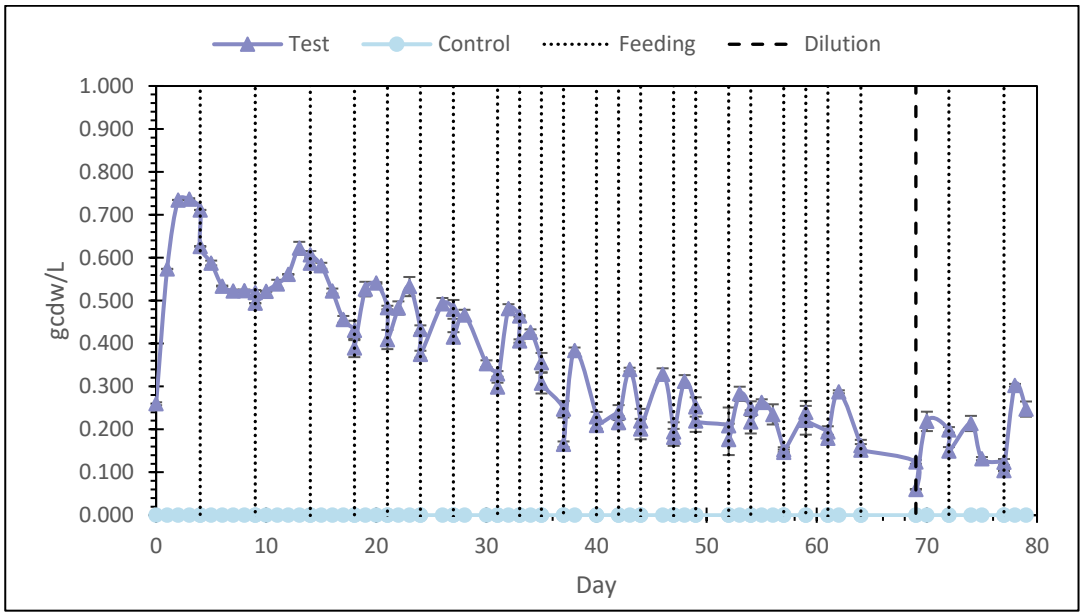

Figure 4.25. Biomass concentration of the sucrose-containing reactors in Set 2 based on OD measurements at 660 nm wavelength. Error bars represent upper and lower range of duplicate reactors.

This observation was also verified with the calibration curve constructed for the sucrose-adapted strains of *R. capsulatus* YO3. Calibration curves for *R. capsulatus* YO3 can be seen in Appendix C Figure C. 2 and Figure C. 3. Comparing the two calibration equations, it was seen that sucrose-adapted strains had a higher slope (y = 0.47x and y = 0.70x for non-adapted and sucrose adapted strains, respectively). In other words, for the same OD reading, sucrose adapted strain yields higher cdw in the presence of NaCl compared to non-adapted strain. This observation may translate to the loss of coloration of the strains. Gradual decrease in the biomass concentration in sucrose-containing reactors throughout the operation can be seen more clearly in the Figure 4.26 below. Dilution on Day 69 was aimed to observe whether reactors would regain their color (consequently, cdw values) during the first days of reactor operation (Days 0 – 12). For this reason, reactors were diluted to decrease the Na^+ concentration and conductivity values, however the inhibition of the biomass due to high Na^+ concentration was observed to be irreversible. In other words, reactors did not regain their color after being exposed to extremely high Na^+ and/or salinity values.

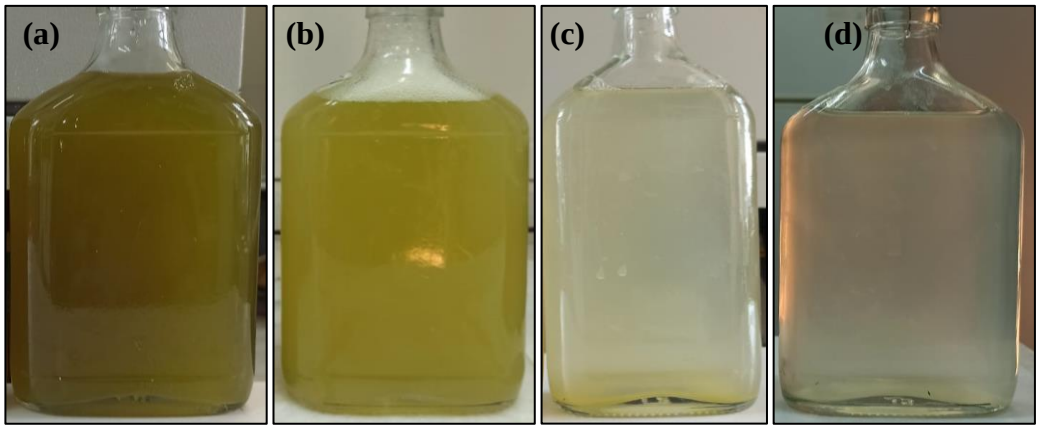

Figure 4.26. *R. capsulatus* YO3 after days of operation in sucrose-containing medium, (a) Day 12, (b) Day 25, (c) Day 48 and (d) Day 79.

Sodium concentration in the sucrose-containing reactors as well as the conductivities of the reactors can be seen in Figure 4.27. Since the sodium input to the reactors was only through feeding and pH adjustment and that the sucrose feed requires much less amount of NaOH to adjust the pH of the feed to 6.80, increase in the Na^+

concentrations of the sucrose-containing reactors were milder relatively to the acetate-containing reactors, in which every feed had been a pulse of Na^+ injection.

As seen in Figure 4.27, there was a gradual increase in Na^+ concentration throughout the operation. Peak sodium concentration was observed as 5127 ± 46 $mgNa^+/L$, after the feeding on Day 61. This result is significant due to the fact that, the following day of the peak Na^+ concentration, maximum rate of biogas production as well as one of the highest H_2 productivities throughout the operation of the set was observed as 16.3 ± 3.1 mL/h and 0.65 ± 0.13 mmol/L·h, respectively for rate of gas production and H_2 productivity (Figure 4.30 and Figure 4.32).

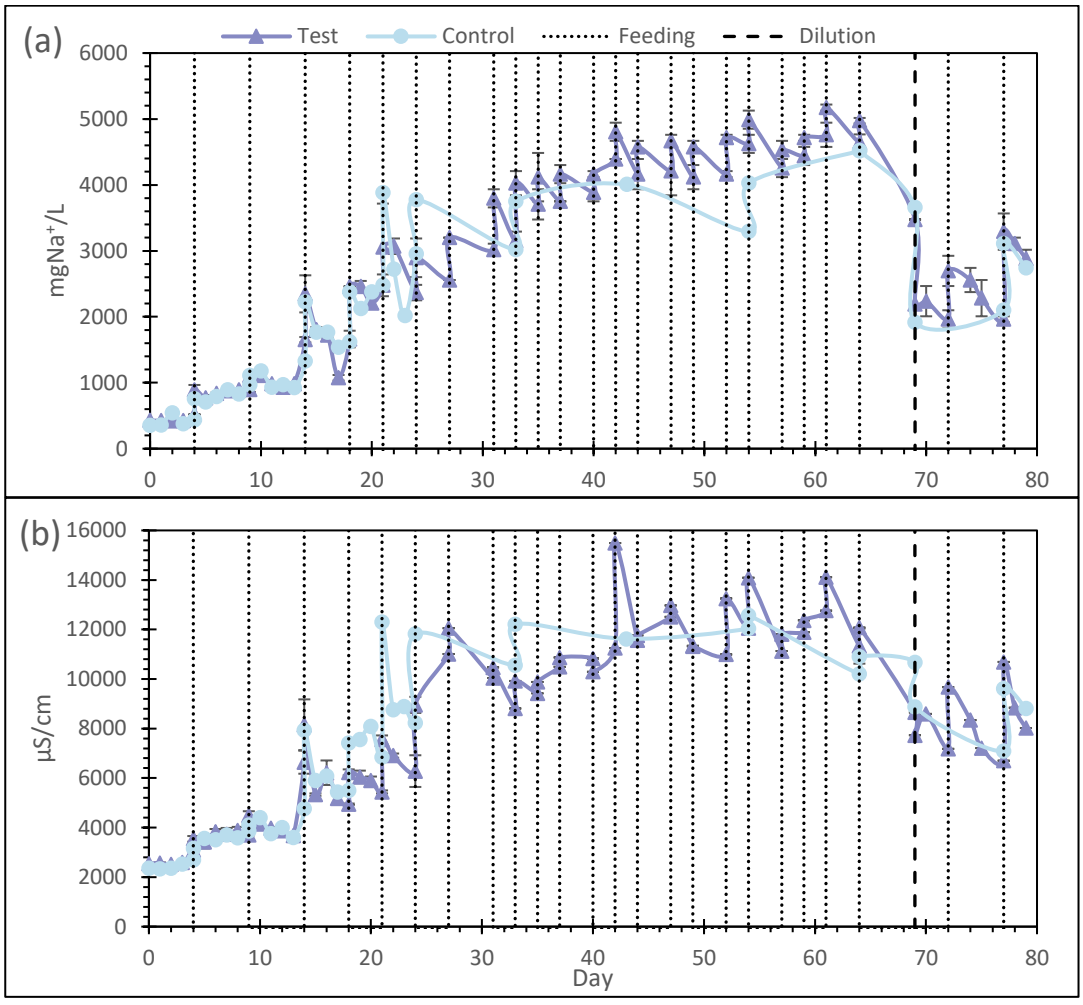

Figure 4.27. (a) Sodium concentrations and (b) conductivities of the sucrose-containing reactors in Set 2 operation. Error bars indicate upper and lower data ranges of duplicate reactors.

Concentrations of sucrose and organic acids are given in Figure 4.28 and Figure 4.29, respectively. Apart from the first 3 weeks of operation, sucrose concentrations in the reactors maintained almost stable around 11 mM, and had been fed once its concentration had decreased around 5.50 mM. Sucrose gradually accumulated in the control reactor due to the absence of microbial activity and eventually became almost equal to the feed sucrose concentration.

Organic acids accumulation differed in sucrose-containing reactors compared to acetate-containing reactors, due to the number of carbon atoms in the substrate, sucrose. It is observed that acetic acid, formic acid, butyric acid, valeric acid and hexanoic acid were the prevalent organic acids that were accumulated in the reactors with the consumption of sucrose, although the accumulation amount and period differed drastically from the acetate-containing reactors.

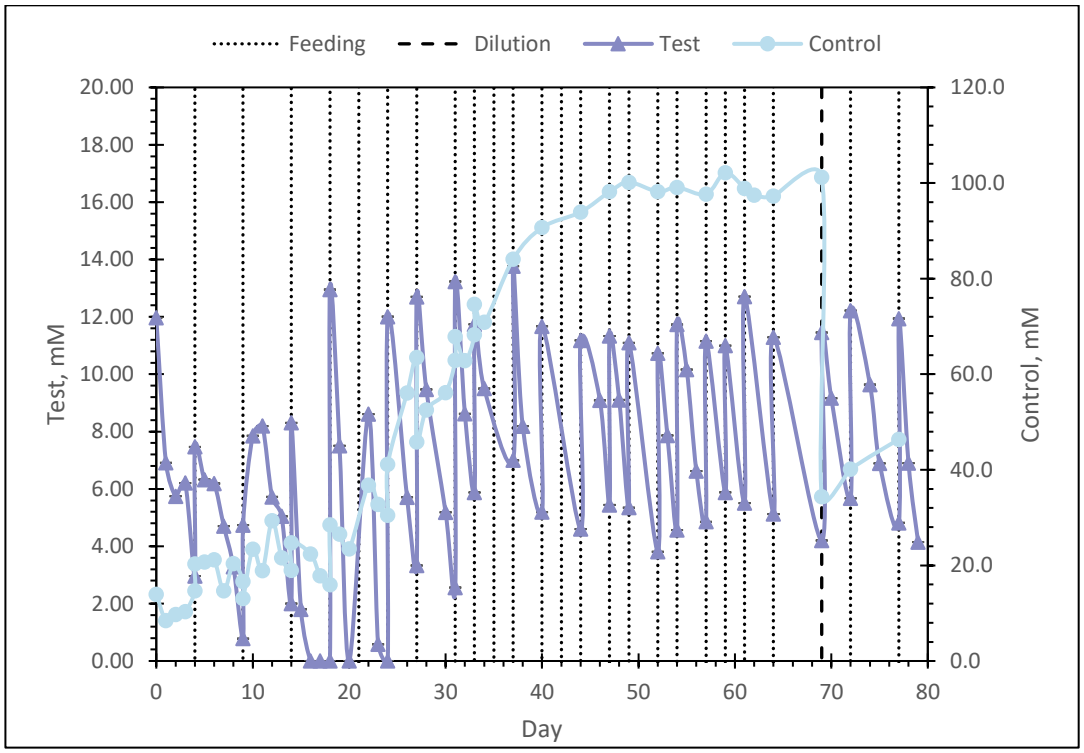

Figure 4.28. Sucrose analysis of sucrose-containing reactors of Set 2. Error bars (Error bar size < Symbol size) represent the high and low data ranges of duplicate test reactors. Control reactor was operated as single reactor.

As expected, almost no organic acids had been produced in the control reactor (Figure 4.29a). In the test reactors, at the beginning of the set operation, valeric acid was prevailing in the test reactors, along with acetic acid and relatively small concentrations of formic acid. Hexanoic acid was observed to increase in concentration until peaking at Day 5 at 48 ± 7 mM and never reached this concentration again throughout the operation. Valeric acid also peaked during this timeframe, at Day 6 as 45 ± 1 mM. It was observed that a shift had occurred with 3rd feed at Day 14, with a clear increase in concentrations of acetic and butyric acid and a decrease in hexanoic acid. Acetic and butyric acid peaked on Day 38 as 49 ± 2 mM and Day 33 as 109 ± 7 mM respectively. Another shift was observed to occur after those peak values of acetic and butyric acids, where formic and isobutyric acids started to be accumulated again with butyric acid decreasing. Dilution of the reactors at Day 69 effectively reduced the concentrations of all the side products back to their initial values, with gas production resuming (Figure 4.30). No PHB production or increase in the cdw of the reactors was observed (Figure 4.25 and Figure 4.33, respectively).

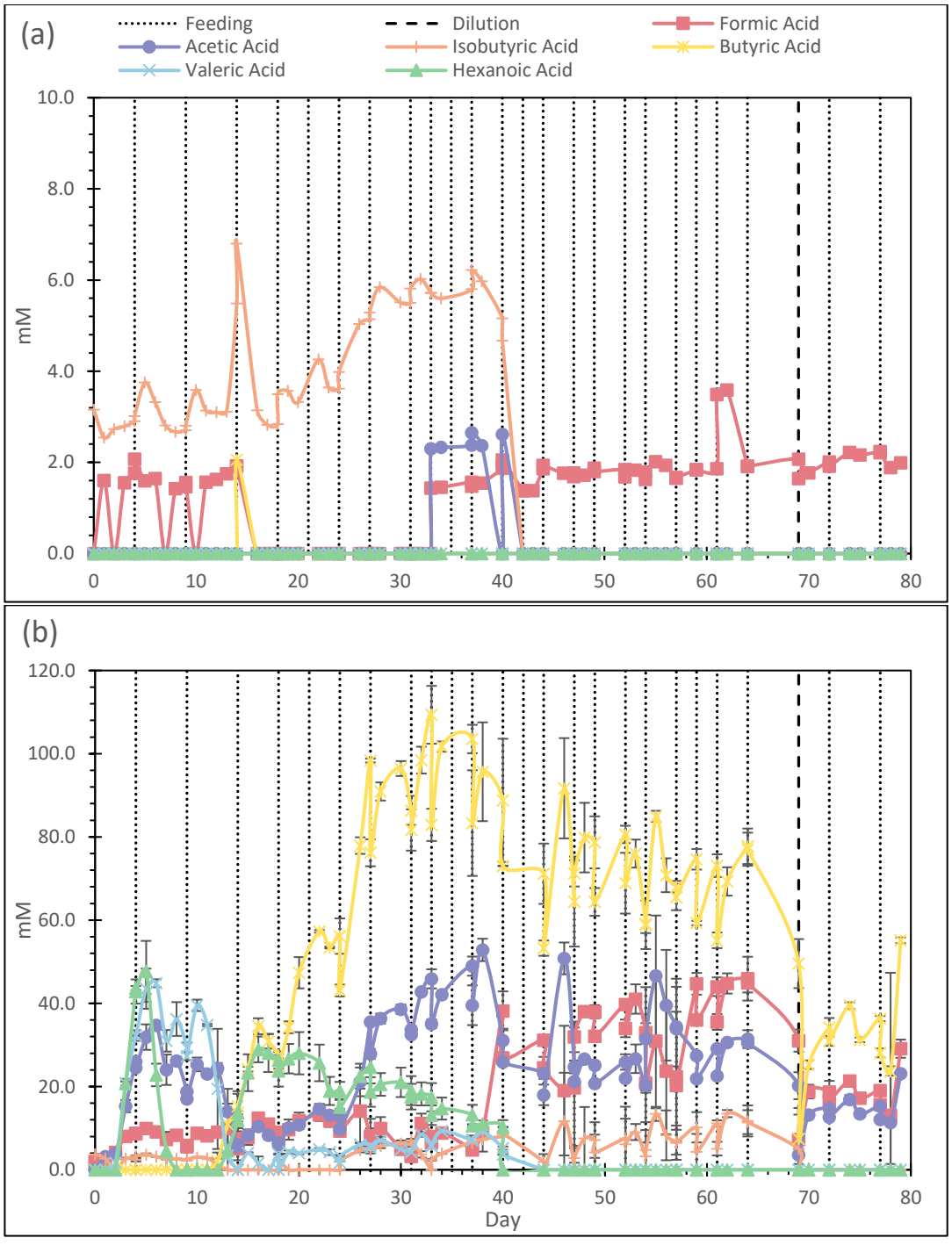

Figure 4.29. Organic acids analysis of sucrose-containing reactors of Set 2, (a) Control reactor (b) Test reactors. Error bars represent the high and low data ranges of duplicate test reactors. Control reactor was operated as single reactor.

4.2.2.2 Hydrogen and CO_2 Production

Biogas production of sucrose-containing reactors can be seen in Figure 4.30 below. Total gas production in sucrose-containing reactors was observed to be almost double the gas production of acetate-containing reactors. However, produced biogas in sucrose-containing reactors included up to 50 % CO_2 compared to 10 % average CO_2 in acetate-containing reactors. Cumulative biogas production at the end of Day 79 was observed to be 7024 mL, with highest rate of gas production observed at Day 62 as 16 ± 3 mL/h. This day with highest gas production is significant for the fact that it was the first lighting period after being kept in dark for 12 hours. This observation would mean that there was a need for an adaptation period which occurred while being in the dark for 12 hours. The following 12 hours of lighting period can be considered as the removal of stress conditions (absence of light) and gas production spiked. Following next days of L/D cycle (after Day 62), gas production was reversed back to the trend during the continuous lighting operation. In other words, there was H_2 production even in the dark, indicating that a dark fermentative pathway plays a major role in H_2 production in sucrose-containing reactors.

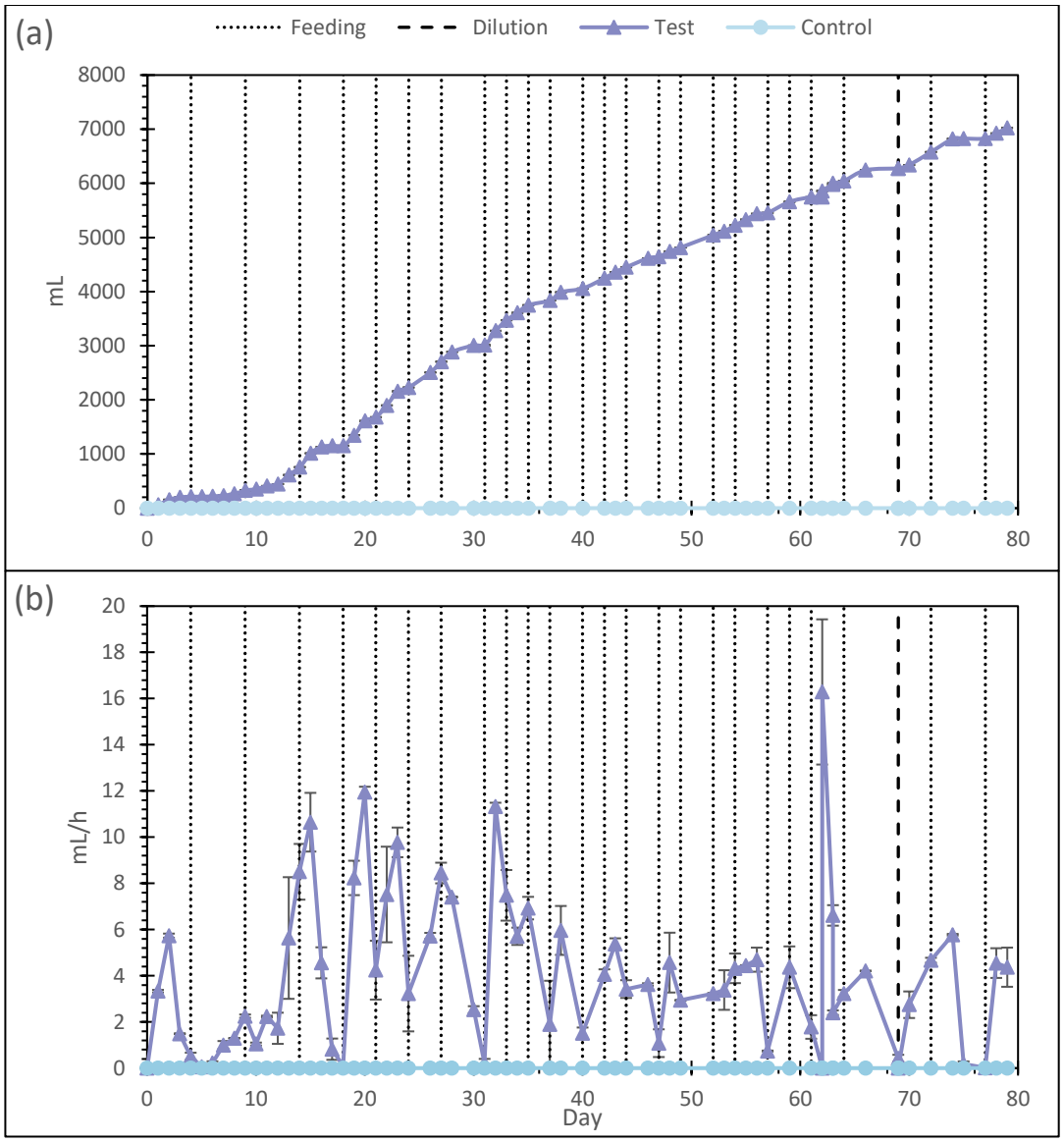

Figure 4.30. (a) Cumulative and (b) hourly biogas production of sucrose-containing reactors in Set 2. Error bars indicate upper and lower data ranges of duplicate test reactors.

Produced biogas is analyzed with GC to translate to H_2 and CO_2 productions of the reactors. Headspace gas composition throughout the operation can be seen in Figure 4.31 below. On average, about 40 – 50 % of the headspace was composed of CO_2 with the remainder being H_2 in test reactors. This high percentage of CO_2 was not observed in acetate-containing reactors. There might be a number of explanations for this, with primary reason being that the acetic acid is directly involved in cellular

metabolism during the organic acid cycle. This would result in skipping the CO_2 producing glycolytic pathway in acetate-containing reactors. Another reason is the pH difference of acetate-containing and sucrose-containing reactors. pH of the former was not controlled and observed to be mostly stable around 7-50-7.70 (Figure 4.15) whereas pH of the latter readjusted to be around 6.80 (Figure 4.24) with every feeding. Relatively higher pH of the working volume of acetate-containing reactors might have acted as a CO_2 sink in the reactors, which is later observed during Set 3 as well (See Section 4.3).

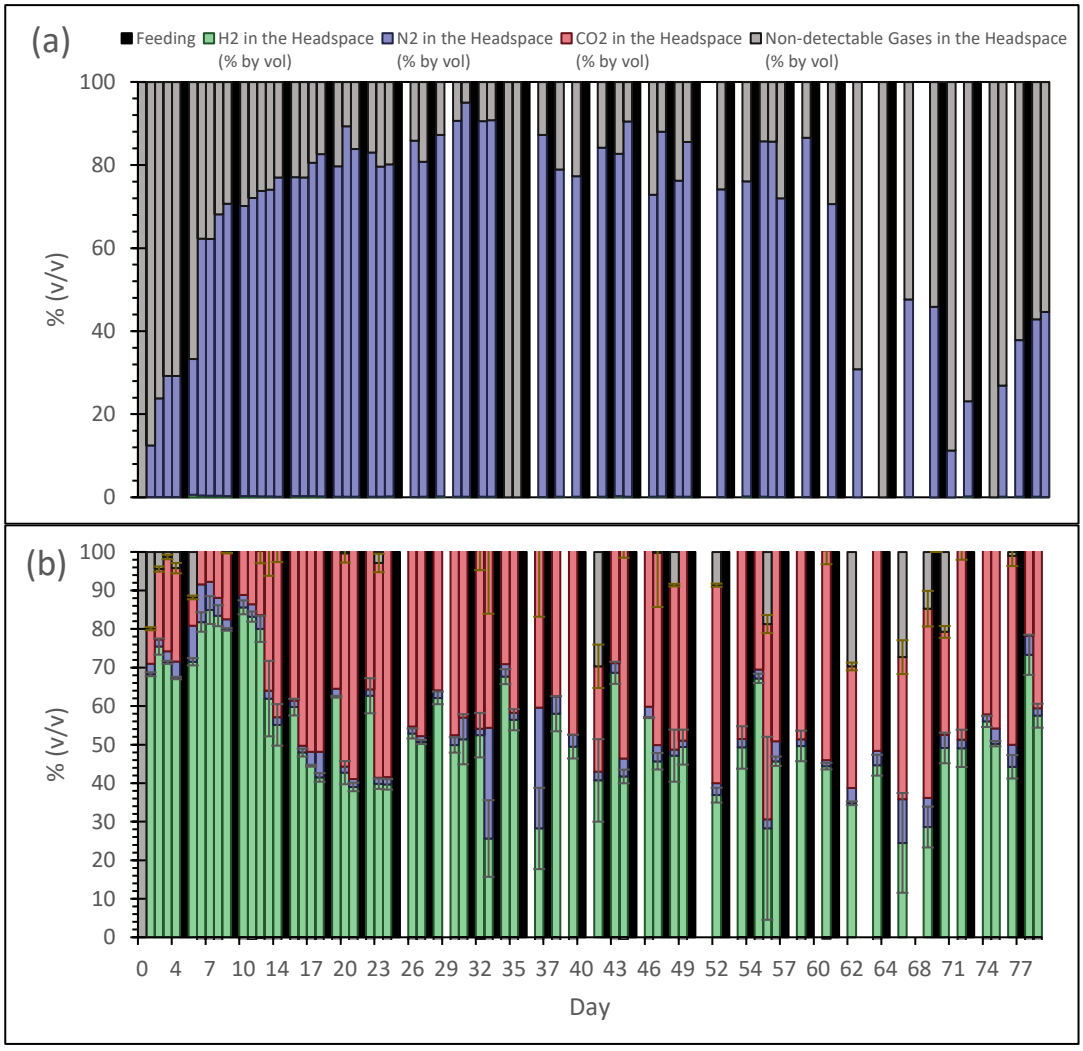

Figure 4.31. Headspace gas composition of sucrose-containing (a) control reactor and (b) test reactors throughout Set 2 operation. Error bars represent the high and low ranges of duplicate test reactors.

Cumulative production and productivities for H_2 and CO_2 are given in Figure 4.32. During the first days of operation, average CO_2 content was observed to be around 20 %, then suddenly reaching to 50 % after 3rd feeding on Day 14. With 3rd feed, Na^+ concentration was also observed to reach 2348 ± 281 mgNa^+/L. This might also indicate a critical Na^+ concentration in sucrose reactors, where hydrogen was produced with higher percentage but at a less rate with Na^+ concentrations below 2 g/L. After reaching above 2 gNa^+/L, increase in rate of production but decrease in percent of occupied volume of H_2 in headspace was observed. In other words, both H_2 and CO_2 production were enhanced after reaching 2 gNa^+/L of Na^+ concentration.

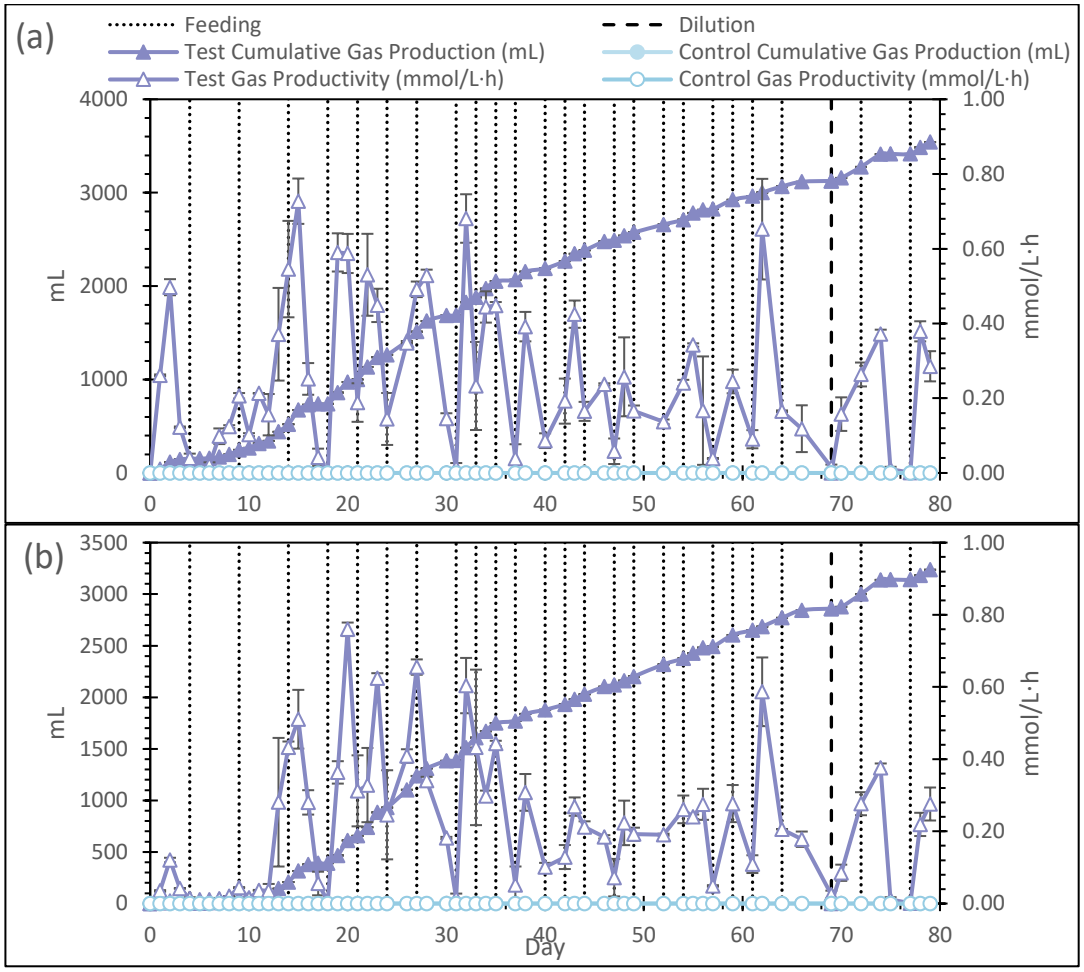

Figure 4.32. (a) Cumulative H_2 production and H_2 productivities and (b) cumulative CO_2 production and CO_2 productivities observed in sucrose-containing reactors of Set 2. Error bars represent the high and low data ranges of duplicate test reactors.

Maximum H_2 productivity was observed as 0.73 ± 0.06 mmolH_2/L·h, on Day 15 with CO_2 productivity for the day being 0.51 ± 0.08 mmolCO_2/L·h. Maximum CO_2 productivity was observed on Day 20, as 0.76 ± 0.02 mmolCO_2/L·h with H_2 productivity for the day being 0.59 ± 0.05 mmolH_2/L·h. Reactors responded very well to the feeding, with gas production spiking the following day after feeding, substrate rapidly degrading and gas production ceasing suddenly, awaiting next feeding.

4.2.2.3 PHB Production

PHB accumulation throughout the operation of Set 2 can be seen in Figure 4.33 below. Interestingly, PHB production was minimal in sucrose-containing reactors, reaching peak value of 3.3 ± 0.4 % cdw on day 9. There had been observable PHB until 3rd feeding at Day 18; however, after that, no PHB was observed in sucrose-containing reactors.

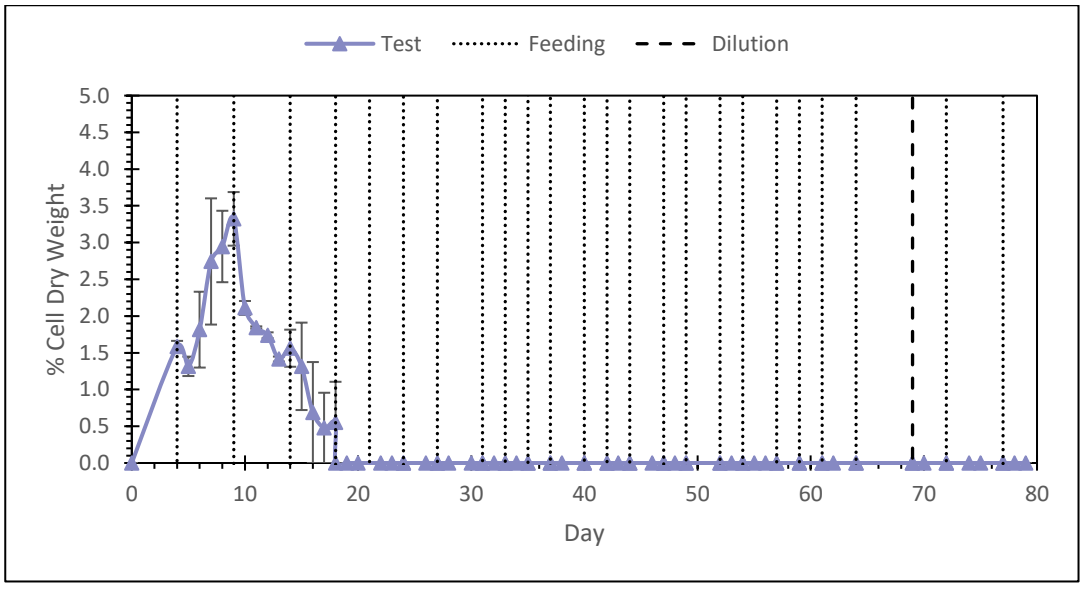

Figure 4.33. PHB Accumulation of sucrose-containing reactors of Set 2. Error bars represent high and low accumulating test reactors.

There might be possible reasons why there was not any PHB accumulated in sucrose-containing reactors, with the primary reason being the concentration of the sucrose

in the reactors. As can be seen from both sucrose consumption graphs (Figure 4.29) as well as gas production graphs (Figure 4.30), affinity of the strain to sucrose is quite high and there is seldom more than 3 days between each feed. This proved that the sucrose was degraded much more rapidly than acetic acid containing same moles of C atoms. Therefore, further experiments should be performed with increasing sucrose concentrations in the media to provide much higher C/N ratio than that of acetate-containing reactors, since high C/N ratio is the most critical parameter in terms of PHB production (See Section 2.2.2).

Another reason might be the absence of pH stress. Despite of the high Na+ concentrations reaching up to 5000 mgNa^+/L and conductivity values up to 12000 µS/cm, which might be even inhibitory, pH was always below 7.00, ranging in 6.00 – 6.80 (Figure 4.24 and Figure 4.27 for pH and Na^+/Conductivity, respectively). In addition, during the PHB peaking period of Days 7 – 9, Na^+ and conductivity values were around 1000 mgNa+/L and 4000 µS/cm. These values are significantly lower than 4000 mgNa+/L and 7000 µS/cm observed in acetate-containing reactors during PHB peaking periods (Days 36 – 38). The absence of a second stress, in addition to pH, might have led to very low PHB production.

The other reason could be the acclimation of the microorganisms to the media. It was seen that the response of the reactors to changing environmental conditions was rapid. During the light/dark cycle operation in Phase I of the reactors, only in the first dark period hydrogen was not produced. Starting from the second dark period, hydrogen production resumed even in the absence of light, indicating the role of another metabolic pathway, i.e., dark fermentation, other than photofermentation. It is also a must to take larger volume of biomass samples from sucrose-containing reactors, as biomass concentration in the reactors decreased drastically, as seen in Figure 4.25. The small amount of biomass that was analyzed for its PHB content might not have yielded PHB that is above the limit of quantification of the GC. In other words, even if PHB is well above 50 % of cdw, it might have not been able to be observed due to the small volume of biomass analyzed for its PHB content. Therefore, more biomass sample is required which requires larger sampling volume.

4.2.3 Summary of Results of Set 2

Results of Set 2 for both acetate-containing reactors and sucrose-containing reactors can be seen in Figure 4.44 and Figure 4.35. It was seen that with equal moles of C maintained in reactors in the form of two different substrates, the pathway can change drastically. Acetate-containing reactors accumulated up to almost 60 %cdw of PHB, while it was practically nonexistent in sucrose-containing reactors. Sucrose-containing reactors however, reached up to a maximum of 0.73 mmol/L·h of H_2 productivity, which is among the highest observed in the literature. In comparison, acetate-containing reactors had 0.56 mmol/L·h of maximum H_2 productivity. It was also proven in this set that the strain can survive up to 5 g/L of Na^+ concentrations.

To reach higher PHB accumulation, trials with higher sucrose concentrations should be made. Also, since the highest PHB accumulation in acetate-containing reactors was observed at elevated pH values of 7.96, another set with acetate as the substrate should be operated with pH of the working volume being the variable parameter in the operation.

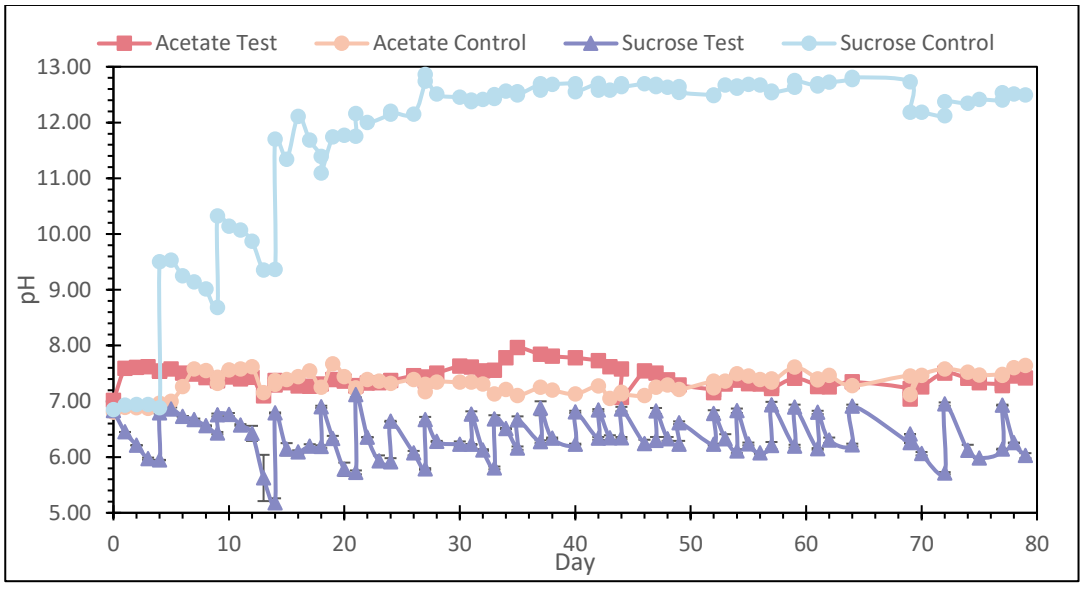

Figure 4.34. pH of acetate-containing and sucrose-containing reactors throughout the operation of Set 2. Error bars indicate the upper and lower data ranges of test reactors. Single reactor was operated as control for both substrates.

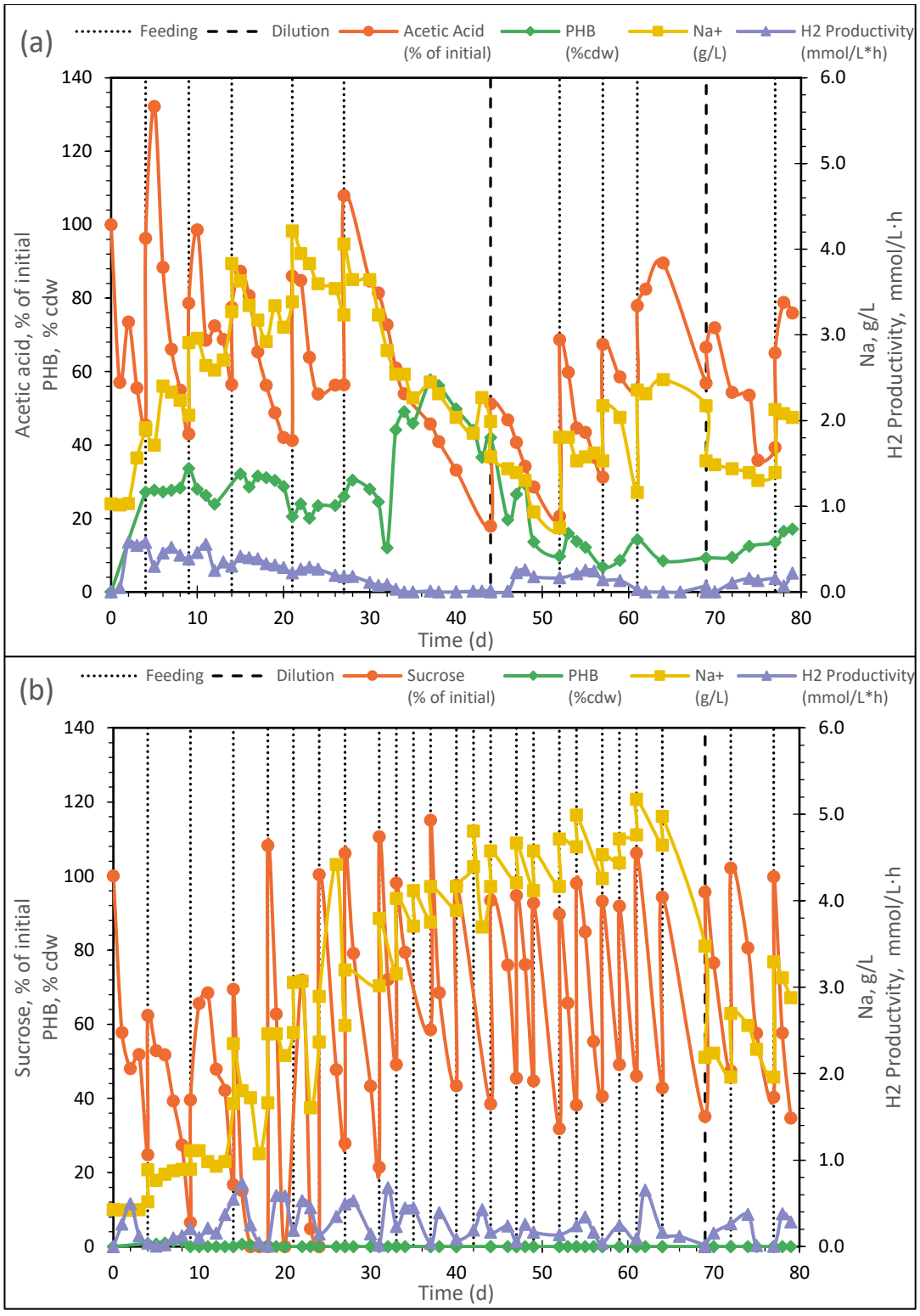

Figure 4.35. Summary of the results obtained in Set 2 with (a) Acetate-containing reactors and (b) Sucrose-containing reactors.

4.3 Results of Set 3: Effect of pH

Third set was operated over the course of 24 days in batch-mode, with only one feeding done during operation. Based on the results obtained from the operation of Set 2, where high PHB accumulation was observed at elevated pH levels in acetate-containing reactors, a total of 3 reactor types (each run in duplicate) were operated in Set 3 with three different pH levels maintained in the reactors, containing acetic acid as the primary carbon source. Every parameter other than pH of the reactors were kept same in all reactors. The pH levels were kept constant throughout the operation period. This set was described in two phases, as seen in Table 4.4 below.

Table 4.4. Phases of operation in Set 3 for all reactors

Phase	***Days***	***Description of the Phase***
I	0-15	Low Na^+ conditions before feeding.
II	16-24	High Na^+ conditions after feeding.

Phase I, Days 0-4 was characterized by lag phase and thus PHB analysis was not performed. Days 5-15 and Days 16-24 include daily PHB analyses and can be considered as operation in low and high Na^+ concentrations, respectively.

4.3.1 Operational Indicators

Three different pH values, namely 7.00, 7.70 and 8.50, were selected as the variable parameter. To keep the pH levels constant at predetermined values, each day, after sampling for pH and other analyses, the pH of the reactor content was elevated with 0.5 M NaOH solution and/or decreased with 0.5 M HCl solution as needed. pH of the reactors during operation of the set is given below in Figure 4.36. Throughout the operation of the set, it was observed that pH 7.00 reactors (R7.00) tend to increase in pH, pH 8.50 reactors (R8.50) tend to decrease, and pH 7.70 reactors (R7.70) remained relatively stable.

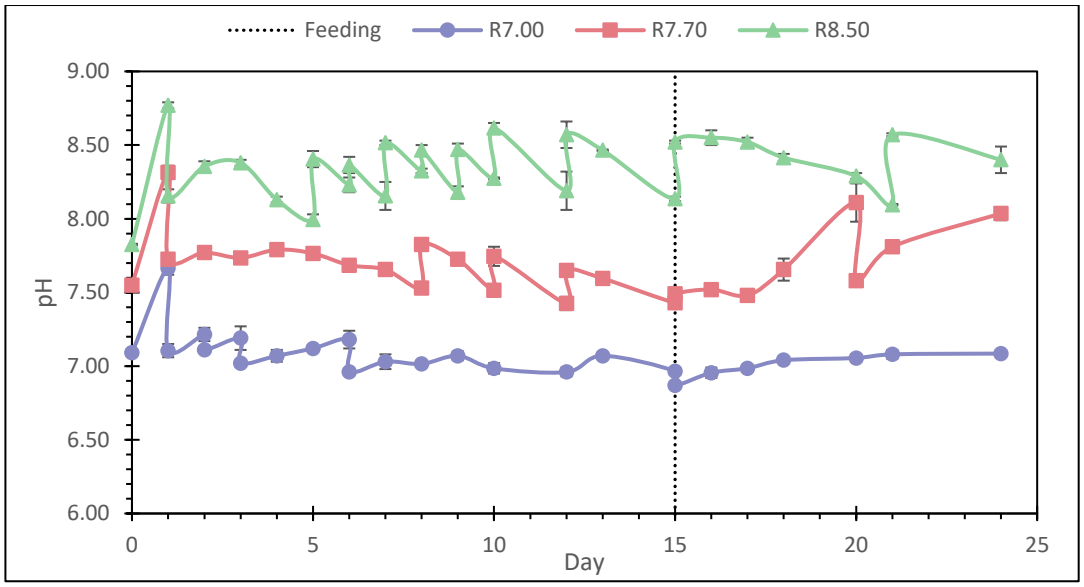

Figure 4.36. pH of the reactors during Set 3 operation. Error bars indicate upper and lower values of duplicate reactors.

Biomass concentration in the reactors can be seen in Figure 4.37. Maximum biomass concentrations as well as the growth rate of the reactors decreased with increasing operational pH. Maximum biomass concentrations were observed at either Day 5 or Day 6 as 0.910 ± 0.004 gcdw/L, 0.846 ± 0.005 gcdw/L and 0.645 ± 0.008 gcdw/L in the order of increasing operational pH. Until Day 5, sampling volume was 5 mL, afterwards increased to 20 mL for PHB analysis. Increased sampling volume had a definite negative effect on the biomass concentration, enhanced with the absence of the feed. Without abundant carbon and nitrogen in the reactors, biomass washed out earlier than Set 2 (where acetic acid concentration had never been allowed to decrease lower than $C_0/2$). Trends for biomass growth for all different operational pH values were observed to be similar. Feeding was proved to have a positive effect on the growth of both R7.00 and R7.70 reactors. Activity of R8.50 had already mostly faded before the feeding on Day 15. With the feeding, the salinity of the reactor contents increased suddenly as expected (Figure 4.38). This, in addition to high operational pH values, proved to be too much stress for the biomass to maintain its activity. Accordingly, biomass did not recover further in R8.50 unlike R7.00 and R7.70 (Figure 4.37).

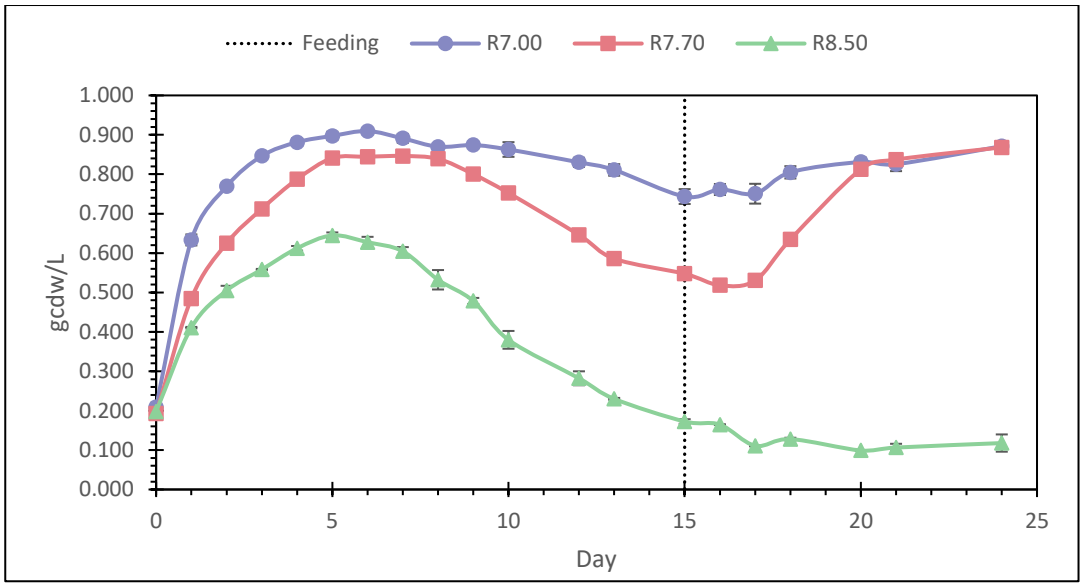

Figure 4.37. Biomass concentrations in the reactors during operation of Set 3. Error bars indicate upper and lower values of duplicate reactors.

Na^+ concentrations of all reactors can be seen in Figure 4.38a. Na^+ concentrations of the reactors maintained stable around 1750 mgNa^+/L and 3250 mgNa^+/L before and after the feeding, respectively. Sudden increase in the Na^+ concentration is due to the high concentration of acetic acid present in the feed requiring high concentrations of NaOH to reach a neutral pH in the feed.

Conductivity values of the reactors remained stable before and after as well, despite daily NaOH or HCl addition to maintain constant pH levels (Figure 4.38b). Despite the similar Na^+ concentrations and electrical conductivity values in all reactors, R7.00 and R7.70 reactors recovered and reached to the levels in cell dry weight as their initial values (Day 4-8). This revealed that YO3 is tolerant to pH levels of 7.70 although recovery rate is relatively slow.

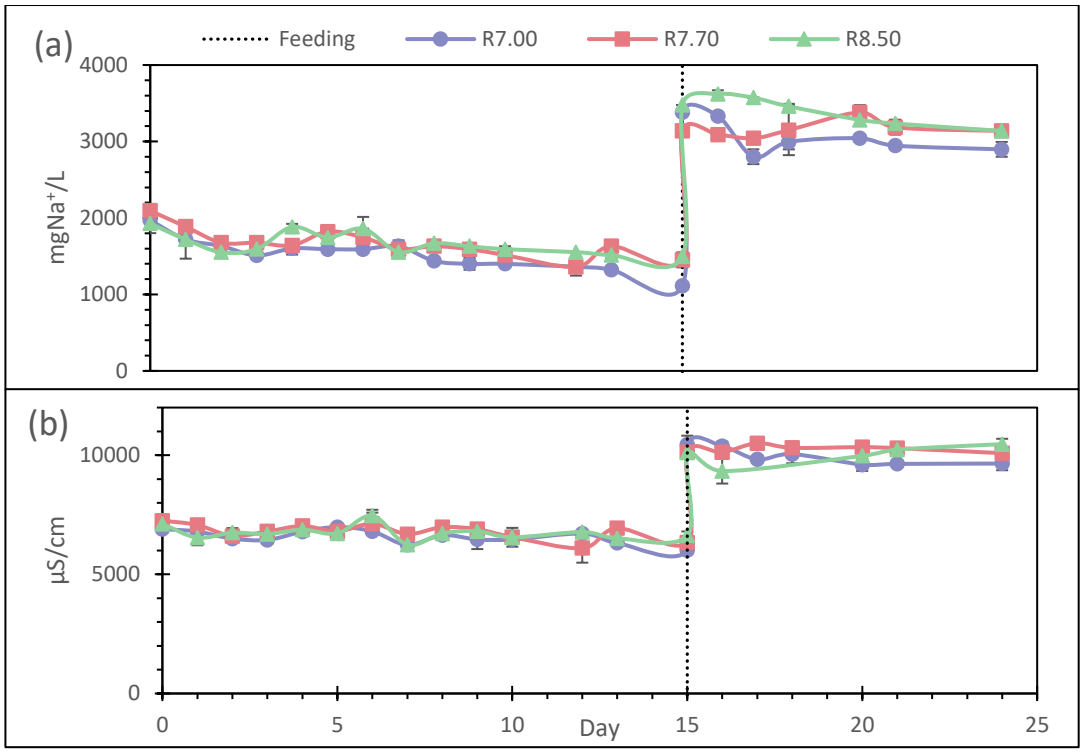

Figure 4.38. (a) Sodium concentrations and (b) conductivities of the reactors during Set 3 operation. Error bars in indicate upper and lower data range of duplicate reactors.

Organic acids analysis for all reactors can be seen in Figure 4.39 below. Similar to the results observed during operation of Set 2, as acetate was utilized as the carbon source, formic acid and hexanoic acid accumulated. Acetic acid consumption and formic acid production rates decreased with increasing operational pH. Contrary to Set 2, valeric acid accumulation was not observed in Set 3, indicating that Na^+ concentrations should be increased above 4 g/L to observe the accumulation of valeric acid. Therefore, organic acid analysis of this set also clarified that the elevated pH observed during the operation of Set 2 had been a result of valeric acid production, which in turn was a result of high Na^+ concentration. Hexanoic acid during the operation of this set was observed to be accumulated more and earlier with increasing pH values. It might also be speculated that the hexanoic acid arises from the components released into the media from non-living cells, since hexanoic acid was usually observed whenever biomass concentrations of the reactors started to decrease rapidly.

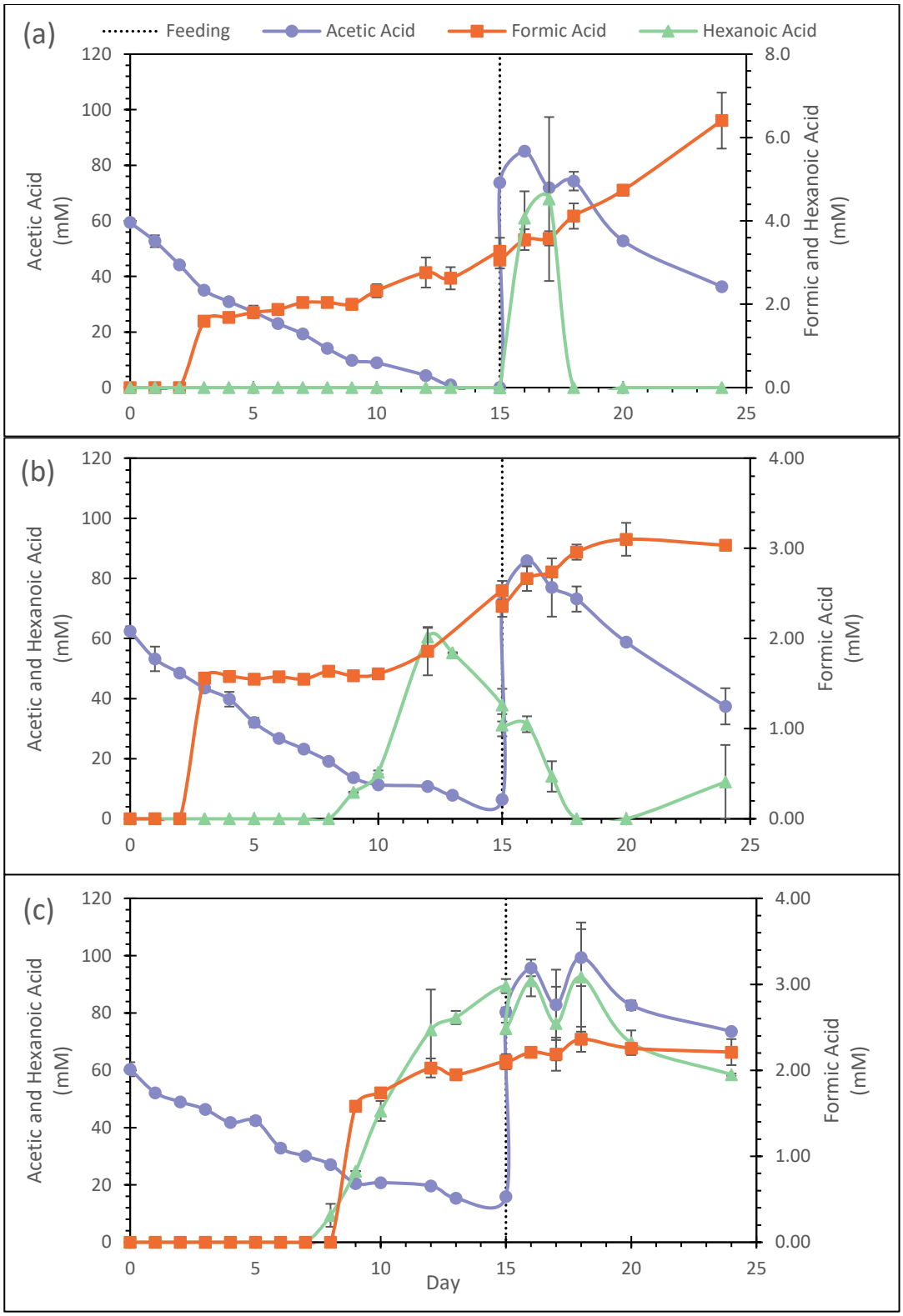

Figure 4.39. Organic acids analysis of Set 3, (a) R7.00, (b) R7.70 and (c) R8.50. Error bars indicate lower and upper data range of duplicate reactors.

4.3.2 Hydrogen and CO_2 Production

Produced gas in Set 3 was also collected by 100 mL sterile injectors. Cumulative biogas production and rate of biogas production can be seen in Figure 4.40 below for all reactors. With increasing operational pH, lower cumulative gas production was observed during operation. Until Phase II (feeding), R7.70 reactors had produced more gas in total, whereas after feeding R7.00 reactors surpassed them. Maximum rate of gas production was slightly higher in R7.00 reactors as 4.20 ± 0.05 mL/h compared to 3.70 ± 0.15 mL/h and 2.38 ± 0.04 mL/h for R7.70 and R8.50 reactors, respectively.

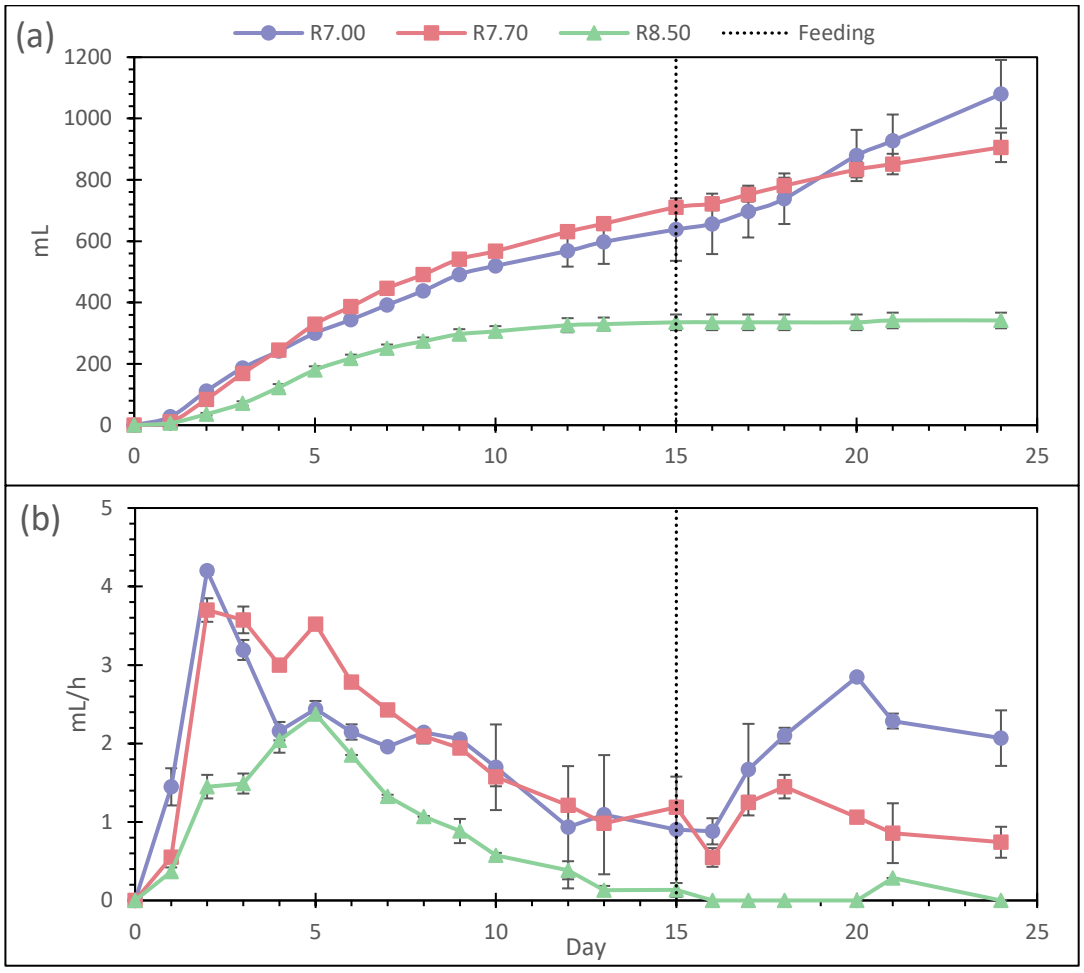

Figure 4.40. (a) Cumulative and (b) hourly biogas production of all reactors in Set 3. Error bars represent upper and lower range of duplicate reactors.

Headspace gas composition of the reactors can be seen in Figure 4.41 and translated into H_2 and CO_2 in Figure 4.42 and Figure 4.43, respectively.

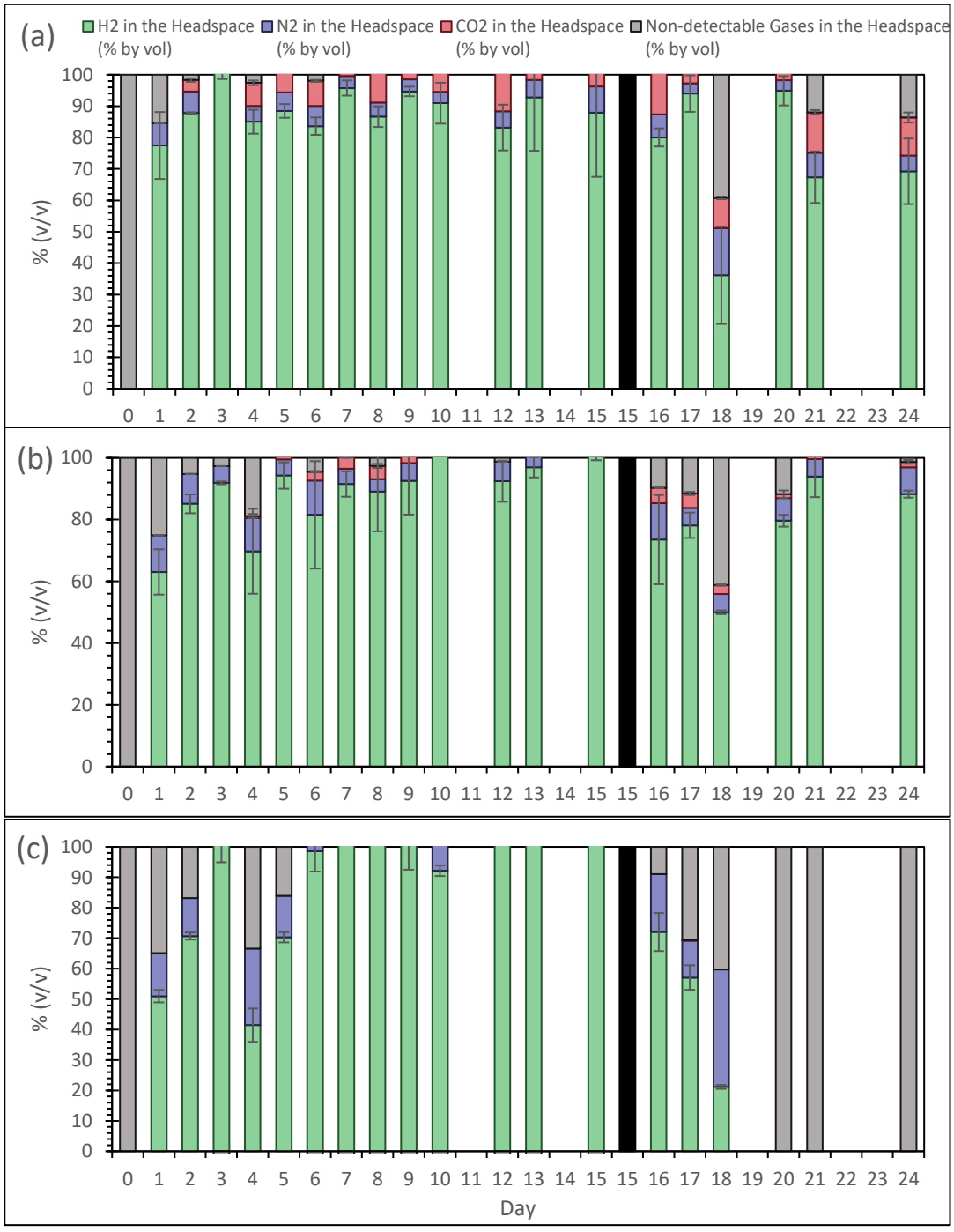

Figure 4.41. Headspace gas composition of (a) R7.00 (b) R7.70 and (c) R8.50 reactors during Set 3 operation. Error bars indicate upper and lower data ranges of duplicate reactors. Black bars indicate the feeding on day 15.

With increased operational pH, lower CO_2 percentages were observed. This observation is most likely due to the pH of the system though, with high pH in the effective volume of the reactors act as an effective CO_2 sink. Therefore, it should be noted that some of the CO_2 produced in the reactors remain dissolved in the liquid.

Cumulative H_2 production and H_2 productivities of all the reactors can be seen in Figure 4.42. Hydrogen production of the reactors were observed to be similar with total gas production of the reactors owing to high percentage of H_2 in the produced gas (Figure 4.41 and Figure 4.42). Cumulative hydrogen productions of the reactors were recorded as 927 ± 117 mL, 785 ± 23 mL and 282 ± 11 mL in the order of increasing operational pH. Relatively high difference in duplicates of R7.00 reactors was due to the failing of the gas collection syringe adapter connected to the reactor stopper, which had been cracked on Day 10 and could not be identified until Day 15. Maximum hydrogen productivities were observed as 0.42 ± 0.01 mmol/L·h, 0.37 ± 0.02 mmol/L·and 0.21 ± 0.01 mmol/L·h in the order of increasing operational pH. It was noted that as operational pH increased, time needed to reach maximum H_2 productivity also increased.

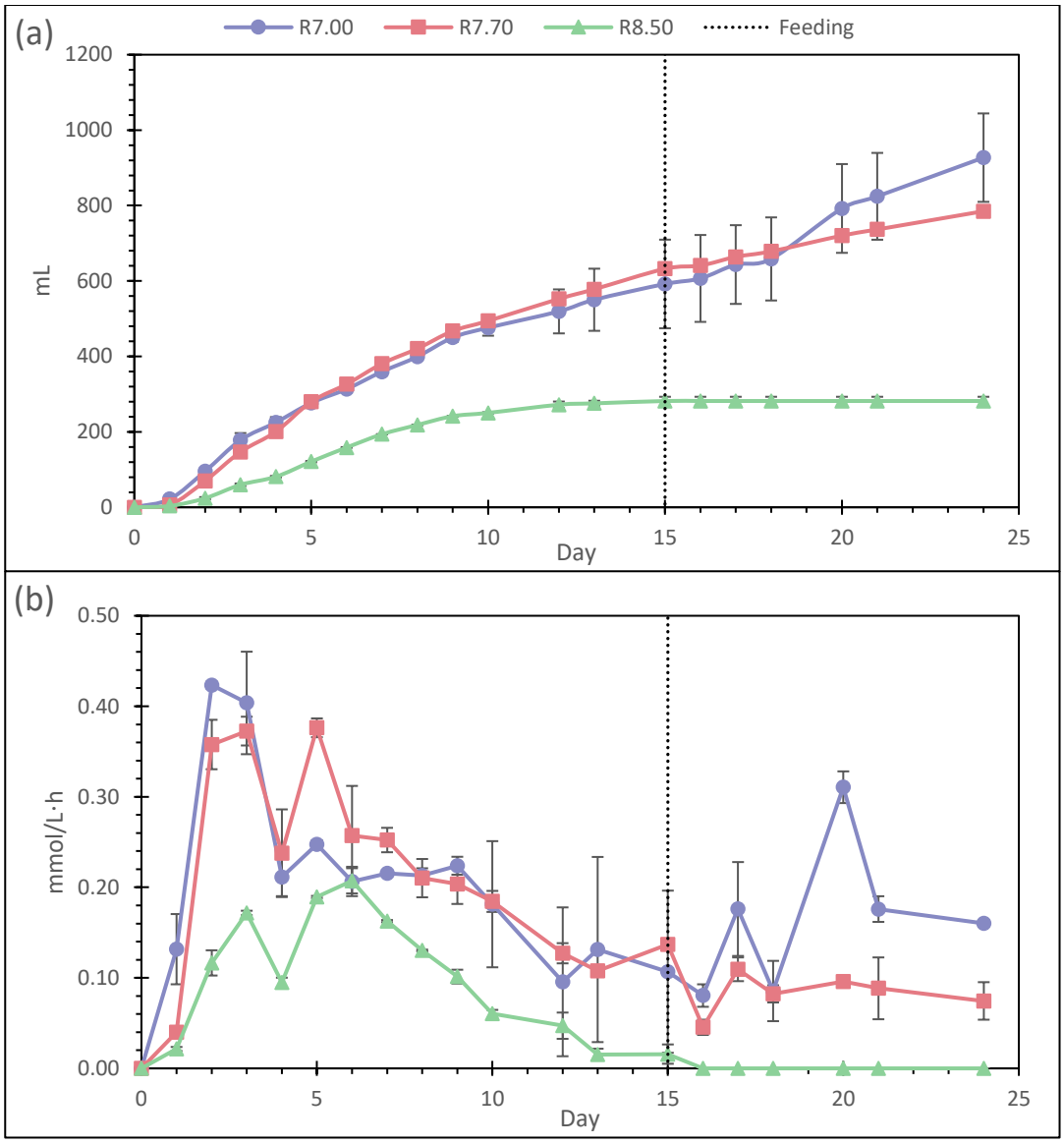

Figure 4.42. (a) Cumulative H_2 production and (b) H_2 productivities in Set 3. Error bars represent upper and lower data range of duplicate reactors.

Cumulative CO_2 production and CO_2 productivities of all the reactors can be seen in Figure 4.43 below. CO_2 also followed a similar pattern where cumulative production as well as productivities decreased with increasing operational pH. Cumulative CO_2 production was observed as 122 ± 18 mL and 22 ± 2 mL for R7.00 and R7.70 reactors, respectively. No CO_2 production was observed in R8.50 reactors, most probably due to the fact that at high pH, reactor content acted as a CO_2 sink, as mentioned above.

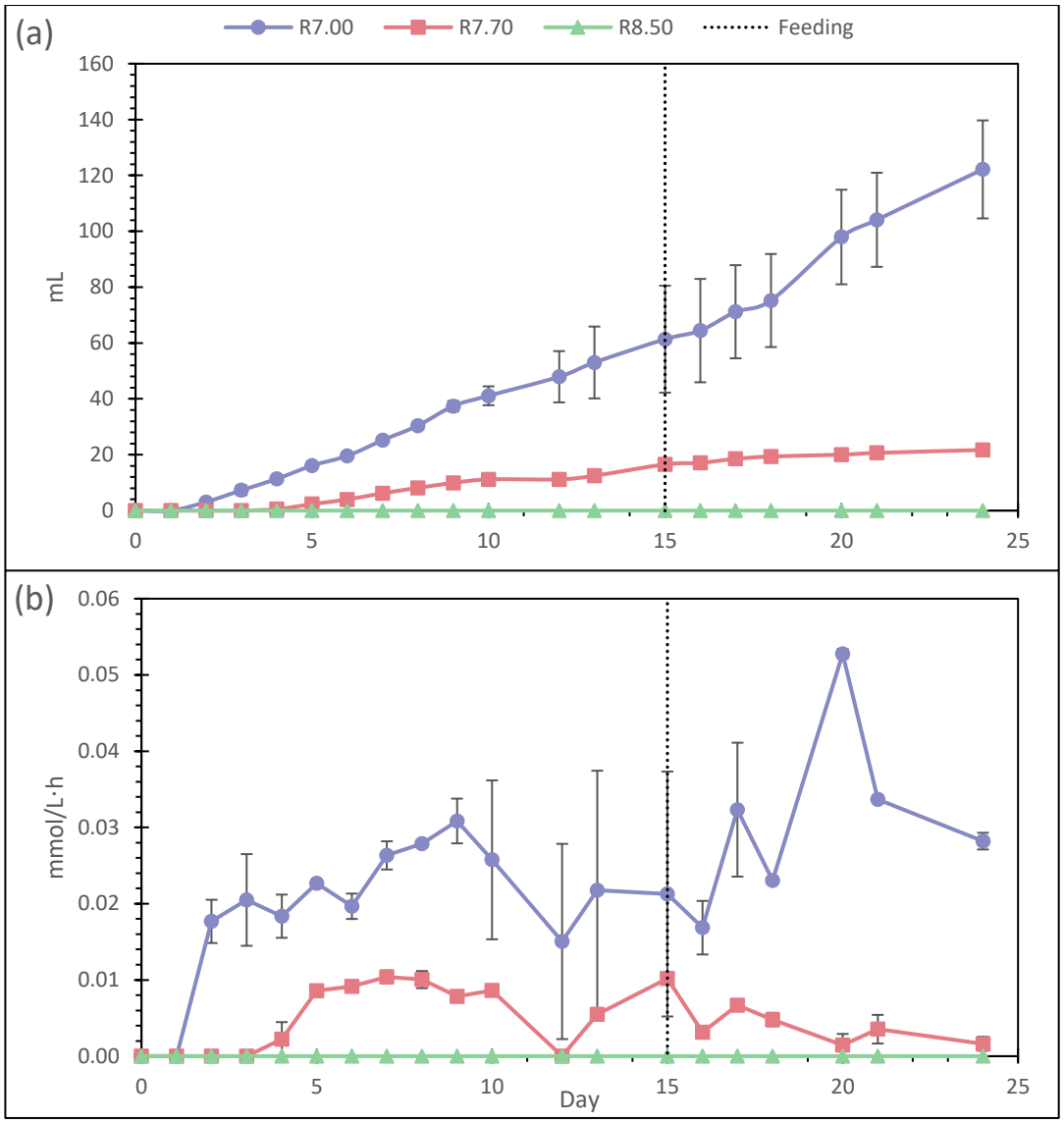

Figure 4.43. (a) Cumulative CO_2 production and (b) CO_2 productivities in Set 3. Error bars represent upper and lower data range of duplicate reactors.

4.3.3 PHB Production

PHB analysis results can be observed on Figure 4.44. For R7.00 reactors, maximum PHB accumulation was observed as 39.8 ± 1.8 % of cdw, on Day 9. For R7.70 reactors, maximum value was observed as 33.6 ± 2.0 % of cdw, on the last day of reactor operation, Day 24. pH 8.50 reactors peaked on Day 8 with PHB accumulation being 57.5 ± 0.2 % of cdw.

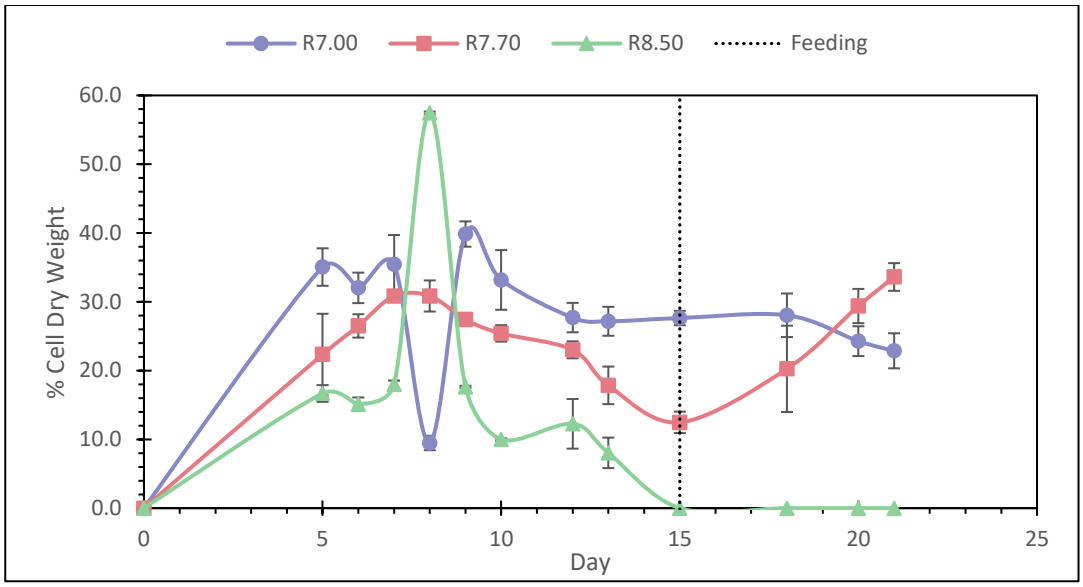

Figure 4.44. PHB Accumulation of Set 3. Error bars represent high and low PHB data of the reactors.

It was speculated after Set 2 that pH of 7.80 – 8.00 might have been the triggering parameter in increasing PHB content of YO3. Therefore, three operational pH values were selected in designing and conducting Set 3. As expected, the highest operational pH of 8.50 led to the highest PHB content of almost 60 %. However, apparently, it was consumed due to stressful conditions of that high pH. Also observed from the gas production data, R8.50 reactors had already ceased activity before the feeding on Day 15. However, it was observed in R7.70 reactors that, feeding and consequently increase in Na^+ concentrations enhanced PHB accumulation, as well as the growth rate mentioned previously (See Figure 4.37). R7.70 reactors were stopped before observing the peak PHB accumulation, therefore repeat of the study for prolonged operation periods should be conducted. Even relatively high pH close to 8.00 might be searched for potential increase in PHB production, as was the pH range detected in Set 2 (Figure 4.15 and Figure 4.23). PHB accumulation of R7.00 reactors were relatively stable throughout the operation at an average of 30 % with peak value of 39.8 ± 1.8 % cdw.

4.3.4 Summary of Results of Set 3

Major parameters of the reactors operated in Set 3, namely acetic acid concentration, PHB accumulation, Na^+ concentration and H_2 productivities are given in Figure 4.45.

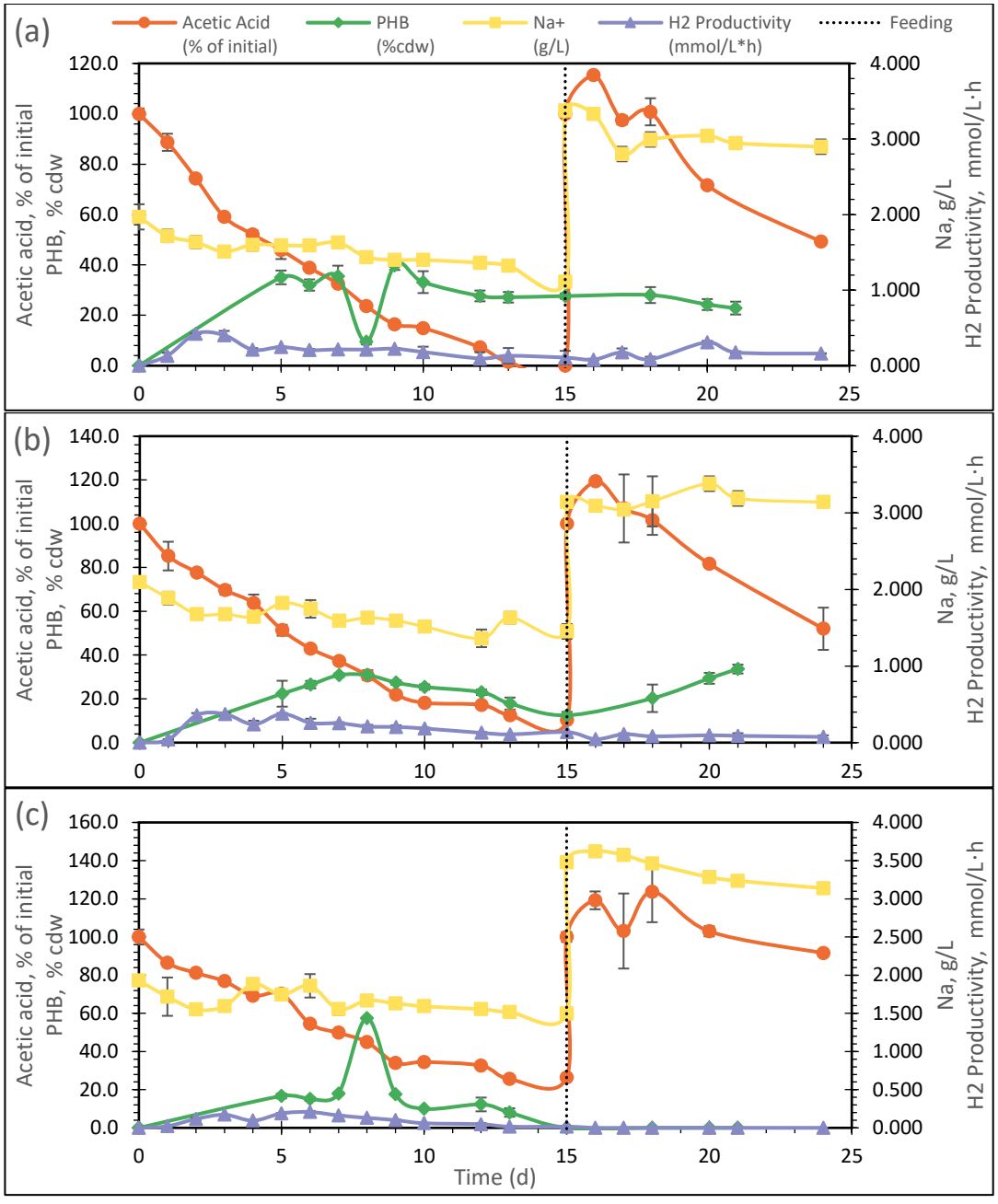

Figure 4.45. Summary of the results obtained in Set 3 for (a) R7.00, (b) R7.70 and (c) R8.50 reactors. Error bars represent upper and lower data ranges of duplicate reactors.

Rate of degradation of acetic acid decreased with increasing pH in the reactors, i.e., acetate was consumed fastest in the low pH reactors. H_2 productivities were observed to be highest at the point where substrate degraded most rapidly for all reactors. In terms of PHB accumulation, based on the observations in Set 3, R7.00 appear as the best performing reactors, however further confirmation with R7.70 should be done until the peak value in PHB is observed. Combining the information that is obtained from both Set 2 and Set 3, it is clear that Set 2 should be mimicked with constant pH values at 7.70 or 8.00 and feeding should be done until Na^+ concentrations in the reactors increase without hindering the activity of the reactors. Contrary to Set 2, valeric acid accumulation was not observed in Set 3, perhaps due to insufficient duration of operation. This is another reason why a further study should be performed for extended periods of time, at least until peak concentration of valeric acid accumulation would be observed. Operational pH of 8.50 combined with sudden doubling of Na+ concentration and/or higher conductivity/salinity proved to be too much of a stress for the reactors to endure.

In terms of H_2 production, R7.00 reactors also perform best compared to other reactors. However, R7.70 reactors were observed to surpass the biomass concentrations of R7.00 reactors, for the first time, in Set 3 operation. Given enough time after the feeding, high biomass concentration in R7.70 reactors might potentially result in more H_2 productivity.

It is clear that R7.70 reactors performed best in terms of adaptation to high Na^+ concentrations and/or high salinity values. This high Na^+ concentration and/or high salinity values/mid pH conditions provide the best stress conditions for a balance between growth of microorganisms and PHB accumulation.

CHAPTER 5

CONCLUSION

This chapter summarizes the results obtained and discussions that were made from the operation of three sets within the scope of this thesis study. Significant observations were given under the Section 5.1, whereas speculations that could not be verified through current methods employed are given under Section 5.2.

5.1 Set Outcomes

Set 1

- A separate formation occurred after centrifuging YO3 strain, which consequently resulted in drastic differences in observed PHB accumulation. Therefore, the whole pellet after centrifuging should be taken to be methanolysed.
- Obtaining the dry pellets homogenously with separate formations was very impractical and prone to errors. This was proven by comparing PHB accumulation of the obtained dry pellet and resuspended dry pellet, and observing much higher PHB accumulation with resuspended pellet.
- Effect of drying proved to be insignificant with WT strain, with both resuspended biomass and dried biomass yielding approximately same PHB accumulation.
- For YO3 strain, dried strain proved to yield much less PHB, which was also due to the occurrence of a secondary formation during centrifuging of YO3 samples.
- PHB accumulation was approximately the same for dried WT and YO3 samples, indicating that some of the YO3 cells might have become fragile due to high PHB accumulation and been destroyed during centrifugation.

- PHB losses that might have resulted from the methanolysis were higher in YO3 reactors. 2 mg of PHB standard that was added externally to the samples were quantified as less than 2 mg, therefore indicating a possible secondary metabolite interfering with assumed 100 % efficient methanolysis.

Set 2 – Acetate-Containing Reactors

- pH was left uncontrolled using acetate as the carbon source. Throughout the operation, buffering capacity of the medium was observed to be sufficient and pH was observed to not fluctuate drastically.
- With increasing sodium concentrations with every feed, then non-existent organic acids started to accumulate. Along with the increase in valerate and hexanoate, pH also rose up to almost 8.00. In this pH range, highest PHB accumulation throughout the set was observed as around 65 % cdw.
- It was speculated that the increase in PHB was mainly linked to the increase in pH and Na^+ concentrations, of which pH also depending on a number of factors.
    - 4000 mgNa^+/L marked the beginning of the decline in hydrogen production and increase in valeric acid production in the reactors.
    - As valeric acid accumulated in the reactors, pH gradually rose to 8.00.
    - This was followed by increase in PHB production.
- It was speculated that there had been double stress conditions caused by the increase in pH and sodium concentration. Therefore, Set 3 was planned to be operated at various pH levels and constant sodium concentrations, aiming to separate the effect of pH and Na^+ from each other.
- Compared to some of the other species of PNSB in the literature (See Section 2.4), very high PHB accumulation of 57.7 ± 5.2 % of cell dry weight was observed.

Set 2 – Sucrose-Containing Reactors

- In sucrose-containing reactors, PHB accumulation was minimal, whereas hydrogen production was significantly higher than that of acetate-containing reactors.
- In set-up of sucrose-containing reactors, moles of C atoms in the media had been selected to be equal to that of acetate-containing reactors, therefore might have been too low for PHB accumulation.
    - During the operation it was seen that sucrose was consumed much more rapidly than acetate with significant pH drops in the reactors accompanying substrate utilization.
    - It is possible that the sucrose concentration in the reactors favored H_2 production rather than PHB, hence no production was observed.
- Relative low pH of 6.30 – 6.80 that was adjusted in the reactors might not have provided enough stress conditions for the accumulation of PHB. Comparing acetate-containing and sucrose-containing reactors, PHB was peaked when the pH value of the former peaked as well. In sucrose-containing reactors, pH was never allowed to fluctuate to disrupt or alter the operation of the reactors.
- Compared to other PNSB species in the literature, high H_2 productivity of 0.73 ± 0.06 mmol/L·h was reached.

Set 3

- A clear observation of effect of both pH and Na^+ was able to be made in Set 3. It was seen that biomass concentration, hydrogen productivity and PHB production decreased with increasing pH under constant Na^+ concentrations.
- It cannot be said that pH was the only factor enhancing the PHB accumulation observed in the Set 2. Following the sudden Na^+ spike in the reactors due to the feeding, double stress conditions prevailed in the reactors as speculated previously.

- The stress was too much for R8.50 reactors, hence activity of the reactors ceased.
- Double stress caused by Na^+ as well as pH resulted in higher PHB accumulation in reactors R7.70 than R7.00 reactors. It can be said that pH is not the sole parameter resulting in the PHB increase, and that a synergistic effect of pH with Na^+ on PHB accumulation is occurring.

5.2 Future Recommendations

For both acetate-containing and sucrose-containing reactors, it is not known whether the increase in the concentration of the carbon source would increase the PHB accumulation, as not many studies have been done using *R. capsulatus* YO3. Further studies may be conducted with increasing carbon concentrations in the media while keeping every other parameter constant. Especially with sucrose-containing reactors, further investigations should be done to observe any PHB accumulation.

Another possible study is that, since a strong link between Na^+ – Valeric acid – pH – PHB was observed, using heavier organic acids (such as butyrate, valerate, hexanoate) as the carbon source should be considered.

After the feeding that was done at Day 15 of Set 3, R8.50 reactors never recovered. It was also seen that R7.70 reactors recovered and PHB production increased; however, the set was ceased before seeing the PHB peak. Therefore, it can be said that "had it been recovered", R8.50 reactors might have accumulated more PHB than R7.70 reactors. pH 8.50 was too much, however another study may be conducted while maintaining a pH of 8.00 in the reactors. Comparing Set 2 acetate-containing reactors and Set 3, it is worth investigating the two stress conditions (moderate Na^+ of 2000 mg/L and pH 8.0) at the same time to achieve high PHB accumulation while maintaining the biomass in the reactors, contrary to R8.50 reactors in Set 3 which had faded due to high Na^+/salinity and pH.

In order to clarify the effect of salinity and Na^+, studies performed with cations such as K^+ in addition to Na^+ can be conducted at constant conductivity values. Effect of pH should also be considered in these studies. i.e., performing a similar study to Set 3 with overall conductivity values divided in between Na^+ and K^+ ions might allow decoupling the effect of Na^+ from conductivity. As an example, instead of utilizing x M of NaOH solution, pH could be adjusted with a mixture of x/2 M NaOH + x/2 KOH solution. This practice would allow for much less input of Na^+ to the reactors during pH adjustment, while keeping the conductivity values on par with Set 3.

To further investigate the possible losses during PHB analysis, a calibration must be done using a commercially available hydroxybutyric acid methyl ester solution. Said solution should be diluted to contain exact same moles of hydroxybutyric acid methyl ester as the standard solutions prepared from the derivatization of PHB standard. Comparing the peak signals obtained from the GC, it should be possible to verify the efficiency of the PHB analysis method. In other words, whether PHB standard is fully monomerized or not has not been completely verified in this study and comparison of results with hydroxybutyric acid methyl ester solution should achieve that.

REFERENCES

Agyekum, E. B., Nutakor, C., Agwa, A. M., & Kamel, S. (2022). A Critical Review of Renewable Hydrogen Production Methods: Factors Affecting Their Scale-Up and Its Role in Future Energy Generation. In *Membranes* (Vol. 12, Issue 2). MDPI. https://doi.org/10.3390/membranes12020173

Ajanovic, A., Sayer, M., & Haas, R. (2022). The economics and the environmental benignity of different colors of hydrogen. *International Journal of Hydrogen Energy*, *47*(57), 24136–24154. https://doi.org/10.1016/j.ijhydene.2022.02.094

Anderson, A. J., & Dawes, E. A. (1990). Occurrence, metabolism, metabolic role, and industrial uses of bacterial polyhydroxyalkanoates. *Microbiological Reviews*, *54*(4), 450–472. https://doi.org/10.1128/mr.54.4.450-472.1990

Androga, D. D., Ozgur, E., Gunduz, U., Yucel, M., & Eroglu, I. (2011). Factors affecting the longterm stability of biomass and hydrogen productivity in outdoor photofermentation. *International Journal of Hydrogen Energy*, *36*(17), 11369–11378. https://doi.org/10.1016/j.ijhydene.2010.12.054

Angenent, L. T., Karim, K., Al-Dahhan, M. H., Wrenn, B. A., & Domíguez-Espinosa, R. (2004). Production of bioenergy and biochemicals from industrial and agricultural wastewater. In *Trends in Biotechnology* (Vol. 22, Issue 9, pp. 477–485). https://doi.org/10.1016/j.tibtech.2004.07.001

Atilhan, S., Park, S., El-Halwagi, M. M., Atilhan, M., Moore, M., & Nielsen, R. B. (2021). Green hydrogen as an alternative fuel for the shipping industry. In *Current Opinion in Chemical Engineering* (Vol. 31). Elsevier Ltd. https://doi.org/10.1016/j.coche.2020.100668

Avcioglu, S. G., Ozgur, E., Eroglu, I., Yucel, M., & Gunduz, U. (2011). Biohydrogen production in an outdoor panel photobioreactor on dark fermentation effluent of molasses. *International Journal of Hydrogen Energy*, *36*(17), 11360–11368. https://doi.org/10.1016/j.ijhydene.2010.12.046

Azwar, M. Y., Hussain, M. A., & Abdul-Wahab, A. K. (2014). Development of biohydrogen production by photobiological, fermentation and electrochemical processes: A review. In *Renewable and Sustainable Energy Reviews* (Vol. 31, pp. 158–173). https://doi.org/10.1016/j.rser.2013.11.022

Basak, N., & Das, D. (2007). The prospect of purple non-sulfur (PNS) photosynthetic bacteria for hydrogen production: The present state of the art. *World Journal of Microbiology and Biotechnology*, *23*(1), 31–42. https://doi.org/10.1007/s11274-006-9190-9

Biebl, H., & Pfennig, N. (1981). Isolation of Members of the Family Rhodospirillaceae. In M. P. Starr (Ed.), *The Prokaryotes* (pp. 267–273). Springer-Verlag.

Boran, E., Özgür, E., van der Burg, J., Yücel, M., Gündüz, U., & Eroglu, I. (2010). Biological hydrogen production by Rhodobacter capsulatus in solar tubular photo bioreactor. *Journal of Cleaner Production*, *18*(SUPPL. 1). https://doi.org/10.1016/j.jclepro.2010.03.018

Boran, E., Özgür, E., Yücel, M., Gündüz, U., & Eroglu, I. (2012). Biohydrogen production by Rhodobacter capsulatus Hup - mutant in pilot solar tubular photobioreactor. *International Journal of Hydrogen Energy*, *37*(21), 16437–16445. https://doi.org/10.1016/j.ijhydene.2012.02.171

Brandl, H., Gross, R. A., Lenz, R. W., Lloyd, R., & Fuller, R. C. (1991). The accumulation of poly(3-hydroxyalkanoates) in Rhodobacter sphaeroides. In *Arch Microbiol* (Vol. 155).

Braunegg, G., Sonnleimer, B., & Lafferty, R. M. (1978). A Rapid Gas Chromatographic Method for the Determination of Poly-β-hydroxybutyric Acid in Microbial Biomass. In *European J. Appl. Microbiol. Biotechnol* (Vol. 6).

Chee, J.-Y., Yoga, S.-S., Lau, N.-S., Ling, S.-C., Abed, R. M. M., & Sudesh, K. (2010). Bacterially Produced Polyhydroxyalkanoate (PHA): Converting

Renewable Resources into Bioplastics. In A. Méndez-Vilas (Ed.), *Current Research, Technology and Education Topics in Applied Microbiology and Microbial Biotechnology* (pp. 1395–1404). Formatex Research Center.

Chen, L., Qi, Z., Zhang, S., Su, J., & Somorjai, G. A. (2020). Catalytic hydrogen production from methane: A review on recent progress and prospect. *Catalysts*, *10*(8). https://doi.org/10.3390/catal10080858

Choi, J., & Lee, S. Y. (1997). Process analysis and economic evaluation for Poly(3-hydroxybutyrate) production by fermentation. *Bioprocess Engineering*, *17*(6), 335. https://doi.org/10.1007/s004490050394

Chung, Y. J., Cha, H. J., Yeo, J. S., & Yoo, Y. J. E. (1997). Production of poly(3-hydroxybutyric-co-3-hydroxyvaleric)acid using propionic acid by pH regulation. *Journal of Fermentation and Bioengineering*, *83*(5), 492–495. https://doi.org/10.1016/S0922-338X(97)83009-7

Cui, Y., Barford, J. P., & Renneberg, R. (2007). Gas chromatographic determination of poly(3-hydroxybutyrate) with alkaline hydrolysis and acid esterification. *Analytical Letters*, *40*(15), 2915–2924. https://doi.org/10.1080/00032710701603959

Dincer, I. (2012). Green methods for hydrogen production. *International Journal of Hydrogen Energy*, *37*(2), 1954–1971. https://doi.org/10.1016/j.ijhydene.2011.03.173

Dincer, I., & Acar, C. (2014). Review and evaluation of hydrogen production methods for better sustainability. *International Journal of Hydrogen Energy*, *40*(34), 11094–11111. https://doi.org/10.1016/j.ijhydene.2014.12.035

Du, G., & Yu, J. (2002). Green technology for conversion of food scraps to biodegradable thermoplastic polyhydroxyalkanoates. *Environmental Science and Technology*, *36*(24), 5511–5516. https://doi.org/10.1021/es011110o

Durand, A., Bourbon, M. L., Steunou, A. S., Khalfaoui-Hassani, B., Legrand, C., Legrand, A., Astier, C., & Ouchane, S. (2018). Biogenesis of the bacterial cbb3 cytochrome c oxidase: Active subcomplexes support a sequential assembly model. *Journal of Biological Chemistry*, *293*(3), 808–818. https://doi.org/10.1074/jbc.M117.805184

Dutta, A., Appel, A. M., & Shaw, W. J. (2018). Designing electrochemically reversible H 2 oxidation and production catalysts. In *Nature Reviews Chemistry* (Vol. 2, Issue 9, pp. 244–252). Nature Publishing Group. https://doi.org/10.1038/s41570-018-0032-8

Elkahlout, K., Alipour, S., Eroglu, I., Gunduz, U., & Yucel, M. (2017). Long-term biological hydrogen production by agar immobilized Rhodobacter capsulatus in a sequential batch photobioreactor. *Bioprocess and Biosystems Engineering*, *40*(4), 589–599. https://doi.org/10.1007/s00449-016-1723-5

El-malek, F. A., Khairy, H., Farag, A., & Omar, S. (2020). The sustainability of microbial bioplastics, production and applications. *International Journal of Biological Macromolecules*, *157*, 319–328. https://doi.org/10.1016/j.ijbiomac.2020.04.076

Eng, G., Bywater, I., & Hendtlass, C. (Eds.). (2008). *New Zealand Energy Information Handbook* (3rd ed.). New Zealand Centre for Advanced Engineering.

Eroglu, E., & Melis, A. (2011). Photobiological hydrogen production: Recent advances and state of the art. *Bioresource Technology*, *102*(18), 8403–8413. https://doi.org/10.1016/j.biortech.2011.03.026

Fajobi, M. A., Loto, R. T., & Oluwole, O. O. (2019). "Crude distillation overhead system": Corrosion and Control. *Journal of Physics: Conference Series*, *1378*(4). https://doi.org/10.1088/1742-6596/1378/4/042090

Gebicki, J., Modigell, M., Schumacher, M., van der Burg, J., & Roebroeck, E. (2010). Comparison of two reactor concepts for anoxygenic H2 production by

Rhodobacter capsulatus. *Journal of Cleaner Production*, *18*(SUPPL. 1). https://doi.org/10.1016/j.jclepro.2010.05.023

Golomysova, A., Gomelsky, M., & Ivanov, P. S. (2010). Flux balance analysis of photoheterotrophic growth of purple nonsulfur bacteria relevant to biohydrogen production. *International Journal of Hydrogen Energy*, *35*(23), 12751–12760. https://doi.org/10.1016/j.ijhydene.2010.08.133

Gorenflo, V., Schmack, G., Vogel, R., & Steinbüchel, A. (2001). Development of a process for the biotechnological large-scale production of 4-hydroxyvalerate-containing polyesters and characterization of their physical and mechanical properties. *Biomacromolecules*, *2*(1), 45–57. https://doi.org/10.1021/bm0000992

Hambourger, M., Gervaldo, M., Svedruzic, D., King, P. W., Gust, D., Ghirardi, M., Moore, A. L., & Moore, T. A. (2008). [FeFe]-hydrogenase-catalyzed H2 production in a photoelectrochemical biofuel cell. *Journal of the American Chemical Society*, *130*(6), 2015–2022. https://doi.org/10.1021/ja077691k

Hejazi, P., Vasheghani-Farahani, E., & Yamini, Y. (2003). Supercritical Fluid Disruption of Ralstonia eutropha for Poly(β-hydroxybutyrate) Recovery. *Biotechnology Progress*, *19*(5), 1519–1523. https://doi.org/10.1021/bp034010q

Higuchi-Takeuchi, M., & Numata, K. (2019). Acetate-Inducing Metabolic States Enhance Polyhydroxyalkanoate Production in Marine Purple Non-sulfur Bacteria Under Aerobic Conditions. *Frontiers in Bioengineering and Biotechnology*, *7*. https://doi.org/10.3389/fbioe.2019.00118

Hong, Y. C., Lee, S. J., Shin, D. H., Kim, Y. J., Lee, B. J., Cho, S. Y., & Chang, H. S. (2012). Syngas production from gasification of brown coal in a microwave torch plasma. *Energy*, *47*(1), 36–40. https://doi.org/10.1016/j.energy.2012.05.008

Howarth, R. W., & Jacobson, M. Z. (2021). How green is blue hydrogen? *Energy Science and Engineering*, *9*(10), 1676–1687. https://doi.org/10.1002/ese3.956

Hustede, E., Steinbüchel, A., & Schlegel, H. G. (1993). Relationship between the photoproduction of hydrogen and the accumulation of PHB in non-sulphur purple bacteria. *Applied Microbiology and Biotechnology*, *39*(1), 87–93. https://doi.org/10.1007/BF00166854

Imhoff, J. F., Trüper, H. G., & Pfennig, N. (1984). Rearrangement of the Species and Genera of the Phototrophic "Purple Nonsulfur Bacteria". *International Journal of Systematic Bacteriology*, 340–343.

Ingale, G. U., Kwon, H. M., Jeong, S., Park, D., Kim, W., Bang, B., Lim, Y. il, Kim, S. W., Kang, Y. B., Mun, J., Jun, S., & Lee, U. (2022). Assessment of Greenhouse Gas Emissions from Hydrogen Production Processes: Turquoise Hydrogen vs. Steam Methane Reforming. *Energies*, *15*(22). https://doi.org/10.3390/en15228679

International Energy Agency. (2022). *World Energy Outlook 2022*. www.iea.org/t&c/

Ishaq, H., Dincer, I., & Crawford, C. (2022). A review on hydrogen production and utilization: Challenges and opportunities. *International Journal of Hydrogen Energy*, *47*(62), 26238–26264. https://doi.org/10.1016/j.ijhydene.2021.11.149

Jacquel, N., Lo, C. W., Wei, Y. H., Wu, H. S., & Wang, S. S. (2008). Isolation and purification of bacterial poly(3-hydroxyalkanoates). In *Biochemical Engineering Journal* (Vol. 39, Issue 1, pp. 15–27). Elsevier. https://doi.org/10.1016/j.bej.2007.11.029

Johnson, K., van Geest, J., Kleerebezem, R., & van Loosdrecht, M. C. M. (2010). Short- and long-term temperature effects on aerobic polyhydroxybutyrate producing mixed cultures. *Water Research*, *44*(6), 1689–1700. https://doi.org/10.1016/j.watres.2009.11.022

Jung, H. R., Choi, T. R., Han, Y. H., Park, Y. L., Park, J. Y., Song, H. S., Yang, S. Y., Bhatia, S. K., Gurav, R., Park, H. A., Namgung, S., Choi, K. Y., & Yang, Y. H. (2020). Production of blue-colored polyhydroxybutyrate (PHB) by one-

pot production and coextraction of indigo and PHB from recombinant Escherichia coli. *Dyes and Pigments*, *173*. https://doi.org/10.1016/j.dyepig.2019.107889

Kadier, A., Simayi, Y., Abdeshahian, P., Azman, N. F., Chandrasekhar, K., & Kalil, M. S. (2016). A comprehensive review of microbial electrolysis cells (MEC) reactor designs and configurations for sustainable hydrogen gas production. In *Alexandria Engineering Journal* (Vol. 55, Issue 1, pp. 427–443). Elsevier B.V. https://doi.org/10.1016/j.aej.2015.10.008

Kapdan, I. K., & Kargi, F. (2006). Bio-hydrogen production from waste materials. In *Enzyme and Microbial Technology* (Vol. 38, Issue 5, pp. 569–582). https://doi.org/10.1016/j.enzmictec.2005.09.015

Kapritchkoff, F. M., Viotti, A. P., Alli, R. C. P., Zuccolo, M., Pradella, J. G. C., Maiorano, A. E., Miranda, E. A., & Bonomi, A. (2006). Enzymatic recovery and purification of polyhydroxybutyrate produced by Ralstonia eutropha. *Journal of Biotechnology*, *122*(4), 453–462. https://doi.org/10.1016/j.jbiotec.2005.09.009

Kars, G., Gündüz, U., Rakhely, G., Yücel, M., Eroğlu, I., & Kovacs, K. L. (2008). Improved hydrogen production by uptake hydrogenase deficient mutant strain of Rhodobacter sphaeroides O.U.001. *International Journal of Hydrogen Energy*, *33*(12), 3056–3060. https://doi.org/10.1016/j.ijhydene.2008.01.037

Kayfeci, M., Keçebaş, A., & Bayat, M. (2019). Hydrogen production. In *Solar Hydrogen Production: Processes, Systems and Technologies* (pp. 45–83). Elsevier. https://doi.org/10.1016/B978-0-12-814853-2.00003-5

Keshavarz, T., & Roy, I. (2010). Polyhydroxyalkanoates: bioplastics with a green agenda. In *Current Opinion in Microbiology* (Vol. 13, Issue 3, pp. 321–326). https://doi.org/10.1016/j.mib.2010.02.006

Kim, B. S., Lee, S. C., Lee, S. Y., Chang, H. N., Chang, Y. K., & Woo, S. I. (1994). Production of poly(3-hydroxybutyric acid) by fed-batch culture of Alcaligenes

eutrophus with glucose concentration control. *Biotechnology and Bioengineering*, *43*(9), 892–898. https://doi.org/10.1002/bit.260430908

Kim, B. S., Lee, S. Y., & Chang, H. N. (1992). Production of poly-B-hydroxybutyrate by fed-batch culture of recombinant Escherichia coli. *Biotechnology Letters*, *14*(9), 811–816. https://doi.org/10.1007/BF01029144

Kim, M. S., Baek, J. S., & Lee, J. K. (2006). Comparison of H2 accumulation by Rhodobacter sphaeroides KD131 and its uptake hydrogenase and PHB synthase deficient mutant. *International Journal of Hydrogen Energy*, *31*(1), 121–127. https://doi.org/10.1016/j.ijhydene.2004.10.023

Kim, M. S., Kim, D. H., Cha, J., & Lee, J. K. (2012). Effect of carbon and nitrogen sources on photo-fermentative H 2 production associated with nitrogenase, uptake hydrogenase activity, and PHB accumulation in Rhodobacter sphaeroides KD131. *Bioresource Technology*, *116*, 179–183. https://doi.org/10.1016/j.biortech.2012.04.011

Koku, H., Eroo Glu, I., Und Uz B, U. G., Ucel, M. Y., & Urker, L. T. (2002). Aspects of the metabolism of hydrogen production by Rhodobacter sphaeroides. In *International Journal of Hydrogen Energy* (Vol. 27). www.elsevier.com/locate/ijhydene

Koul, Y., Devda, V., Varjani, S., Guo, W., Ngo, H. H., Taherzadeh, M. J., Chang, J. S., Wong, J. W. C., Bilal, M., Kim, S. H., Bui, X. T., & Parra-Saldívar, R. (2022). Microbial electrolysis: a promising approach for treatment and resource recovery from industrial wastewater. In *Bioengineered* (Vol. 13, Issue 4, pp. 8115–8134). Taylor and Francis Ltd. https://doi.org/10.1080/21655979.2022.2051842

Koutinas, A. A., Xu, Y., Wang, R., & Webb, C. (2007). Polyhydroxybutyrate production from a novel feedstock derived from a wheat-based biorefinery. *Enzyme and Microbial Technology*, *40*(5), 1035–1044. https://doi.org/10.1016/j.enzmictec.2006.08.002

Koyama, N., & Doi, Y. (1995). Continuous production of poly(3-hydroxybutyrate-co-3-hyhroxyvalerate) byAlcaligenes eutrophus. *Biotechnology Letters*, *17*(3), 281–284. https://doi.org/10.1007/BF01190637

Kranz, R. G., Gabbert, K. K., Locke, T. A., & Madigan, M. T. (1997). Polyhydroxyalkanoate Production in Rhodobacter capsulatus: Genes, Mutants, Expression, and Physiology. In *APPLIED AND ENVIRONMENTAL MICROBIOLOGY* (Vol. 63, Issue 8). http://aem.asm.org/

Krishna, C., & van Loosdrecht, M. C. M. (1999). Effect of temperature on storage polymers and settleability of activated sludge. *Water Research*, *33*(10), 2374–2382. https://doi.org/10.1016/S0043-1354(98)00445-X

Lagioia, G., Spinelli, M. P., & Amicarelli, V. (2022). Blue and green hydrogen energy to meet European Union decarbonisation objectives. An overview of perspectives and the current state of affairs. *International Journal of Hydrogen Energy*. https://doi.org/10.1016/j.ijhydene.2022.10.044

Lamb, J. J., & Lien, K. M. (2020). Promising Selected Biohydrogen Solutions. In *Hydrogen, Biomass and Bioenergy* (pp. 119–132). Elsevier. https://doi.org/10.1016/b978-0-08-102629-8.00007-4

Lang, A. S., Zhaxybayeva, O., & Beatty, J. T. (2012). Gene transfer agents: Phage-like elements of genetic exchange. In *Nature Reviews Microbiology* (Vol. 10, Issue 7, pp. 472–482). https://doi.org/10.1038/nrmicro2802

Lee, H. S., Vermaas, W. F. J., & Rittmann, B. E. (2010). Biological hydrogen production: Prospects and challenges. In *Trends in Biotechnology* (Vol. 28, Issue 5, pp. 262–271). https://doi.org/10.1016/j.tibtech.2010.01.007

Lee, S. Y. (1996). Bacterial polyhydroxyalkanoates. *Biotechnology and Bioengineering*, *49*(1), 1–14. https://doi.org/10.1002/(SICI)1097-0290(19960105)49:1<1::AID-BIT1>3.0.CO;2-P

Liangqi, Z., Jingfan, X., Tao, F., & Haibin, W. (2006). Synthesis of poly (3-hydroxybutyrate-co-3-hydroxyoctanoate) by a Sinorhizobium fredii strain. *Letters in Applied Microbiology*, *42*(4), 344–349. https://doi.org/10.1111/j.1472-765X.2006.01852.x

Luengo, J. M., García, B., Sandoval, A., Naharro, G., & Olivera, E. R. (2003). Bioplastics from microorganisms. In *Current Opinion in Microbiology* (Vol. 6, Issue 3, pp. 251–260). Elsevier Ltd. https://doi.org/10.1016/S1369-5274(03)00040-7

Madison, L. L., & Huisman, G. W. (1999). Metabolic Engineering of Poly(3-Hydroxyalkanoates): From DNA to Plastic. In *MICROBIOLOGY AND MOLECULAR BIOLOGY REVIEWS* (Vol. 63, Issue 1). http://mmbr.asm.org/

Mahidhara, G., Burrow, H., Sasikala, C., & Ramana, C. v. (2019). Biological hydrogen production: molecular and electrolytic perspectives. In *World Journal of Microbiology and Biotechnology* (Vol. 35, Issue 8). Springer Netherlands. https://doi.org/10.1007/s11274-019-2692-z

Marchessault, R. H., Monasterios, C. J., & Lepoutre, P. (1990). Properties of Poly-β-Hydroxyalkanoate Latex: Nascent Morphology, Film Formation and Surface Chemistry. In *Novel Biodegradable Microbial Polymers* (pp. 97–112). Springer Netherlands. https://doi.org/10.1007/978-94-009-2129-0_9

Martino, M., Ruocco, C., Meloni, E., Pullumbi, P., & Palma, V. (2021). Main hydrogen production processes: An overview. In *Catalysts* (Vol. 11, Issue 5). MDPI. https://doi.org/10.3390/catal11050547

McCay, M. H., & Shafiee, S. (2020). Hydrogen: An energy carrier. In *Future Energy: Improved, Sustainable and Clean Options for Our Planet* (pp. 475–493). Elsevier. https://doi.org/10.1016/B978-0-08-102886-5.00022-0

McKinlay, J. B. (2014). *Systems Biology of Photobiological Hydrogen Production by Purple Non-sulfur Bacteria* (pp. 155–176). https://doi.org/10.1007/978-94-017-8554-9_7

Melis, A., & Melnicki, M. R. (2006). Integrated biological hydrogen production. *International Journal of Hydrogen Energy*, *31*(11), 1563–1573. https://doi.org/10.1016/j.ijhydene.2006.06.038

Merki, D., & Hu, X. (2011). Recent developments of molybdenum and tungsten sulfides as hydrogen evolution catalysts. In *Energy and Environmental Science* (Vol. 4, Issue 10, pp. 3878–3888). https://doi.org/10.1039/c1ee01970h

Merugu, R., Girisham, S., & Reddy, S. M. (2010). Production of PHB (Poly-hydroxybutyrate) by Rhodopseudomonas palustris KU003 and Rhodobacter capsulatus KU002 Under Phosphate Limitation. *International Journal of Applied Biology and Pharmaceutical Technology*. www.ijabpt.com

Merugu, R., & Rao, A. S. (2015). Optimization of Polyhydroxybutyrate production by two phototrophic bacteria Rhodobacter capsulatus KU002 and Rhodopseudomonas palustris KU003. *Available Online Www.Jocpr.Com Journal of Chemical and Pharmaceutical Research*, *7*(12), 260–264. www.jocpr.com

Monroy, I., & Buitrón, G. (2020). Production of polyhydroxybutyrate by pure and mixed cultures of purple non-sulfur bacteria: A review. In *Journal of Biotechnology* (Vol. 317, pp. 39–47). Elsevier B.V. https://doi.org/10.1016/j.jbiotec.2020.04.012

Montiel-Corona, V., & Buitrón, G. (2022). Polyhydroxybutyrate production in one-stage by purple phototrophic bacteria: influence of alkaline pH, ethanol, and C/N ratios. *Biochemical Engineering Journal*, 108715. https://doi.org/10.1016/j.bej.2022.108715

Nikolaidis, P., & Poullikkas, A. (2017). A comparative overview of hydrogen production processes. In *Renewable and Sustainable Energy Reviews* (Vol. 67, pp. 597–611). Elsevier Ltd. https://doi.org/10.1016/j.rser.2016.09.044

Oflaz, B. (2019). *Photofermentative Hydrogen Production from Molasses in Tubular Photobioreactor with pH Control*. Middle East Technical University.

Oflaz, F. B., & Koku, H. (2021). Pilot-scale outdoor photofermentative hydrogen production from molasses using pH control. *International Journal of Hydrogen Energy*, *46*(57), 29160–29172. https://doi.org/10.1016/j.ijhydene.2020.10.086

Oh, Y. K., Raj, S. M., Jung, G. Y., & Park, S. (2011). Current status of the metabolic engineering of microorganisms for biohydrogen production. *Bioresource Technology*, *102*(18), 8357–8367. https://doi.org/10.1016/j.biortech.2011.04.054

Ojumu, T. v., Yu, J., & Solomon, B. O. (2004). Production of Polyhydroxyalkanoates, a bacterial biodegradable polymer. In *African Journal of Biotechnology* (Vol. 3, Issue 1, pp. 18–24). Academic Journals. https://doi.org/10.5897/AJB2004.000-2004

Özgür, E., Uyar, B., Öztürk, Y., Yücel, M., Gündüz, U., & Eroğlu, I. (2010). Biohydrogen production by Rhodobacter capsulatus on acetate at fluctuating temperatures. *Resources, Conservation and Recycling*, *54*(5), 310–314. https://doi.org/10.1016/j.resconrec.2009.06.002

Özkan, E., Uyar, B., Özgür, E., Yücel, M., Eroglu, I., & Gündüz, U. (2012). Photofermentative hydrogen production using dark fermentation effluent of sugar beet thick juice in outdoor conditions. *International Journal of Hydrogen Energy*, *37*(2), 2044–2049. https://doi.org/10.1016/j.ijhydene.2011.06.035

Özsoy, B. (2012). *Hydrogen and Poly-beta-hydroxy Butyric Acid Production and Expression Analyses of Related Genes in Rhodobacter Capsulatus at Different Acetate Concentrations*. Middle East Technical University.

Özsoy Demiriz, B., Kars, G., Yücel, M., Eroğlu, İ., & Gündüz, U. (2019). Hydrogen and poly-B-hydroxybutyric acid production at various acetate concentrations using Rhodobacter capsulatus DSM 1710. *International Journal of Hydrogen Energy*, *44*(32), 17269–17277. https://doi.org/10.1016/j.ijhydene.2019.02.036

Öztürk, Y. (2005). *Characterisation of the Genetically Modified Cytochrome Systems and Their Application to Biohydrogen Production in Rhodobacter Capsulatus*. Middle East Technical University.

Öztürk, Y., Yücel, M., Daldal, F., Mandaci, S., Gündüz, U., Türker, L., & Eroğlu, I. (2006). Hydrogen production by using Rhodobacter capsulatus mutants with genetically modified electron transfer chains. *International Journal of Hydrogen Energy*, *31*(11), 1545–1552. https://doi.org/10.1016/j.ijhydene.2006.06.042

Page, W. J., & Cornish, A. (1993). Growth of Azotobacter vinelandii UWD in Fish Peptone Medium and Simplified Extraction of Poly-,-Hydroxybutyrate. In *APPLIED AND ENVIRONMENTAL MICROBIOLOGY* (Vol. 59, Issue 12). http://aem.asm.org/

Petushkova, E. P., & Tsygankov, A. A. (2017). Acetate metabolism in the purple non-sulfur bacterium Rhodobacter capsulatus. *Biochemistry (Moscow)*, *82*(5), 587–605. https://doi.org/10.1134/S0006297917050078

Rhee, Y. H., Jang, J.-H., & Rogers, P. L. (1993). Production of copolymer consisting of 3-hydroxybutyrate and 3-hydroxyvalerate by fed-batch culture of Alcaligenes SP. SH-69. *Biotechnology Letters*, *15*(4), 377–382. https://doi.org/10.1007/BF00128280

Rousseau, R., Etcheverry, L., Roubaud, E., Basséguy, R., Délia-Dupuy, M.-L., & Bergel, A. (2020). Microbial electrolysis cell (MEC): Strengths, weaknesses and research needs from electrochemical engineering standpoint. *Journal of Applied Energy*, *257*(113938). https://doi.org/10.1016/j.apenergy.2019.113938ï

Roychowdhury, S., Cox, D., & Levandowsky, M. (1988). Production of hydrogen by microbial fermentation. *International Journal of Hydrogen Energy*, *13*(7), 407–410. https://doi.org/10.1016/0360-3199(88)90126-7

Sagir, E., Alipour, S., Elkahlout, K., Koku, H., Gunduz, U., Eroglu, I., & Yucel, M. (2017). Scale-up studies for stable, long-term indoor and outdoor production of hydrogen by immobilized Rhodobacter capsulatus. *International Journal of Hydrogen Energy*, *42*(36), 22743–22755. https://doi.org/10.1016/j.ijhydene.2017.07.240

Sakurai, H., Masukawa, H., Kitashima, M., & Inoue, K. (2013). Photobiological hydrogen production: Bioenergetics and challenges for its practical application. In *Journal of Photochemistry and Photobiology C: Photochemistry Reviews* (Vol. 17, pp. 1–25). https://doi.org/10.1016/j.jphotochemrev.2013.05.001

Sasikala, K., Ramana, C., Raghuveerrao, P., & Subrahmanyam, M. (1990). Effect of gas phase on the photoproduction of hydrogen and substrate conversion efficiency in the photosynthetic bacterium Rhodobacter sphaeroides O.U. 001. *International Journal of Hydrogen Energy*, *15*(11), 795–797. https://doi.org/10.1016/0360-3199(90)90015-Q

Sato, T., Inoue, K., Sakurai, H., & Nagashima, K. V. P. (2017). Effects of the deletion of hup genes encoding the uptake hydrogenase on the activity of hydrogen production in the purple photosynthetic bacterium rubrivivax gelatinosus IL144. *Journal of General and Applied Microbiology*, *63*(5), 274–279. https://doi.org/10.2323/jgam.2017.01.003

Schneider, S., Bajohr, S., Graf, F., & Kolb, T. (2020). State of the Art of Hydrogen Production via Pyrolysis of Natural Gas. In *ChemBioEng Reviews* (Vol. 7, Issue 5, pp. 150–158). Wiley-Blackwell. https://doi.org/10.1002/cben.202000014

Schulze, C., Juraschek, M., Herrmann, C., & Thiede, S. (2017). Energy Analysis of Bioplastics Processing. *Procedia CIRP*, *61*, 600–605. https://doi.org/10.1016/j.procir.2016.11.181

Sevinç, P., Gündüz, U., Eroglu, I., & Yücel, M. (2012). Kinetic analysis of photosynthetic growth, hydrogen production and dual substrate utilization by

Rhodobacter capsulatus. *International Journal of Hydrogen Energy*, *37*(21), 16430–16436. https://doi.org/10.1016/j.ijhydene.2012.02.176

Seyitoglu, S. S., Dincer, I., & Kilicarslan, A. (2017). Energy and exergy analyses of hydrogen production by coal gasification. *International Journal of Hydrogen Energy*, *42*(4), 2592–2600. https://doi.org/10.1016/j.ijhydene.2016.08.228

Shang, L., Jiang, M., Ho, &, & Chang, N. (2003). Poly(3-hydroxybutyrate) synthesis in fed-batch culture of Ralstonia eutropha with phosphate limitation under different glucose concentrations. In *Biotechnology Letters* (Vol. 25).

Sirohi, R., Prakash Pandey, J., Kumar Gaur, V., Gnansounou, E., & Sindhu, R. (2020). Critical overview of biomass feedstocks as sustainable substrates for the production of polyhydroxybutyrate (PHB). In *Bioresource Technology* (Vol. 311). Elsevier Ltd. https://doi.org/10.1016/j.biortech.2020.123536

Stams, A. J. M., & Plugge, C. M. (2009). Electron transfer in syntrophic communities of anaerobic bacteria and archaea. In *Nature Reviews Microbiology* (Vol. 7, Issue 8, pp. 568–577). https://doi.org/10.1038/nrmicro2166

Statistical Review of World Energy 2022. (2022).

Steinbüchel, A., & Füchtenbusch, B. (1998). Bacterial and other biological systems for polyester production. *Trends in Biotechnology*, *16*(10), 419–427. https://doi.org/10.1016/S0167-7799(98)01194-9

Sudesh, K., & Iwata, T. (2008). Sustainability of biobased and biodegradable plastics. In *Clean - Soil, Air, Water* (Vol. 36, Issues 5–6, pp. 433–442). https://doi.org/10.1002/clen.200700183

Tarlan, E. (2022). *Product Analysis for Photobiological Production of Hydrogen*. Middle East Technical University

Tetteh, D. A., & Salehi, S. (2023). The Blue Hydrogen Economy: A Promising Option for the Near-to-Mid-Term Energy Transition. *Journal of Energy Resources Technology*, *145*(4). https://doi.org/10.1115/1.4055205

Tiang, M. F., Fitri Hanipa, M. A., Abdul, P. M., Jahim, J. M. d., Mahmod, S. S., Takriff, M. S., Lay, C. H., Reungsang, A., & Wu, S. Y. (2020). Recent advanced biotechnological strategies to enhance photo-fermentative biohydrogen production by purple non-sulphur bacteria: An overview. In *International Journal of Hydrogen Energy* (Vol. 45, Issue 24, pp. 13211–13230). Elsevier Ltd. https://doi.org/10.1016/j.ijhydene.2020.03.033

Tsuge, T. (2002). Metabolic improvements and use of inexpensive carbon sources in microbial production of polyhydroxyalkanoates. *Journal of Bioscience and Bioengineering*, *94*(6), 579–584. https://doi.org/10.1016/S1389-1723(02)80198-0

Ursúa, A., Gandía, L. M., & Sanchis, P. (2012). Hydrogen production from water electrolysis: Current status and future trends. *Proceedings of the IEEE*, *100*(2), 410–426. https://doi.org/10.1109/JPROC.2011.2156750

Uyar, B. (2008). *Hydrogen Production by Microorganisms in Solar Bioreactor*. Middle East Technical University.

Uyar, B., Eroglu, I., Yücel, M., Gündüz, U., & Türker, L. (2007). Effect of light intensity, wavelength and illumination protocol on hydrogen production in photobioreactors. *International Journal of Hydrogen Energy*, *32*(18), 4670–4677. https://doi.org/10.1016/j.ijhydene.2007.07.002

Uyar, B., Gürgan, M., Özgür, E., Gündüz, U., Yücel, M., & Eroglu, I. (2015). Hydrogen production by hup- mutant and wild-type strains of Rhodobacter capsulatus from dark fermentation effluent of sugar beet thick juice in batch and continuous photobioreactors. *Bioprocess and Biosystems Engineering*, *38*(10), 1935–1942. https://doi.org/10.1007/s00449-015-1435-2

Validation of Analytical Procedures: Text and Methodology Q2(R1). (2005, November). *International Conference on Harmonisation of Technical Requirements for Registration of Pharmaceuticals for Human Use*.

van Niel, C. B. (1944). The Culture, General Physiology, Morphology and Classification of the Non-Sulfur Purple and Brown Bacteria. *Bacteriological Reviews*, *8*(1), 1–118. https://doi.org/10.1128/br.8.1.1-118.1944

van Wegen, R. J., Ling, Y., & Middelberg, A. P. J. (1998). Industrial production of polyhydroxyalkanoates using escherichia coli: An economic analysis. *Chemical Engineering Research and Design*, *76*(3), 417–426. https://doi.org/10.1205/026387698524848

Vignais, P. M., Willison, J. C., & Colbeau, A. (2004). *Chapter 11: Hydrogen Respiration* (pp. 233–260). https://doi.org/10.1007/978-1-4020-3163-2_11

Wang, Y., & Liu, S. (2013). Enzymatic recovery of polyhydroxybutyrate (PHB) from burkholderia cepacia by pancreatin and characterization of Polymer Properties. *Journal of Bioprocess Engineering and Biorefinery*, 2(3), 163–170. https://doi.org/10.1166/jbeb.2013.1058

Wu, S. C., Liou, S. Z., & Lee, C. M. (2012). Correlation between bio-hydrogen production and polyhydroxybutyrate (PHB) synthesis by Rhodopseudomonas palustris WP3-5. *Bioresource Technology*, *113*, 44–50. https://doi.org/10.1016/j.biortech.2012.01.090

Yiğit, D., Ufuk, G., Tiüker, L., & Yücel, M. (1999). Identification of by-products in hydrogen producing bacteria; Rhodobacter sphaeroides O.U. 001 grown in the waste water of a sugar refinery. In *ELSEVIER Journal of Biotechnology* (Vol. 70).

Yu, M., Wang, K., & Vredenburg, H. (2021). Insights into low-carbon hydrogen production methods: Green, blue and aqua hydrogen. *International Journal of Hydrogen Energy*, *46*(41), 21261–21273. https://doi.org/10.1016/j.ijhydene.2021.04.016

APPENDICES

A. COMPOSITIONS OF MEDIA

Table A. 1. MPYE medium composition

Compound	*Concentration*	*Unit*
Bacto Peptone	3.00	g/L
Yeast extract	3.00	g/L
$MgCl_2$	0.32	g/L
$CaCl_2$	0.14	g/L
Agar – agar[1]	15.0	g/L

pH is adjusted to 7.0 using 0.5 M NaOH solution.

Table A. 2. Growth medium composition

Compound	*Concentration*	*Unit*
KH_2PO_4	3.00	g/L
$MgSO_4 \cdot 7H_2O$	0.50	g/L
$CaCl_2.2H_2O$	0.05	g/L
CH_3COOH	20.0	mM
$C_5H_8NO_4Na$	10.0	mM
Vitamin solution (10X Stock)	100	µL/L
Ferric citrate solution (50X Stock)	500	µL/L
Trace element solution (10X Stock)	100	µL/L

pH is adjusted to 6.30 – 6.40 using 5 M NaOH solution.

[1] Media should not be stirred after agar addition, rather should be left to dissolve on its own in autoclave.

Table A. 3. First adaptation medium composition

Compound	***Concentration***	***Unit***
KH_2PO_4	3.00	g/L
$MgSO_4 \cdot 7H_2O$	0.50	g/L
$CaCl_2.2H_2O$	0.05	g/L
CH_3COOH	20.0	mM
$C_{12}H_{22}O_{11}$	5.0	mM
$C_5H_8NO_4Na$	10.0	mM
Vitamin solution (10X Stock)	100	µL/L
Ferric citrate solution (50X Stock)	500	µL/L
Trace element solution (10X Stock)	100	µL/L

pH is adjusted to 6.30 – 6.40 using 5 M NaOH solution.

Table A. 4. Second adaptation medium composition

Compound	***Concentration***	***Unit***
KH_2PO_4	3.00	g/L
$MgSO_4 \cdot 7H_2O$	0.50	g/L
$CaCl_2.2H_2O$	0.05	g/L
$C_{12}H_{22}O_{11}$	5.0	mM
$C_5H_8NO_4Na$	10.0	mM
Vitamin solution (10X Stock)	100	µL/L
Ferric citrate solution (50X Stock)	500	µL/L
Trace element solution (10X Stock)	100	µL/L

pH is adjusted to 6.30 – 6.40 using 5 M NaOH solution.

Table A. 5. PHB and H2 production medium with acetate composition

Compound	***Concentration***	***Unit***
KH_2PO_4	3.00	g/L
$MgSO_4 \cdot 7H_2O$	0.50	g/L
$CaCl_2.2H_2O$	0.05	g/L
CH_3COOH	65.0	mM
$C_5H_8NO_4Na$	2.00	mM
Vitamin Solution (10X Stock)	100	µL/L
Ferric Citrate Solution (50X Stock)	500	µL/L
Trace Element Solution (10X Stock)	100	µL/L

pH is adjusted to desired levels using 5 M NaOH solution.

Table A. 6. PHB and H2 production medium with sucrose composition

Compound	***Concentration***	***Unit***
KH_2PO_4	3.00	g/L
$MgSO_4 \cdot 7H_2O$	0.50	g/L
$CaCl_2.2H_2O$	0.05	g/L
$C_{12}H_{22}O_{11}$	10.8	mM
$C_5H_8NO_4Na$	2.00	mM
Vitamin Solution (10X Stock)	100	µL/L
Ferric Citrate Solution (50X Stock)	500	µL/L
Trace Element Solution (10X Stock)	100	µL/L

pH is adjusted to desired levels using 5 M NaOH solution.

Table A. 7. 10X trace element solution composition[1,2]

Compound	*Concentration*	*Unit*
$ZnCl_2$	700	mg/L
$MnCl_2 \cdot 4H_2O$	1000	mg/L
H_3BO_3	600	mg/L
$CoCl_2 \cdot 6H_2O$	2000	mg/L
$CuCl_2 \cdot 2H_2O$	200	mg/L
$NiCl_2 \cdot 6H_2O$	200	mg/L
$NaMoO_4 \cdot 2H_2O$	400	mg/L
HCl (25% v/v)	10	mL/L

Table A. 8. 10X vitamin solution composition[1,2]

Compound	*Concentration*	*Unit*
Thiamin chloride hydrochloride	5.00	g/L
Niacin (Nicotinic acid)	5.00	g/L
D+ Biotin	0.15	g/L

Table A. 9. 50X ferric citrate solution composition[1,2]

Compound	*Concentration*	*Unit*
Fe-Citrate	50.0	g/L

[1] Trace element, vitamin and ferric-citrate solutions should be prepared using sterile water and filtered through 0.22μm sterile filters. Said solutions should not be subjected to autoclaving to avoid degradation.

[2] Trace element, vitamin and ferric-citrate solutions must not be subjected to daylight or UV light. Should be stored in dark and refrigerated at +4°C.

B. CALCULATION OF FEED CARBON SOURCE CONCENTRATION

General mass balance equation can be written as,

$$m_1 + m_2 = m_3 \quad \text{(B. 1)}$$

Where;

m_1 = mass of carbon source in the reactor after sampling (i.e., before feeding),

m_2 = mass of carbon source in the feed,

m_3 = mass of carbon source in the reactor after feeding.

Writing in terms of concentrations;

$$C_1 * V_1 + C_2 * V_2 = C_3 * V_3 \quad \text{(B. 2)}$$

Rearrange Equation B.2 to reflect the reactor;

$$C_{unfed} * V_{unfed} + C_{feed} * V_{feed} = C_{fed} * V_{fed} \quad \text{(B. 3)}$$

Suppose that the sampling and feeding volume is 20 mL, initial concentration of carbon source is 65 mM, working volume is 350 mL and feeding is done when concentration of the carbon source reaches to half of its initial value, substituting the values;

$$32.5\ \text{mM} * 330\ \text{mL} + C_{feed} * 20\ \text{mL} = 65\ \text{mM} * 350\ \text{mL}$$

Solving for C_{feed},

$$C_{feed} = 601.25\ \text{mM}$$

C. ABSORBANCE SPECTROPHOTOMETER CALIBRATION CURVES FOR CELL DRY WEIGHT DETERMINATION

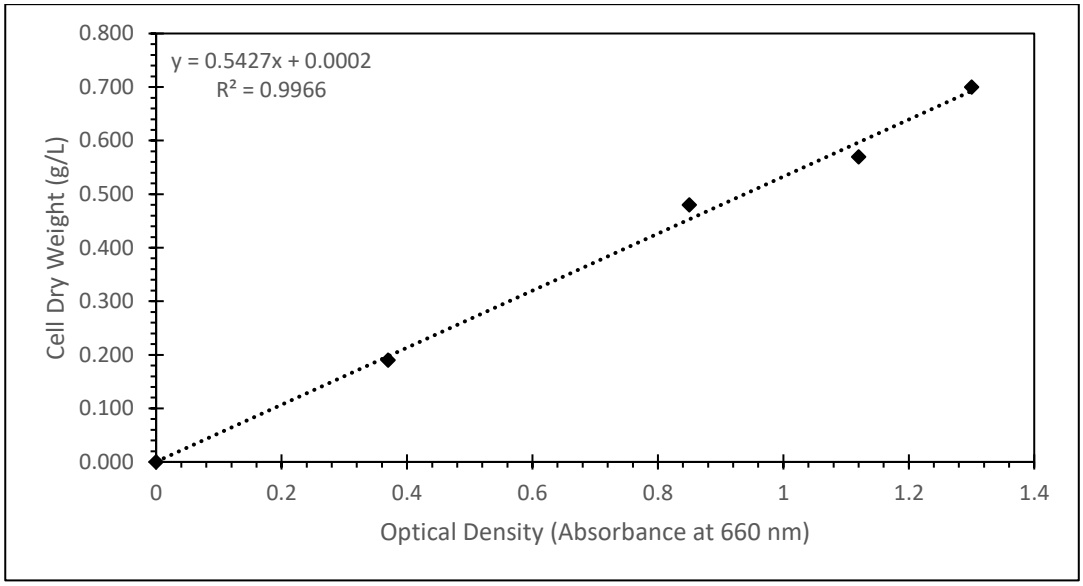

Figure C. 1. *R. capsulatus* WT (DSM1710) cell dry weight vs. optical density calibration curve and equation (Uyar, 2008).

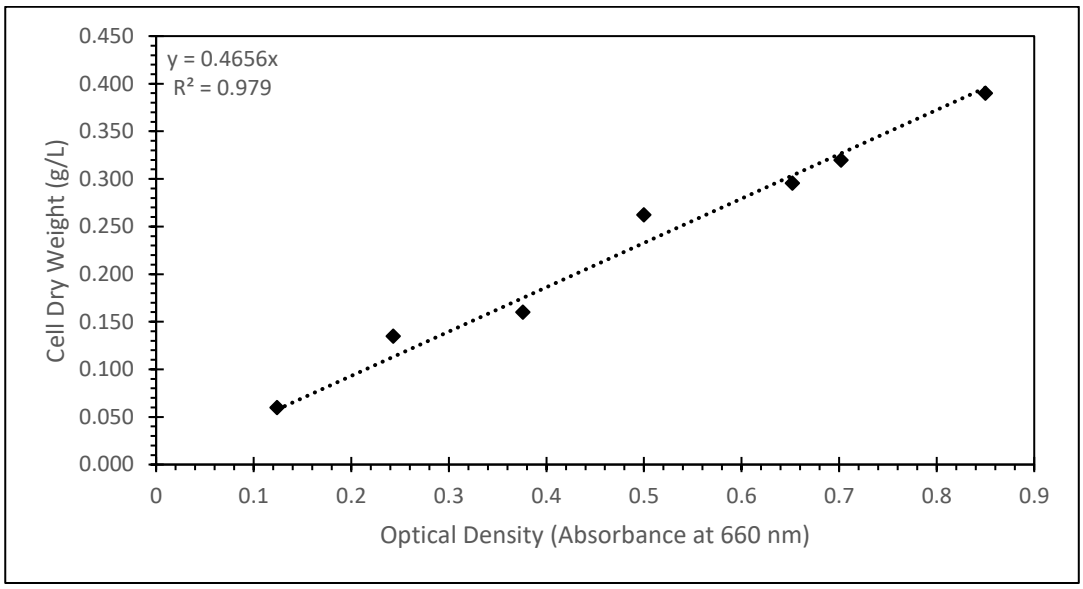

Figure C. 2. *R. capsulatus* YO3 cell dry weight vs. optical density calibration curve and equation (Öztürk, 2005).

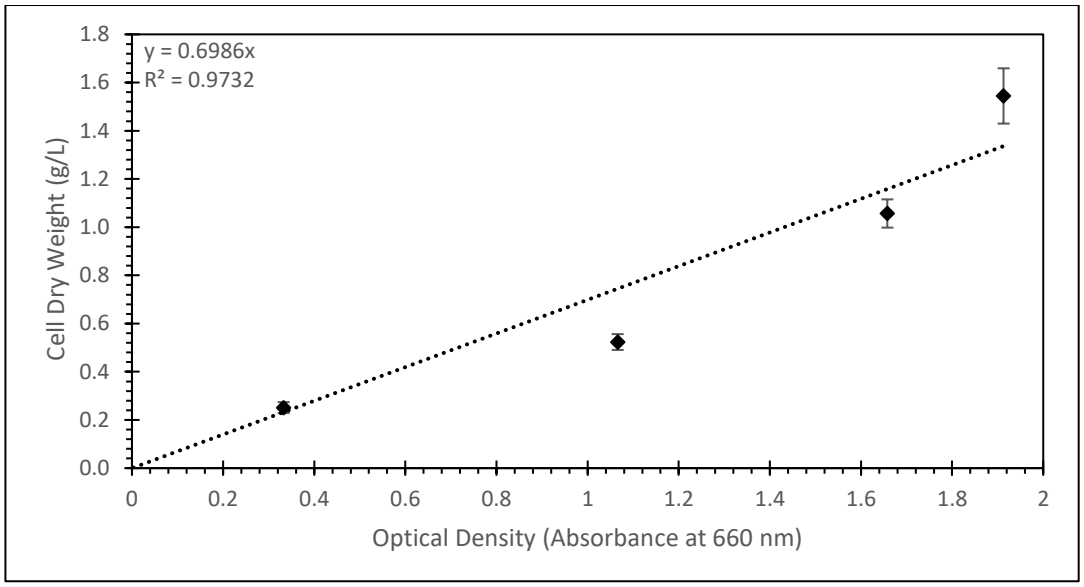

Figure C. 3. Cell dry weight vs. optical density calibration curve and equation for *R. capsulatus* YO3 utilizing sucrose as the carbon source in the presence of 40 mM NaCl (This study).

D. HPLC CALIBRATION CURVES FOR ORGANIC ACIDS AND SUCROSE ANALYSIS

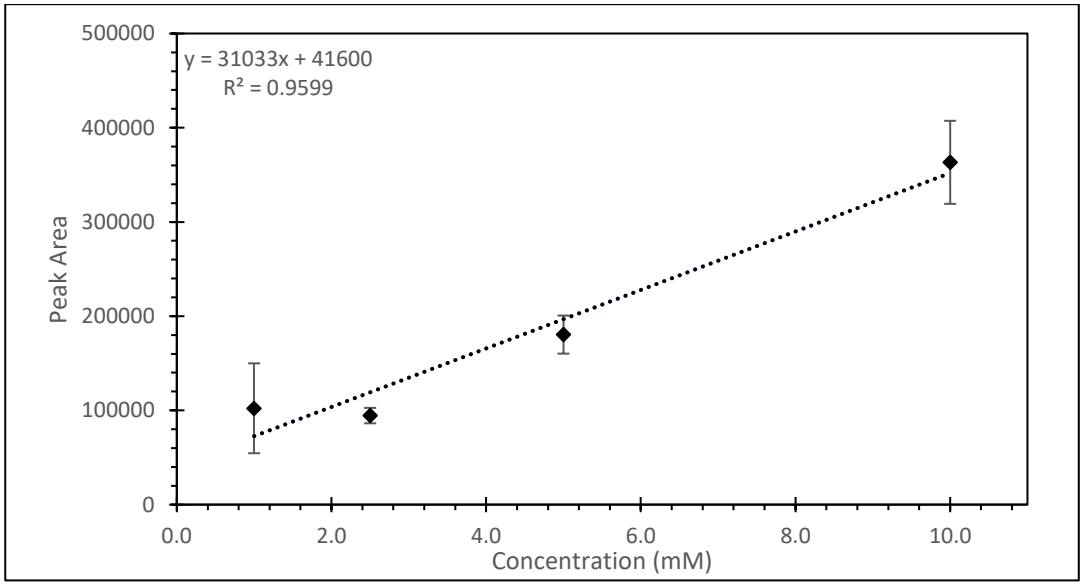

Figure D. 1. Heptanoic acid calibration curve, prepared from 10mM VFA mix. Elution order = 1, Retention Time = 7.9 – 8.3 min.

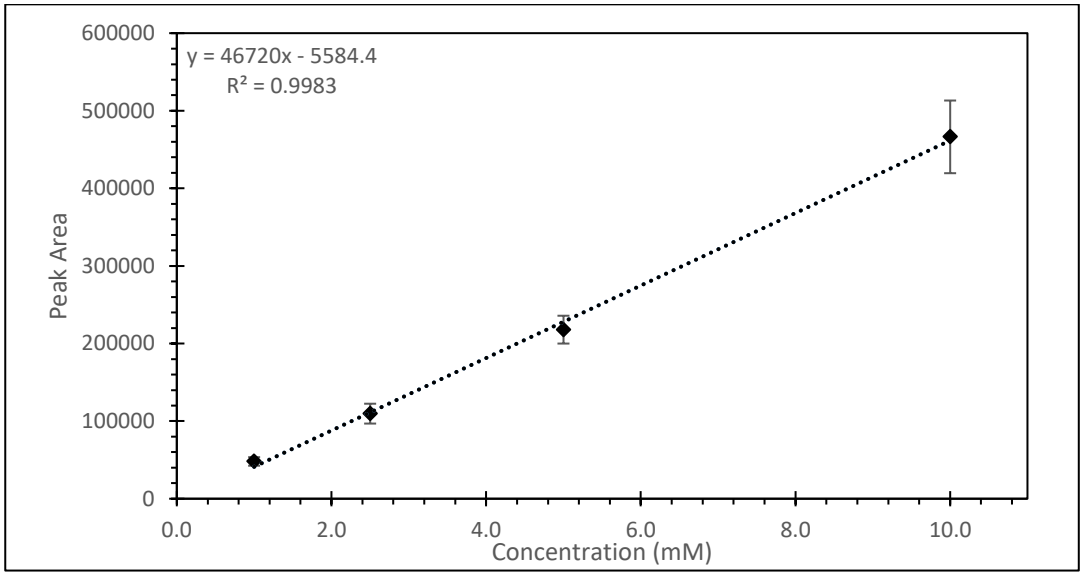

Figure D. 2. Formic acid calibration curve, prepared from 10mM VFA mix. Elution order = 2, Retention Time = 22.1 – 23.4 min.

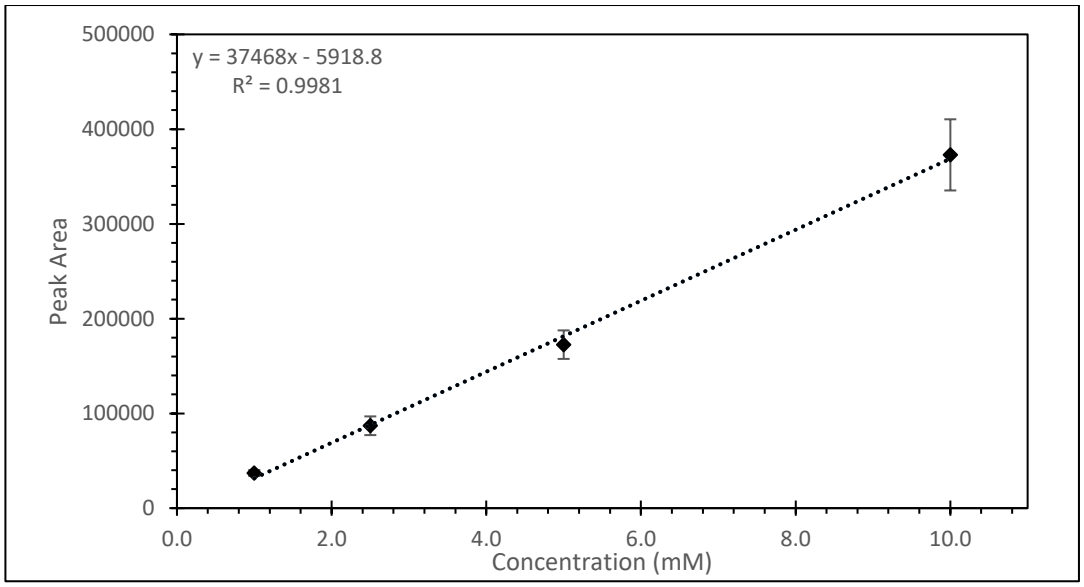

Figure D. 3. Acetic acid calibration curve, prepared from 10mM VFA mix. Elution order = 3, Retention Time = 24.0 – 25.4 min.

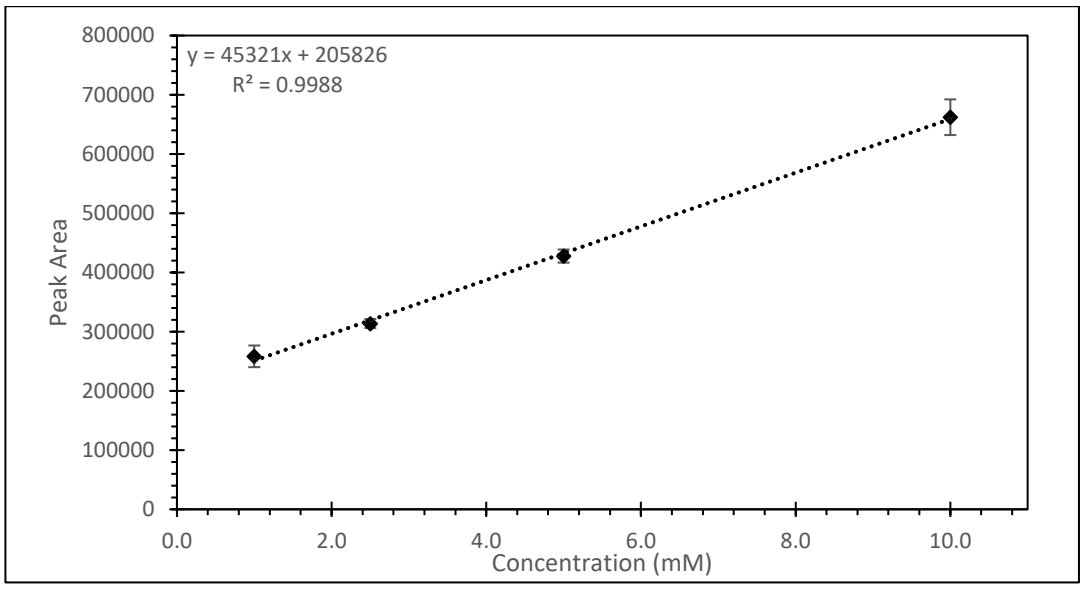

Figure D. 4. Propionic acid calibration curve, prepared from 10mM VFA mix. Elution order = 4, Retention Time = 28.2 – 29.7 min.

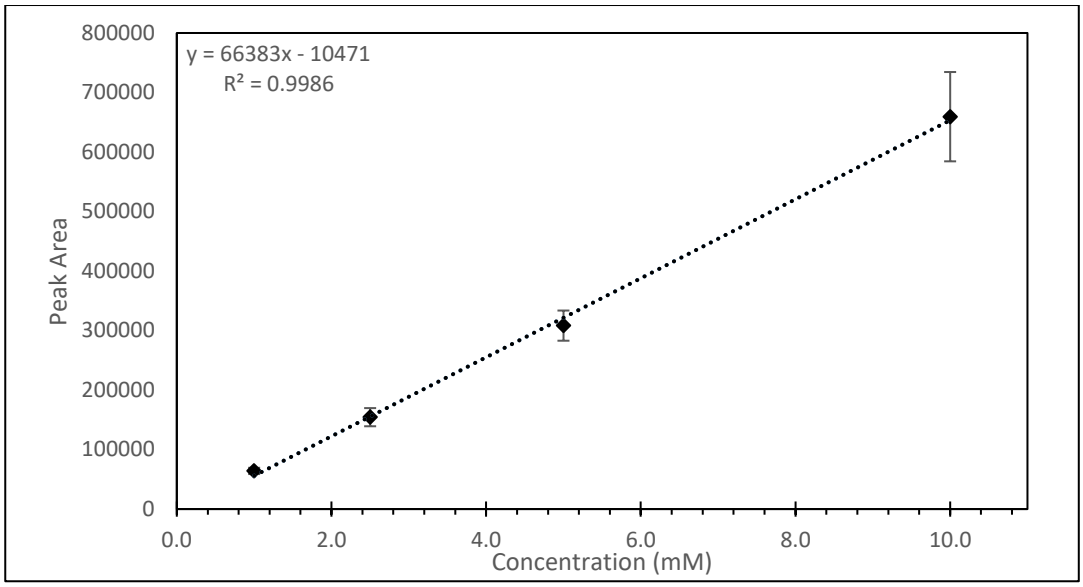

Figure D. 5. Isobutyric acid calibration curve, prepared from 10mM VFA mix. Elution order = 5, Retention Time = 32.1 – 33.5 min.

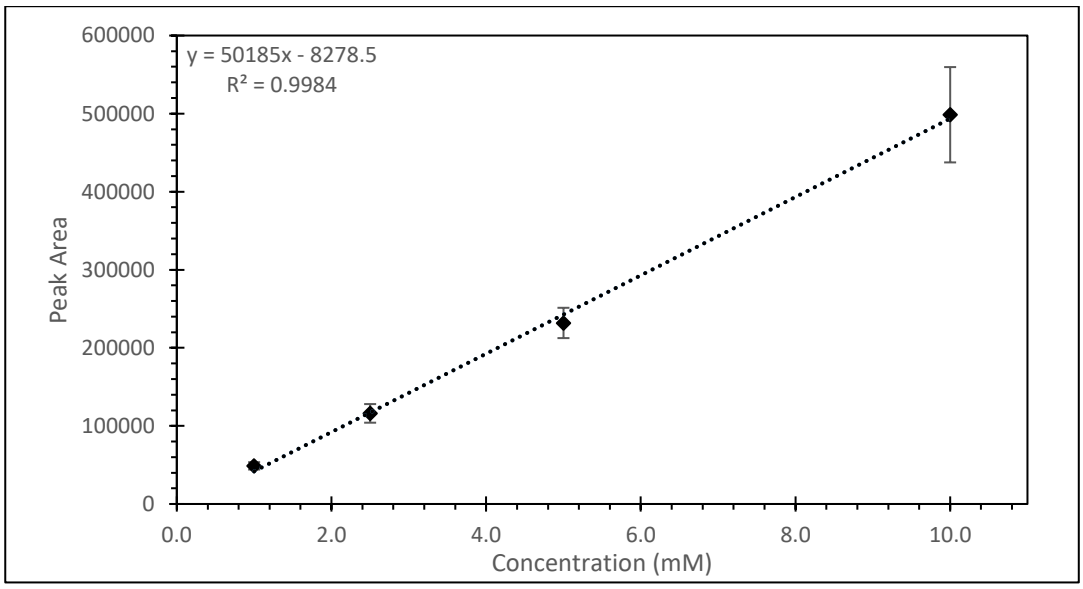

Figure D. 6. Butyric acid calibration curve, prepared from 10mM VFA mix. Elution order = 6, Retention Time = 34.7 – 36.0 min.

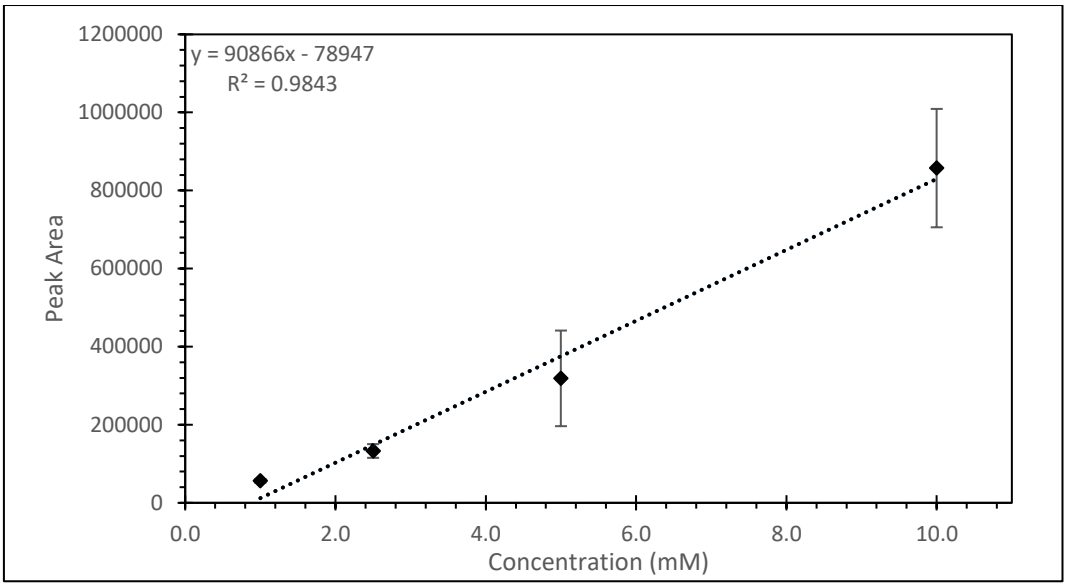

Figure D. 7. Isovaleric acid calibration curve, prepared from 10mM VFA mix. Elution order = 7, Retention Time = 40.3 – 41.5 min.

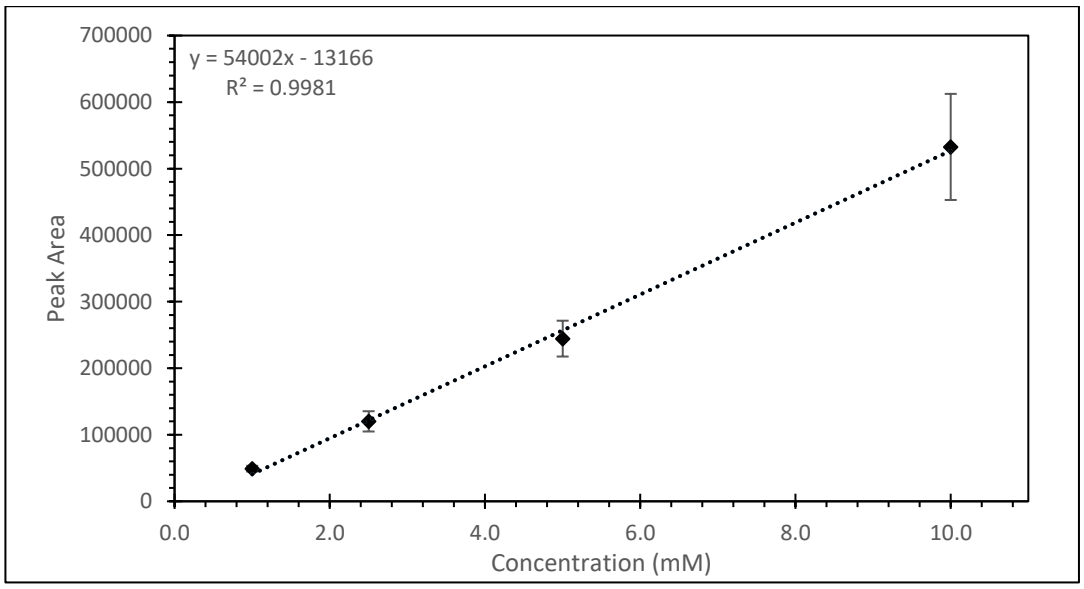

Figure D. 8. Valeric acid calibration curve, prepared from 10mM VFA mix. Elution order = 8, Retention Time = 48.7 – 49.7 min.

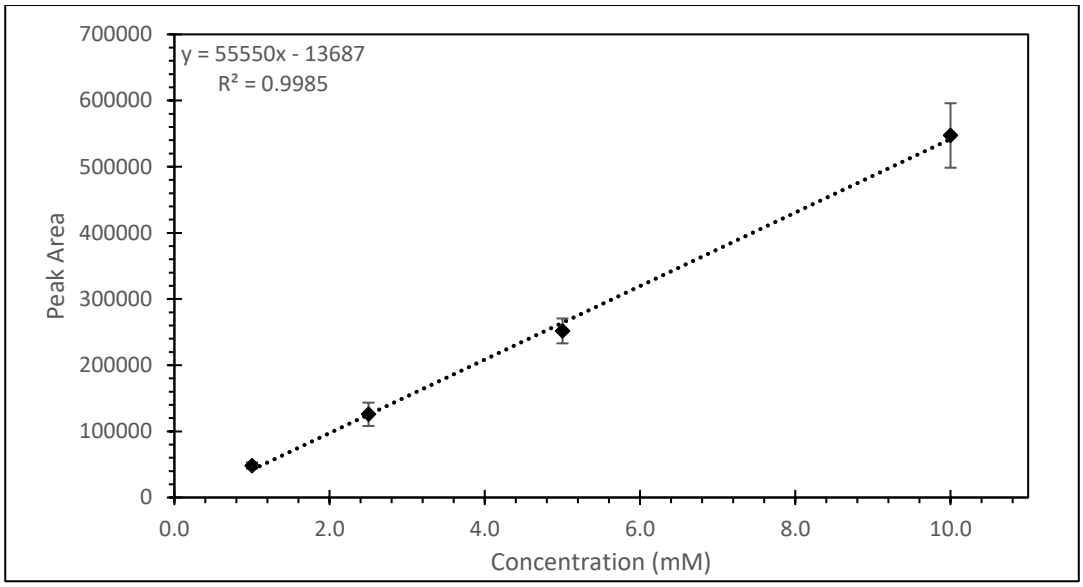

Figure D. 9. Isocaproic acid calibration curve, prepared from 10mM VFA mix. Elution order = 9, Retention Time = 62.6 – 64.1 min.

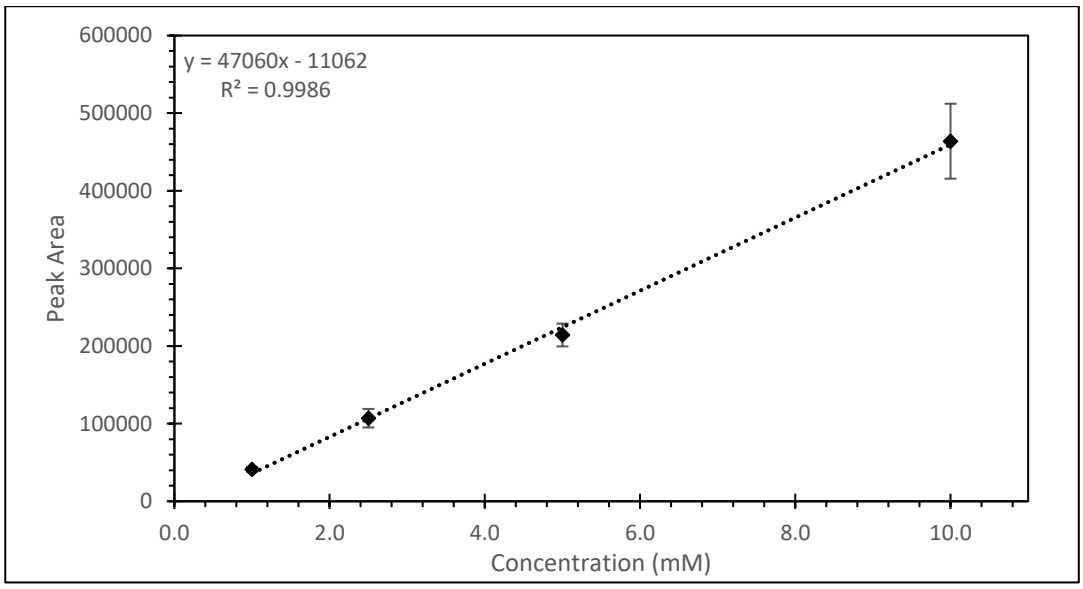

Figure D. 10. Hexanoic acid calibration curve, prepared from 10mM VFA mix. Elution order = 10, Retention Time = 73.1 – 75.3 min.

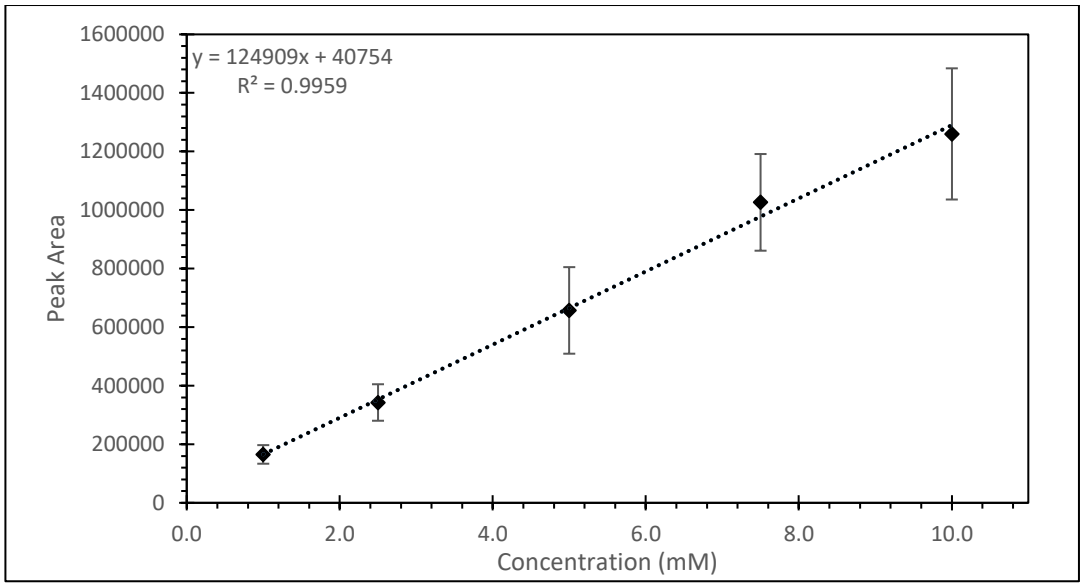

Figure D. 11. Lactic acid calibration curve, prepared from pure lactic acid solution, Fluka, 69775. Retention Time = 20.1 – 21.0 min.

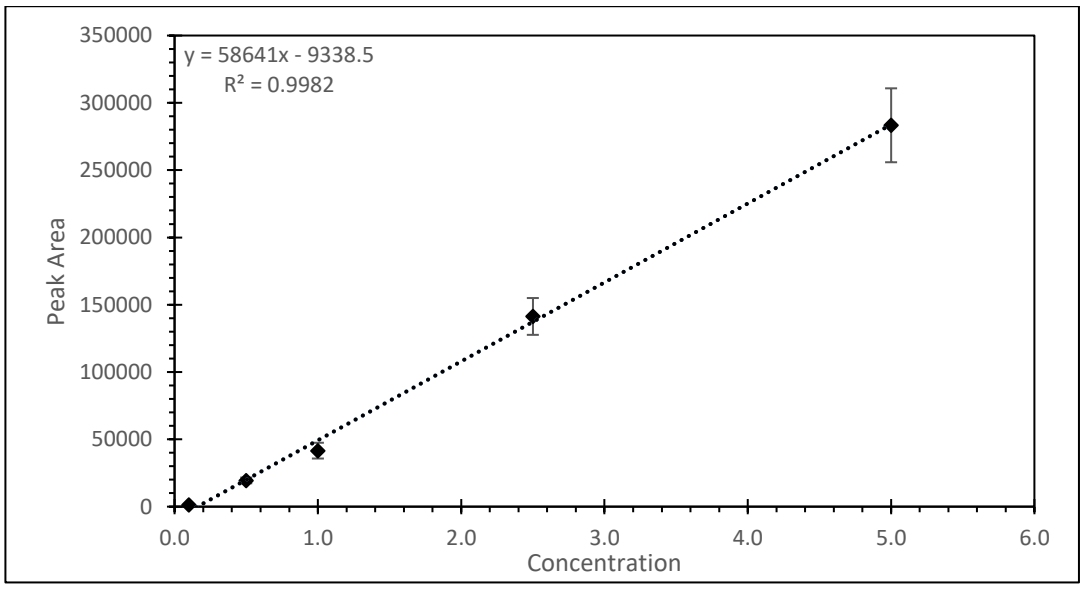

Figure D. 12. Sucrose calibration curve, prepared from laboratory grade sucrose, Merck Millipore, 107651. Retention Time = 11.5 – 12.3 min.

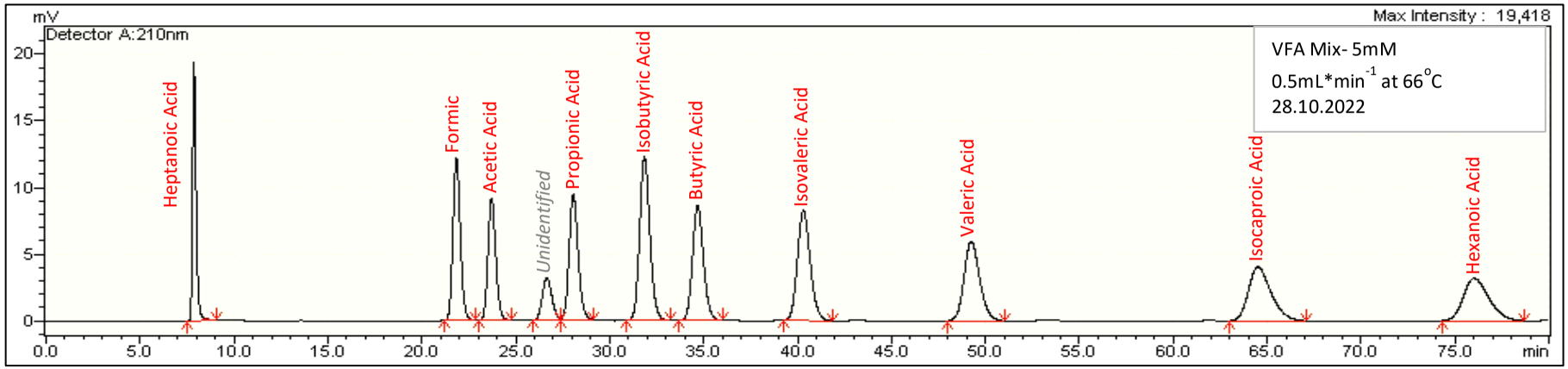

Figure D. 13. Sample chromatogram (signal strength vs. retention time) for organic acids analysis using 5.0 mM VFA mix.

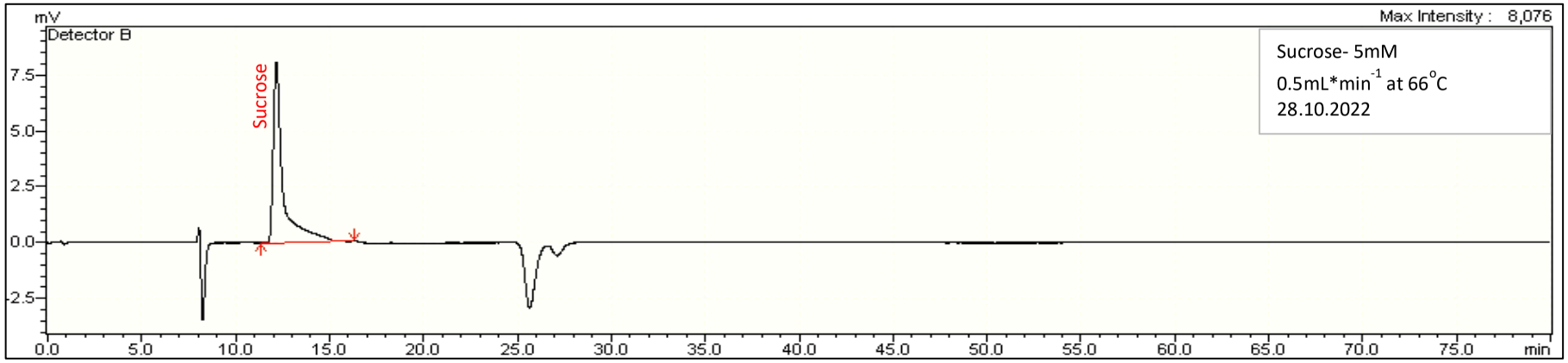

Figure D. 14. Sample chromatogram (signal strength vs. retention time) for sucrose analysis using 5.0 mM laboratory grade sucrose.

E. FLAME PHOTOMETER CALIBRATION CURVE FOR SODIUM CONTENT

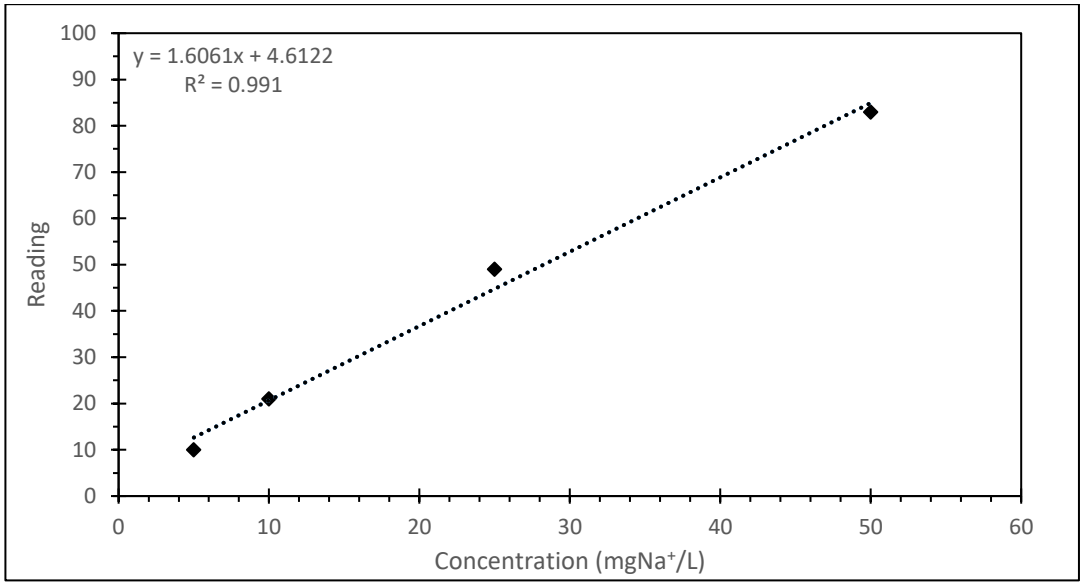

Figure E. 1. Flame photometer calibration curve, dated 02.12.2022 for determination of Na^+ content.

Note that the calibration curve should be reconstructed before every use of the instrument.

F. GC CALIBRATION CURVES FOR HEADSPACE GAS CONTENT

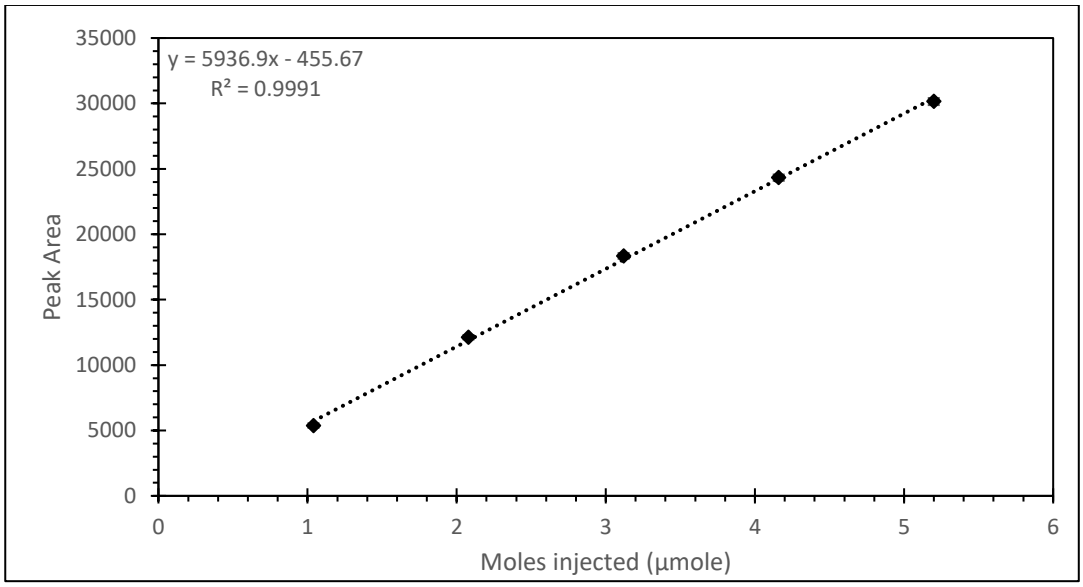

Figure F. 1. H_2 calibration curve. Retention order = 1, Retention Time = 1.3 min.

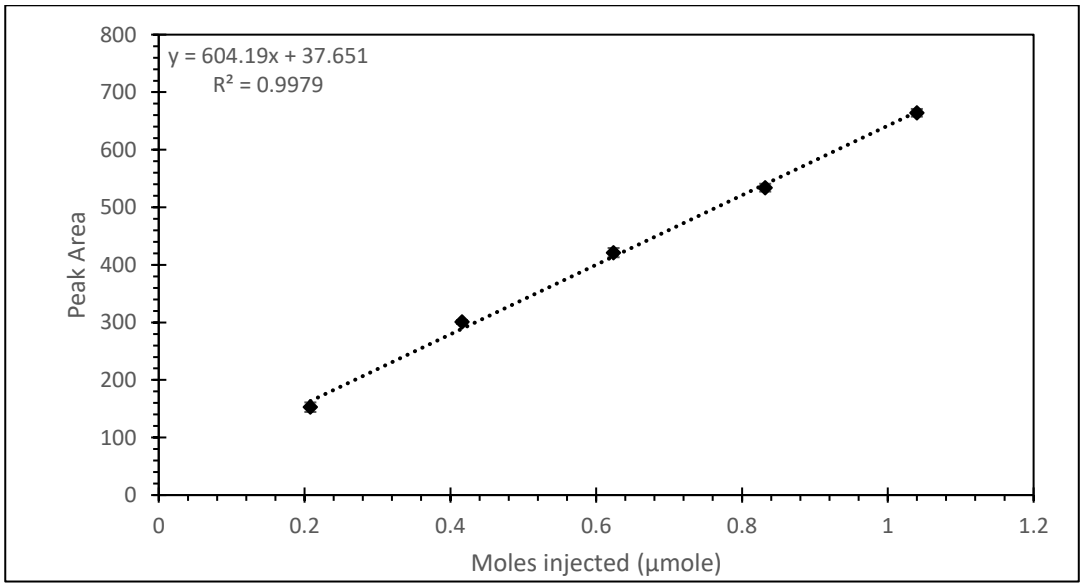

Figure F. 2. N_2 calibration curve. Retention order = 2, Retention Time = 2.2 min.

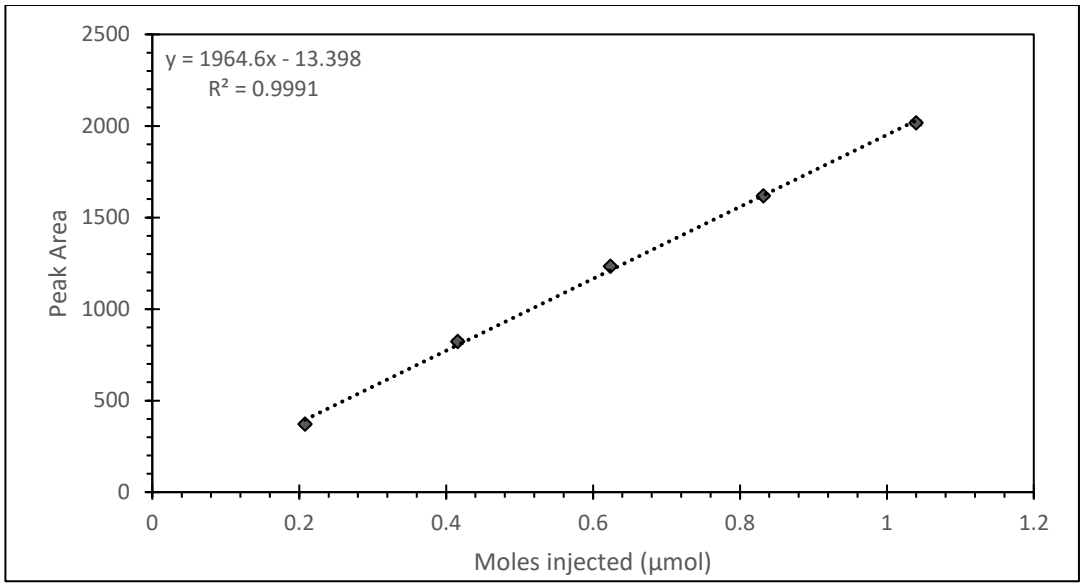

Figure F. 3. CH_4 calibration curve. Retention order = 3, Retention Time = 4.6 min.

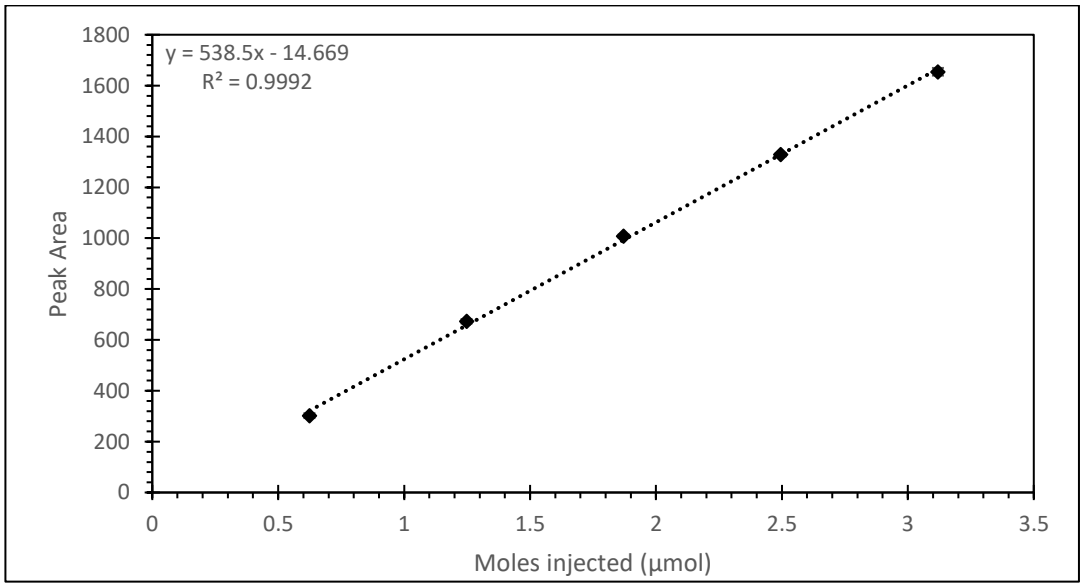

Figure F. 4. CO_2 calibration curve. Retention order = 4, Retention Time = 8.3 min.

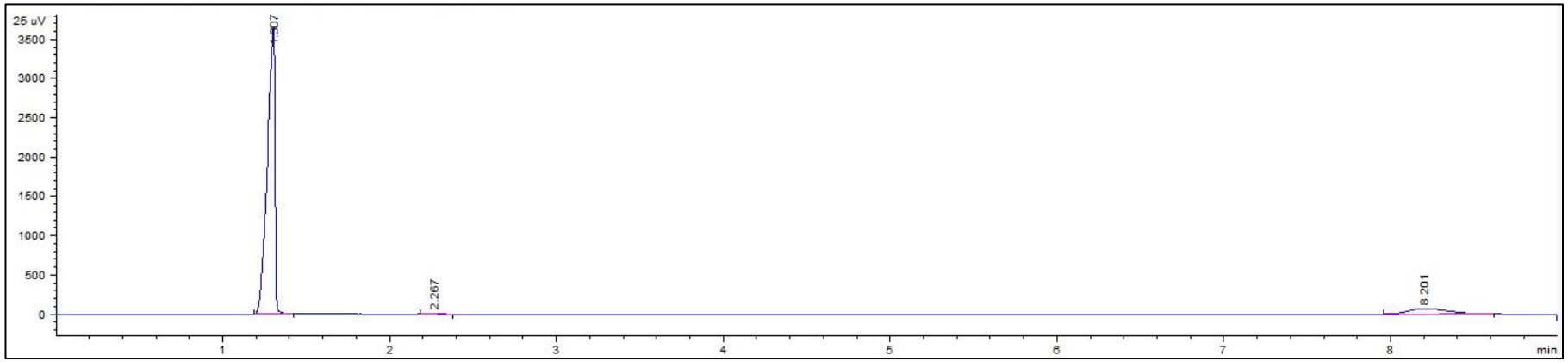

Figure F. 5. Sample chromatogram (signal strength vs. retention time) for headspace gas analysis from a reactor sample dated November 7, 2022.

G. GC CALIBRATION CURVE FOR PHB CONTENT

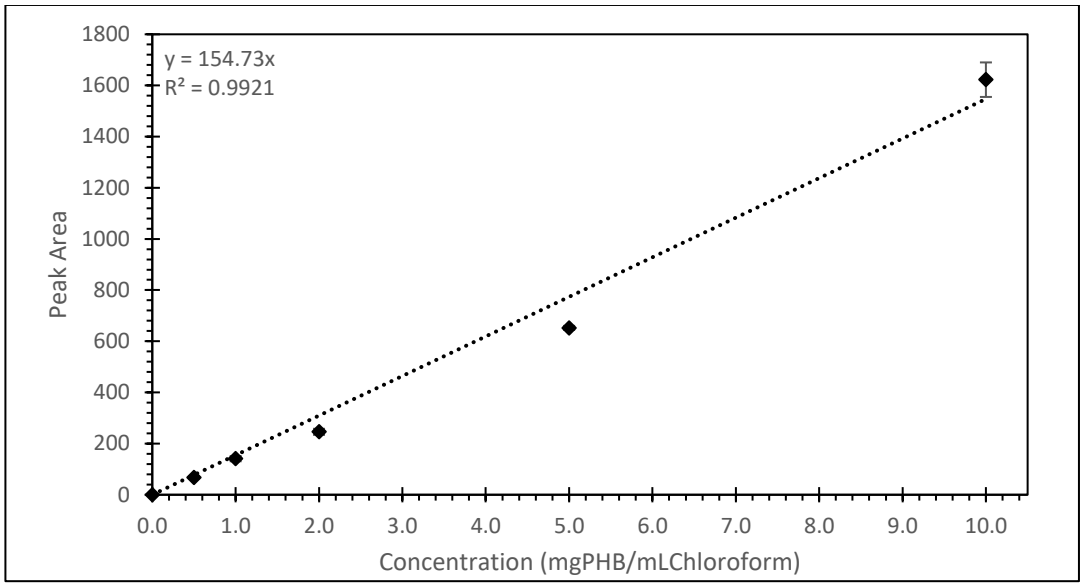

Figure G. 1. PHB calibration curve. Retention Time = 8.8 – 9.0 minutes.

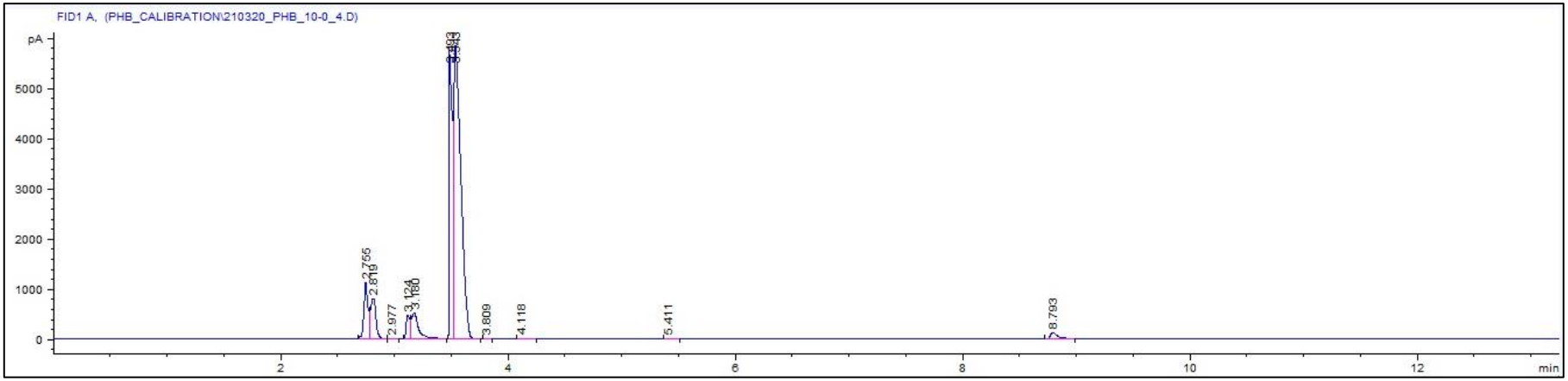

Figure G. 2. Sample chromatogram (signal strength vs. retention time) for PHB analysis using 10 mgPHB/mLChloroform standard solution. Retention time for PHB is 8.8 – 9.0 minutes.

H. RESULTS FOR AC0 REACTOR IN SET 2

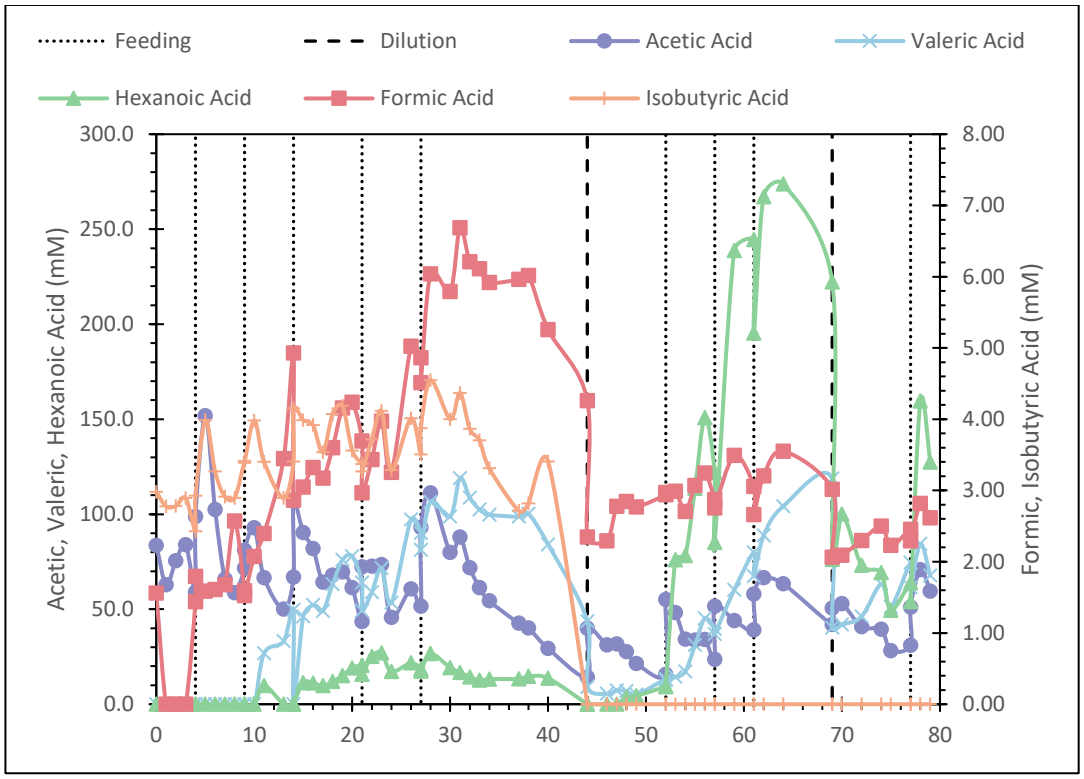

Figure H. 1. Organic acids analysis of acetate-containing control reactor in Set 2. Error bars indicate upper and lower ranges of duplicate reactors

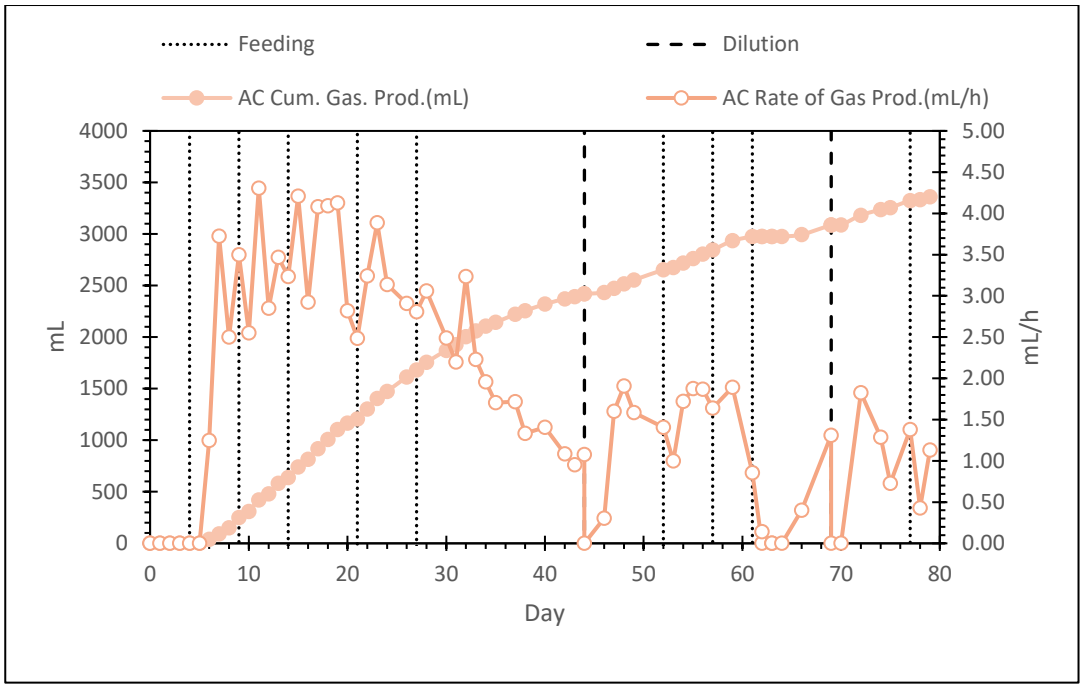

Figure H. 2. Cumulative and hourly biogas production of acetate-containing control reactor in Set 2.

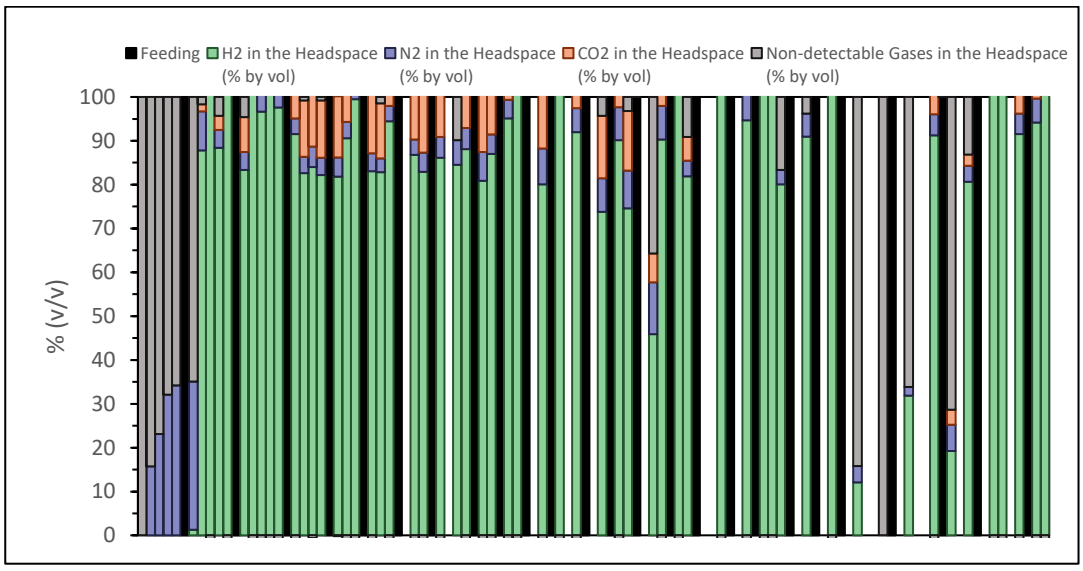

Figure H. 3. Headspace gas composition for acetate-containing control reactor in Set 2.

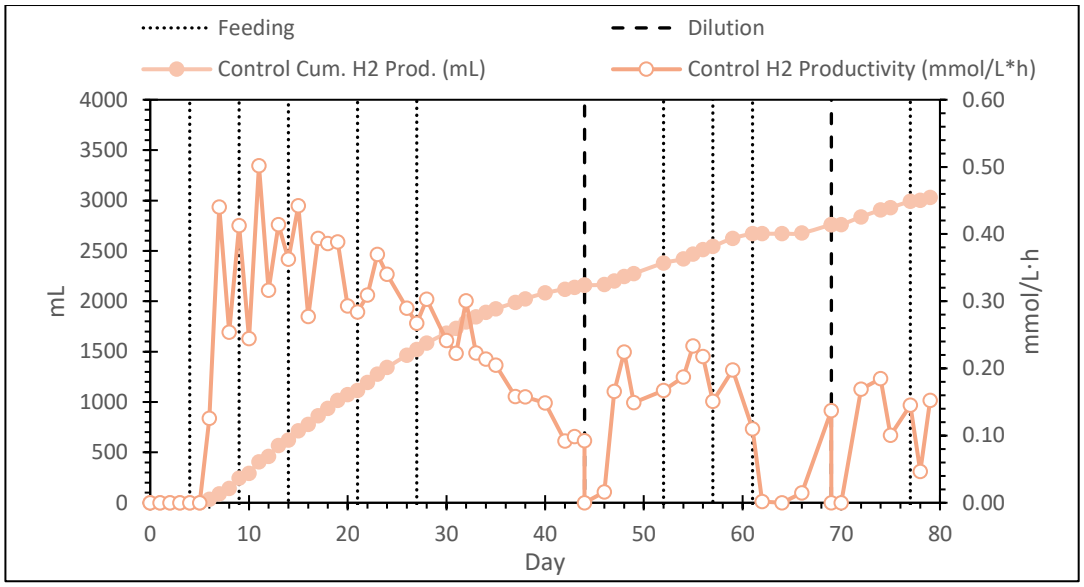

Figure H. 4. Cumulative H_2 production and H_2 productivities observed in acetate-containing control reactor in Set 2.

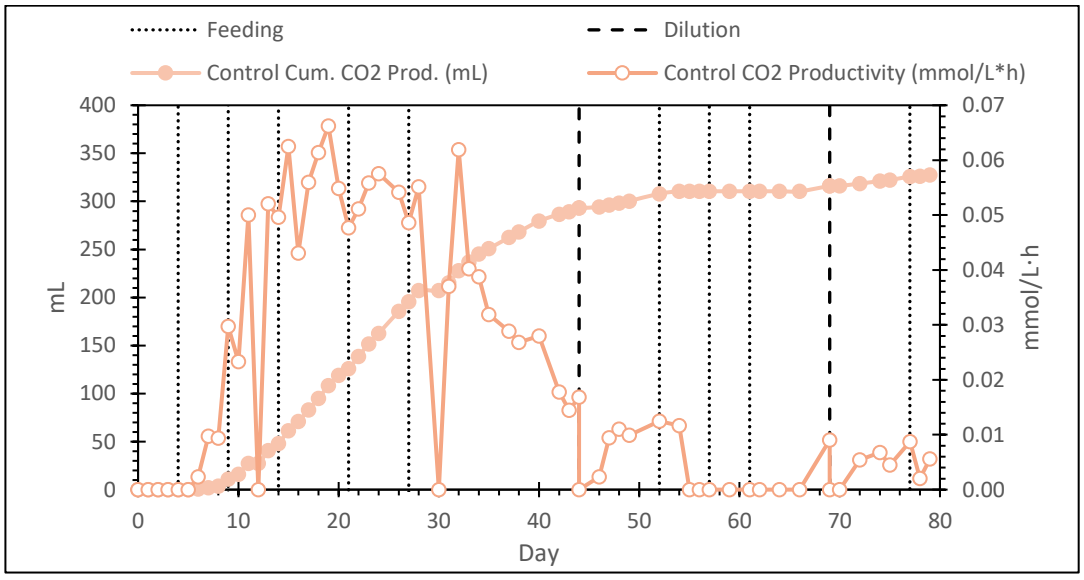

Figure H. 5. Cumulative CO_2 production and CO_2 productivities observed in acetate-containing control reactor of Set 2.